THE ASTROPHYSICAL JOURNAL

AN INTERNATIONAL REVIEW OF SPECTROSCOPY AND ASTRONOMICAL PHYSICS

VOLUME 89 MARCH 1939 NUMBER 2

WILLIAM WALLACE CAMPBELL
1862–1938

J. H. MOORE

William Wallace Campbell, eminent scientist and able administrator, is recognized as a leading astronomer of his generation. Coming to the Lick Observatory only three years after it opened, he was associated with this institution for the remainder of his life as astronomer and director, and later as president of the University of California. His high sense of duty, his idealism, combined with his ability as an investigator, an organizer, and director of research during a long period of service, have left their impress alike upon the observatory and the university.

Born on a farm in Hancock County, Ohio, April 11, 1862, Campbell received his early education in the country schools and the high school of a neighboring village. After teaching in the public schools for a year he entered the University of Michigan, from which he was graduated in 1886 with the degree of B.S. While he was following the regular course in civil engineering, his interests were turned to astronomy by the reading of Newcomb's popular treatise, and during his senior year he elected as many courses as possible in practical and theoretical astronomy. He had now definitely decided to be an astronomer; but, upon graduation, finding no opportunities open to him in this field, he accepted a professorship in mathematics at the University of Colorado. Two years later he returned to the Univer-

sity of Michigan as instructor in astronomy and assistant in the observatory.

At Ann Arbor, in addition to teaching the course in practical astronomy for engineers, Campbell engaged extensively in the observation of comets and the computation of their orbits. Here, in 1888, appeared his first scientific paper, "The Definitive Determination of the Orbit of Comet 1885 III," to be followed within the next three years by eleven others relating to micrometric measures and the orbital elements of comets. It was also during this period that he prepared *A Handbook of Practical Astronomy*, which, in its revised and enlarged form, has been widely used and which is perhaps still one of the best textbooks on the subject. His astronomical experience was further widened by a summer spent as volunteer assistant in the Lick Observatory. Here his enthusiasm and ability for research so impressed Director Holden that a few months later, when Keeler resigned to accept the directorship of the Allegheny Observatory, Campbell was appointed to succeed him and thus in 1901 became astronomer in the Lick Observatory.

The following year he was married to Elizabeth Ballard Thompson, whose rare culture and personal charm made her an ideal companion to her gifted husband. Their happy life was one of constant devotion to each other, and their gracious hospitality a real source of joy to their many friends.

Spectroscopic work at Mount Hamilton had been inaugurated by Keeler with a visual spectroscope designed by him as part of the original equipment for the 36-inch refractor, and with this instrument Campbell took up the observation of the spectra of comets, novae, variable stars, and various classes of bright-line stars. These investigations, which were described in numerous papers appearing during the next few years, are all of a high order and bear eloquent testimony to his remarkable skill and judgment as an observer. Especially should we note his pioneering work relating to the emission lines occurring in the spectra of certain early-type stars, particularly those known as Wolf-Rayet stars; his comprehensive investigation of the spectrum of Nova Aurigae, in which he was the first to identify the nebular lines; and his studies of the variation in relative intensities of the hydrogen and nebulium (N_1 and N_2) lines in

different parts of the Orion nebula. No less important were his spectroscopic observations of Mars in the summer of 1894, in which he sought to detect the presence of water vapor in the Martian atmosphere, by comparing the intensities of the water-vapor lines in the spectra of Mars and the moon. They too were made by the visual method, and from them he concluded that the amount of water vapor in the atmosphere of Mars must be very much less than in that of the earth. This conclusion was amply confirmed fifteen years later by his results obtained with more refined photographic methods, both at Mount Hamilton and on the summit of Mount Whitney.

During these early years at the Lick Observatory Campbell gave serious thought to the problem with which his name will always be associated: the determination of stellar radial velocities. The visual method, which in the skilful hands of his predecessor had given the first satisfactory velocities in the line of sight for fourteen gaseous nebulae and three bright stars, was soon supplanted by the incomparably better one employing the photographic plate. To meet these changed conditions the Mills spectrograph was designed and constructed in accordance with what he conceived to be the essential requirements for this special type of investigation: rigidity of mechanical parts, excellent definition, and maximum light transmission of the optical train. After submitting the instrument to thorough tests and removing certain of its optical defects, Campbell, in 1896, entered upon an ambitious program for the measurement of the radial velocities of all stars in the northern heavens brighter than visual magnitude 5.51. A few years later he published in this *Journal* the classic papers in which were given the results of his measures for some of the bright stars. One need only compare his values with those obtained by previous observers to appreciate the fact that he was the first to solve the problem of the accurate determination of stellar radial velocities. Probable errors which for the best of the earlier measures had averaged about ± 2.6 km/sec were reduced to ± 0.5 km/sec, and for spectra with excellent lines to ± 0.25 km/sec—a precision not surpassed at the present time.

The reasons for this outstanding achievement lay not alone in the fortunate combination of a large telescope and an excellent spectro-

graph especially efficient for this work. It was Campbell's thorough mastery of every essential detail at each step in the process, from the taking of satisfactory spectrograms to their accurate measurement and reduction, that contributed in no small degree to his success.

An important by-product of the program and one quite unexpected was the discovery that a number of the stars were spectroscopic binaries. Three or four such systems were previously known, but by 1900 he and his associate, Mr. Wright, had added no less than thirty-one others. Of the stars observed by them, more than one in nine was shown to have variable velocity. At this time Campbell made the prophetic statement: "It is not improbable that at least one star in five or six will be found to be a spectroscopic binary, and I should not be surprised to see a still larger ratio established." The field of astronomical research thus opened has, in the years that followed, become an exceedingly rich one in which he and his colleagues have made many notable contributions.

During the later part of the period under consideration certain events took place at the Lick Observatory which were important in determining the future development of its activities and in particular those relating to radial-velocity investigations. Professor Keeler had succeeded Dr. Holden as director in 1898, and his brilliant career had been closed by death only two years later. Dr. Campbell's high scientific attainments and his ability as an executive were recognized by his appointment to the directorship in 1901. With the assumption of the heavy administrative duties of this position much of the active work of carrying on the radial-velocity observations was of necessity committed to others, although he maintained general supervision of these researches and occasionally participated in the observing. Thus, for a number of years, the investigations were conducted in collaboration with astronomer Wright and later with astronomer Moore, as well as with other associates for shorter periods.

The urgent need of radial-velocity data for the stars of the southern heavens to supplement those obtained at Mount Hamilton had long been recognized by Dr. Campbell, and, with the object of obtaining them, he organized the D. O. Mills Expedition to Chile. Through the generosity of Mr. D. O. Mills, an observing station,

specially equipped for observations of this kind, was established at Santiago, Chile, in 1903, with astronomer Wright in charge. After the completion of the program for the brighter stars the life of the expedition was extended for many years, which resulted in the addition of very important data for the spectroscopic binaries of the southern sky as well as for the motions of the fainter stars.

Some conception of the magnitude of Dr. Campbell's great work on stellar radial velocities may perhaps be gained from the statement that in the thirty years devoted to it more than 25000 spectrograms of 2770 stars were obtained at Mount Hamilton and at Santiago. The measures of these he submitted to a most thorough investigation for the presence of systematic errors arising from instrumental and other causes. His publication in 1928 of the result of all this labor made available the most extensive and homogeneous set of radial-velocity data for the naked-eye stars of the entire heavens that has thus far been produced. This material was made the basis for a determination of the direction and speed of the solar motion and for other statistical studies relating to the peculiar motions of the stars. A detailed account of these investigations and the results of the entire radial-velocity program were presented in Volume XVI, *Publications of the Lick Observatory*, a work that will always remain a fitting monument to one who contributed so abundantly to our knowledge of stellar motions.

A closely related undertaking was his program of radial-velocity determinations of 101 gaseous nebulae, to which the spectroscopic equipment of the two observatories was devoted for several years, and which yielded data that have proved of the greatest value in studies of galactic rotation. At the same time he conducted in collaboration with Moore extensive researches on the internal motions in several of the larger planetary nebulae, which afforded strong evidence that these objects are expanding and at the same time rotating about their minor axis of figure.

Although Dr. Campbell's major contribution to astronomy was, as he himself regarded it, the accurate determination of stellar radial velocities, his researches were by no means limited to this particular field. Early he became interested in the spectroscopic study of the solar chromosphere and corona—an interest which continued

through the years and which was largely responsible for the important part played by the Lick Observatory in the observation of total solar eclipses. As an eclipse observer he had few equals. Only those who have taken part in the seven eclipse expeditions that he directed can fully appreciate his powers of organization, his skill and resourcefulness in the design and manipulation of instruments, and his thorough attention to every detail essential to success in the critical moments of totality. On all these expeditions he was accompanied by Mrs. Campbell, whose able assistance and thoughtful care lightened many of the burdens incident to eclipse work.

In 1898 he observed his first total eclipse of the sun at Jeur, India. Here he employed a spectrograph of high dispersion in an attempt to "determine the law of rotation of the solar corona" from observations of the green line, λ 5303, near the east and west limbs of the sun. Although his measures indicated a small rotational velocity in the corona, he regarded the result as of doubtful validity. These measures yielded, however, together with those of Lockyer at the same eclipse, the first accurate determination of the wave length of the green coronal radiation. It was also at this eclipse that he obtained the first continuous photographic record of the rapidly changing spectrum at the sun's edge during the few seconds near the beginning and end of totality. The method by which this was accomplished was devised by him, and consists essentially in giving to the plate-holder of the spectrograph a uniform motion in a direction perpendicular to the length of the spectrum. It was again used successfully at the eclipses of 1900, 1905, and 1908, the record of the flash spectrum obtained in Spain (1905) being especially excellent. This method of the "moving plate" has certain obvious advantages over the usual one employing a fixed plate; and at the same time it possesses its own observational difficulties which need not be discussed here. It is sufficient to note that Dr. Campbell was well aware of these and strongly urged that both methods be used, the results obtained with the one furnishing a most important check upon those derived from the other. His beautiful photographs of the flash spectrum on both moving and fixed plates were utilized by Dr. Menzel as the basis for a notable discussion of the complex conditions that exist in the solar chromosphere.

An important part of the equipment for the Australian eclipse in 1922 included a battery of four wide-angle cameras. These were specially designed and mounted under his immediate supervision for a test of a possible deflection of light by the sun's gravitational field—an effect predicted by Einstein from the general theory of relativity. The results of this investigation, made in collaboration with Dr. Trumpler, not only confirmed those obtained by Eddington at the eclipse of 1919 but afforded the most thorough and critical study to which this phenomenon has been subjected.

His researches touching many fields of endeavor are described in his more than three hundred papers and memoirs appearing in scientific journals, and in the publications of astronomical societies and of the Lick Observatory. A number of these relate to the problems connected with the motions of the stars, a subject discussed more at length in the treatise entitled *Stellar Motions*, which was based on his Silliman Lectures delivered in 1910. They attest his versatility, his capacity for clear and accurate statement of the results of investigations, and his keen scientific judgment in the appraisal of their value.

Great as were Dr. Campbell's contributions to the advancement of knowledge, they comprised but a part of that magnificent service which he rendered to astronomy. His able administration and direction of the work of the Lick Observatory for nearly a quarter of a century were largely responsible for the high quality of the researches conducted by this institution. By his ideals of right living and working, by his enthusiasm and industry, and by his consideration for the views of others he gained the respect and admiration of his colleagues and of all those with whom he came in contact. His skill as an administrator and organizer were called upon frequently by his fellow-scientists, and in this wider field also he served with distinction. In 1915 he was president of the American Association for the Advancement of Science, and in the same year the first president of its Pacific Division, which he had helped to organize. From 1922 to 1925 he was president of the International Astronomical Union, in whose organization, in 1919, he had taken a leading part. During the same period he served as president of the American Astronomical Society.

Dr. Campbell's great ability as an organizer and administrator,

combined with his high qualities of mind and character, led the Regents of the University of California to turn to him in a critical situation and to offer him the presidency of that institution. Although he preferred to remain at the observatory and devote himself to his chosen science, the call to duty was for him a command, and he accepted the responsibilities of the office in 1923. He still retained, however, the title of director of the observatory and maintained his legal residence at Mount Hamilton in the hope that he might be permitted soon to return; but his sense of duty kept him at his post for seven years, until he reached the age of retirement.

His administration of the university was conducted with breadth of vision, with thorough attention to details and in accordance with those same ideals that had characterized his scientific career. In shaping its policies he was confronted with many difficult problems. These were attacked and solved courageously, with the steadfast purpose of maintaining the highest standards of university life and work. Appreciation of his great service to the state and to the cause of education could not be expressed in words more fitting than those of Regent Chester H. Rowell: "With a hand always gentle but firm and never shirking, President Campbell ruled the University wisely and well."

To this arduous task he had given beyond his strength and as a consequence his health was seriously impaired. After his retirement in 1930 he continued his general scientific activities and in addition to other responsibilities served as president of the National Academy of Sciences from 1931 to 1935. Although at that time he was suffering from ill health and partial blindness, he conducted the affairs of the academy so ably and efficiently that he won added distinction as an administrator.

Recognition of Dr. Campbell's eminent services as a scientist, educator, and executive was accorded by his fellow-workers both at home and abroad through the many honors conferred upon him. He was the recipient of honorary degrees from eight American and foreign universities, of honorary membership in the leading scientific academies and societies throughout the world, the Lalande and Janssen medals of the Paris Academy, the Draper medal of the National Academy, the Bruce medal of the Astronomical Society of the

Pacific, and the gold medal of the Royal Astronomical Society. The international character of his achievements was further signalized by the bestowal upon him of decorations with gold insignia: by Belgium, as commander of the Order of Leopold III; by Italy, as commander of the Crown; by France, as officer of the Legion of Honor.

The malady with which he was stricken during the last year of the presidency of the University, and against which he had struggled so courageously, continued its relentless march, taking heavy toll of his physical and mental powers. It led to his death on June 14, 1938. Dr. Campbell is survived by his widow and their three sons—Wallace, Douglas, and Kenneth. To his family and to his friends he has left treasured memories of a life dedicated to the service of his fellow-men.

LICK OBSERVATORY
November 12, 1938

ERNEST WILLIAM BROWN
1866–1938

FRANK SCHLESINGER

Ernest William Brown was born at Hull, England, on November 29, 1866, the only son of William and Emma (Martin) Brown. He was educated at East Riding College, where he showed an aptitude for mathematics, and it was decided that he was to go on to Cambridge University. He was graduated with the degree B.A. in 1887 as sixth wrangler and was elected a fellow of Christ's College. Then, as now, Cambridge excelled in mathematical training without giving much thought to what application the student was to make of this training. It is interesting to note that, upon graduation, Brown applied for a post as a meteorologist, fortunately (for astronomy) unsuccessfully. In 1891 he received and accepted a place as professor of applied mathematics at Haverford College near Philadelphia, where he remained until 1907, when he was called to Yale as a successor to the late Williard Gibbs (1839–1903). When the Sterling Professorships were founded at Yale in 1921, he was among the first group of three to receive one of these appointments. In 1931 he became the first incumbent of the Williard Gibbs Professorship. The following year he retired, partly on account of ill-health and partly because he wished to be free from his teaching duties. The years of his retirement, in spite of a constant struggle with ill-health, proved to be among the most fruitful of his career.

The Cambridge instructor to whom he was most indebted and upon whom he most relied was George Howard Darwin (1845–1912). It was upon his advice that Brown studied carefully George William Hill's (1838–1913) great memoir of 1877 upon the lunar theory. He became more and more interested in this subject; and when he went to Haverford in 1891, he had resolved to undertake the enormous task of computing the moon's orbit upon this theory. One of the attractions that drew him to Yale was the assurance of a fund for assistance in computing and for publishing the results. Later he had

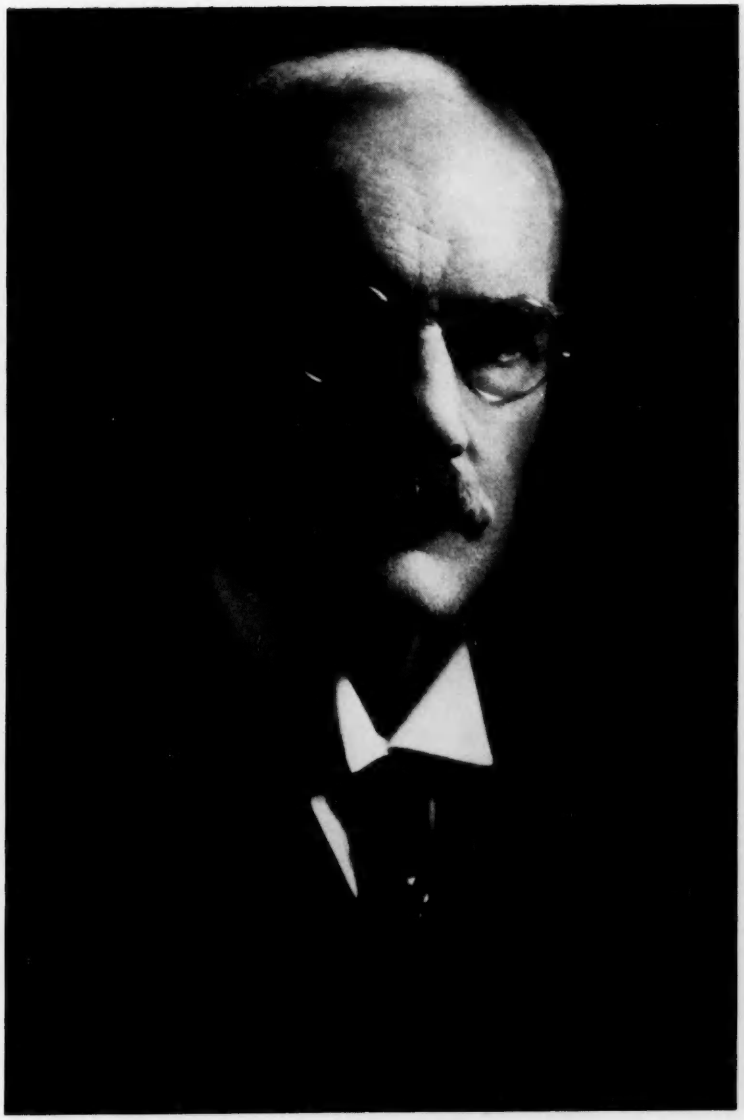

ERNEST WILLIAM BROWN

1866–1938

a number of tempting offers of other posts, including one to succeed his old teacher, Darwin, at Cambridge. But he had become deeply attached to America and, in particular, to his surroundings at New Haven; and there he remained throughout his remaining years.

The computation of the path of the moon occupied him to the practical exclusion of every other research for a full quarter-century; indeed, he was busy with some phase of the lunar theory until within two weeks of his death. He had a superb facility for throwing mathematical expressions into the best form for computing. In this respect he has seldom been equaled in the whole history of applied mathematics. He carried out his work on the moon so accurately and so thoroughly that it is difficult to imagine that it will have to be reviewed or revised in any sense for many decades to come.

The principal object of this laborious task was to see whether the motion of the moon could be accounted for by the attractions of the known bodies in the solar system. It came out that in two respects they apparently fail to do so. The first of these concerns the "secular acceleration" of the moon's place, discovered by Halley (1656–1742) some two centuries earlier. It was suggested by Newcomb (1835–1909) that this may really be a retardation in the rate of rotation of the earth, but it was left to Brown to prove that this is actually so; and more recently two English geophysicists have shown that such a retardation can be accounted for quantitatively by tidal friction in shallow channels like the Irish Sea and Bering Strait. The other respect in which Brown found that gravitation fails to account for the motion of the moon relates to the "fluctuations" (so called by Newcomb), oscillations (in a rough period of several decades) about the moon's mean place. Brown showed that these, too, are due to irregularities in the earth's rotation; their origin is, however, still very obscure.

In the years that Brown was busy on the moon, he made only two investigations of other problems: the relation between the sunspot period and the periods of revolution of Jupiter and Saturn and the cause of the shapes of the spiral arms in extragalactic nebulae. In the latter case he suggested that what we really see are the envelopes of continuous closed orbits of the separate constituents of the nebulae.

Once the moon was at least partly out of the way, Brown turned with great success to other difficult problems in celestial mechanics, like the orbit of the eighth satellite of Jupiter, asteroid gaps, periodic orbits, and the orbits of the Trojan group of asteroids, bodies that form nearly equilateral triangles with Jupiter and the sun. During the last two or three years of his life he concerned himself, again with happy results, with the stellar problem of three bodies in which the masses concerned are of the same order of magnitude.

Throughout the half-century that Brown worked, he never lost the least particle of his enthusiasm for celestial mechanics. Once on the track of a promising lead, he was wont to work himself into a fever of excitement that made it difficult for him to lay it aside. For many years he was accustomed to awake in the small hours of the night; and, after refreshing himself with a draft of coffee from a thermos bottle and with his never failing cigarette, he would work in bed until it was time to arise for a nine o'clock breakfast. This he did wherever he happened to be—whether at home, visiting with friends, or even on shipboard.

Although he was not particularly fond of teaching, he fulfilled these duties with distinction; and he won the respect, admiration, and warm friendship of all his students. He was not in the habit of preparing his lectures very minutely in advance, and as a result he was occasionally stuck. But he always extricated himself promptly, and it was instructive for his students to see how accurately and unerringly his mind worked under such circumstances.

Brown knew how to play as well as to work. In his youth he rowed in the Christ's College boat, and he was addicted to mountain-climbing. He was an excellent performer on the piano to within a few years of his death, before palsy made it impossible for him to strike the keys accurately. He was devoted to music in all its forms and was for a time head of the New Haven Oratorio. He was fond of chess and played a good game. Late in life he took up card-playing but, oddly enough, with only moderate success. He was an authority on nonsense verse; he could recite without a slip long excerpts from Gilbert and Sullivan's operas, from the "Bab Ballads," and from the poems of Lewis Carroll. In earlier years he read the English classics, but later he devoted most of his reading-time to

detective stories. He was an inveterate traveler, especially in his famous Ford motor car, widely known as "Sylvia," which he usually drove at a higher speed than is recommended by the police. He was a constant attendant at the meetings of many scientific societies, although he was not always present during the reading of papers; there is no doubt that his chief object in going was to renew his many friendships among his colleagues.

Like some of his predecessors in celestial mechanics, Brown never married. His household was presided over by his maiden sister, Mildred, two years his junior. For most of her adult life she made the comfort of her distinguished brother her chief, almost her sole, concern; and she succeeded in thoroughly spoiling him. She died some two years before he did, and thereafter his only surviving close relative was a sister who lives in New Zealand.

From his early manhood Brown was affected by bronchial trouble, probably as a result of his rowing activities. Just before his retirement in 1932 he suffered an attack of intestinal ulcers. He refused to take the usual treatment for this complaint, admonishing his physician not to try to prolong his life but to make him as comfortable as possible. Strange to say, this illness cured itself but left him in a much weakened condition. The six years that were left to him were a constant struggle with ill-health. But he went about his work undaunted and unafraid. He died at last of sheer exhaustion on July 22, 1938, in his seventy-second year.

YALE OBSERVATORY
December 6, 1938

THE SPECTRA OF THE SUPERNOVAE IN IC 4182 AND IN NGC 1003*

R. MINKOWSKI

ABSTRACT

Spectrograms of supernova IC 4182 have been obtained until 339 days after maximum and of supernova NGC 1003 until 115 days after maximum. The spectra of these two supernovae differ only in details of minor importance. They may be interpreted as consisting of wide, partly overlapping emission bands; on the earlier spectrograms the width of the narrowest details is about 100 A. After an initial period of about two weeks the spectrum divides into two parts. That to the red of λ 5000 undergoes pronounced changes; bands appear and disappear in a manner resembling the behavior of the emission bands in the spectra of ordinary novae. Below λ 5000 a permanent pattern forms, consisting of one strong and several fainter bands, which shifts, as a whole, gradually toward the red without any significant changes in its intensity distribution. The two parts of the spectrum show pronounced changes in their relative intensities, which emphasize their independence. The red part strengthens at first, and about 40 days after maximum becomes preponderant; it then fades to a minimum intensity about 160 days after maximum, reappears at almost its initial strength about 20 days later, and finally fades out slowly. These changes are not accompanied by any significant change of the pattern in the blue. About 180 days after maximum two narrow bands, with a width of less than 40 A, appear at λ 6299 and λ 6359. Their intensity relative to the rest of the spectrum increases slowly, and they become finally the only observable features in the red.

A comparison of the spectra of supernovae IC 4182 and NGC 1003 with those of the five earlier supernovae for which spectroscopic observations are available indicates that the spectra of all supernovae are practically identical in their composition and in their transformations. A possible exception is S Andromedae, for which, however, only visual observations were made. This similarity extends apparently to even the amount of the red shift in the blue part of the spectrum, which for supernova IC 4182, 339 days after maximum, reached a value of about 125 A.

If the bands are ordinary emission lines, the red shift, which is not accompanied by a change in the width of the bands, cannot be explained as due to a Doppler effect produced by an outward flow of matter without assuming an excessive darkening toward the limb. The explanation of the red shift as due to an increase in the gravitational potential at the surface of the star, in accordance with Zwicky's hypothesis of a collapse of the star, entails the assumption that the bands are negative absorption lines formed by induced transitions in a forbidden line of a highly ionized atom. But this assumption also permits, with fewer restrictions, an interpretation of the red shift as the result of a Doppler effect.

The two narrow bands in the red are probably to be identified as the [*O* I] lines λ 6300 and λ 6364. At present no other identifications can be proposed without reservation. The absence of hydrogen and helium lines indicates a very high degree of ionization; thus, all the bands may be of unknown origin.

INTRODUCTION

Before the discovery of the supernovae in IC 4182 and in NGC 1003 very few spectra of supernovae had been photographed,

* *Contributions from the Mount Wilson Observatory*, No. 602.

even with slitless or low-dispersion spectrographs. Visual observations of Z Centauri and of S Andromedae were the only sources of information on the part of the spectrum from λ 5000 on toward the red. Supernovae IC 4182 and NGC 1003 were both bright enough to be observed with slit spectrographs of moderate dispersion for a considerable time after maximum. By using short-focus Schmidt cameras and films with fast panchromatic emulsions, the observations could be extended to λ 6700. As faster equipment became available while the observations were in progress, spectrograms of supernova IC 4182 covering the whole region from λ 3700 to λ 6700 could be obtained until eleven months after maximum, when approaching conjunction with the sun prevented further observations. Most of the spectrograms of supernova NGC 1003, on the other hand—particularly all the later plates—had still to be obtained with a spectrograph of lower dispersion, which permitted observations only of the region from λ 3700 to λ 5000.

In the study of a phenomenon so complex and so peculiar as the spectrum of a supernova it is inevitable that interpretations of the observations will not agree completely. An impartial report of the spectroscopic data, presented in a form convenient for general discussion, is therefore indispensable. The spectrum of a supernova contains numerous indistinct details, clearly perceptible only on microphotometer tracings. It is virtually impossible for a reader to obtain from tables of wave lengths and from descriptive text an undistorted picture of such a spectrum and the numerous changes that it undergoes. Obviously, the proper means of presentation is a reproduction of microphotometer tracings of the spectrograms, accompanied by a journal giving all the data and remarks pertaining to them. These remarks have appeared desirable in order to draw the attention of the reader to the details, to the question of their reality, and to their variability; they are not intended to prejudice the discussion. In the interests of conciseness, however, it has been advantageous to take a definite point of view as to the character of the spectrum—on which there seems to be general agreement—namely, that the supernova spectrum is composed of wide emission bands. To base remarks on this assumption can hardly be mislead-

ing, although the question whether the supernova spectrum is a pure emission spectrum must remain open for later discussion.

The following instruments have been used:

a) The nebular spectrograph VIA, used with two prisms and with the Rayton camera, attached at the Cassegrain focus of the 100-inch reflector. The linear dispersion is 510 A/mm at $H\gamma$.

b) The nebular spectrograph VIA, used with two prisms and a 3-inch camera, attached at the Cassegrain focus of the 100-inch reflector. The linear dispersion is 220 A/mm at $H\gamma$ and 850 A/mm at $H\alpha$.

c) The same spectrograph as (*b*), attached at the Cassegrain focus of the 60-inch reflector.

d) A new nebular spectrograph VIB, with collimator of 32 inches focal length and two prisms of Schott LF-6 glass, used with a Schmidt camera of 3 inches focal length, corresponding to an aperture ratio of F/1.5. This spectrograph was attached at the Cassegrain focus of the 100-inch reflector. The linear dispersion is 215 A/mm at $H\gamma$ and 950 A/mm at $H\alpha$.

e) A two-prism spectrograph with a Schmidt camera of 6 inches focal length, attached at the Cassegrain focus of the 100-inch reflector. The linear dispersion is 80 A/mm at $H\gamma$ and 370 A/mm at $H\alpha$.

f) The same spectrograph as in (*e*), attached at the Cassegrain focus of the 60-inch reflector.

g) The one-prism spectrograph with 10-inch camera attached at the Cassegrain focus of the 60-inch reflector. The linear dispersion is 73 A/mm at $H\gamma$.

h) The same spectrograph as in (*g*) with 6-inch camera. The linear dispersion is 110 A/mm at $H\gamma$.

i) The one-prism spectrograph with 10-inch camera, attached at the Cassegrain focus of the 100-inch reflector. The linear dispersion is 78 A/mm at $H\gamma$.

j) A one-prism quartz spectrograph with a Schmidt camera of 2 inches focal length.

The tracings have been obtained with the photoelectric microphotometer designed by Dunham. The magnification of the wavelength scale has been adjusted to the dispersion of the different spectrograms so that the scale of all tracings is as similar as possible. Errors due to the considerable distortion of the photographic paper during processing are eliminated with the aid of a co-ordinate system recorded on the paper by the microphotometer. This co-ordinate system has been omitted from the illustrations, however, in order to obtain more legible reproductions. Instead, a more conveniently spaced co-ordinate system has been drawn; this, of course, does not take part in the distortion, and even for tracings of spectrograms

obtained from the same instrument, its abscissas correspond therefore only approximately to fixed values of the wave length.

Wave lengths of characteristic points of the spectrum have been measured and are given above the curves. With very few exceptions, which will be mentioned at their proper places in the journal, the features of the spectra of supernovae are too indistinct to be measured on the spectrograms. Wave lengths have therefore been obtained from another set of tracings, showing the comparison spectrum together with the spectrum of the supernova. The accuracy of such measures is not very high. For all spectra obtained on film, the accuracy is still more impaired by the unavoidable distortions of the film. It is estimated that the errors may be as large as 3 A at the violet end and 15 A at the red end of the spectrum. The uncertainty arising from the diffuseness of most of the details is still larger, however, and remains the predominant source of errors.

The wave lengths given in the figure are those corresponding to the position of the dashed line which connects the number with the curve. The aim has been to give, in this way, wave lengths for all points that may have physical meaning, such as maxima and minima, the edges of very flat maxima and minima, and inflections. The graininess of the photographic emulsion makes it difficult to determine whether minor details of the curves are real or spurious. Narrow details can sometimes be seen more distinctly on the spectrogram than on the tracing. Such features have been marked with a note of exclamation below the curve. When no decision as to the reality of a suspected feature could be reached, a question mark has been used. Scratches and other clearly recognizable defects of the emulsion have been marked with an X.

It is hardly necessary to emphasize that microphotometer tracings do not show true relative intensities. The deflections of the microphotometer are proportional to the light transmitted by the plate; in all the figures the uppermost ordinate corresponds to the deflection zero. Since the shortest usable slit of the photometer was longer than the width of unwidened spectra, the tracings of such spectra suffer an additional distortion of the relative intensities. Rough photometric estimates can be obtained, however, for the widened spectra obtained with spectrograph *f*. Diaphragms can be inserted in this

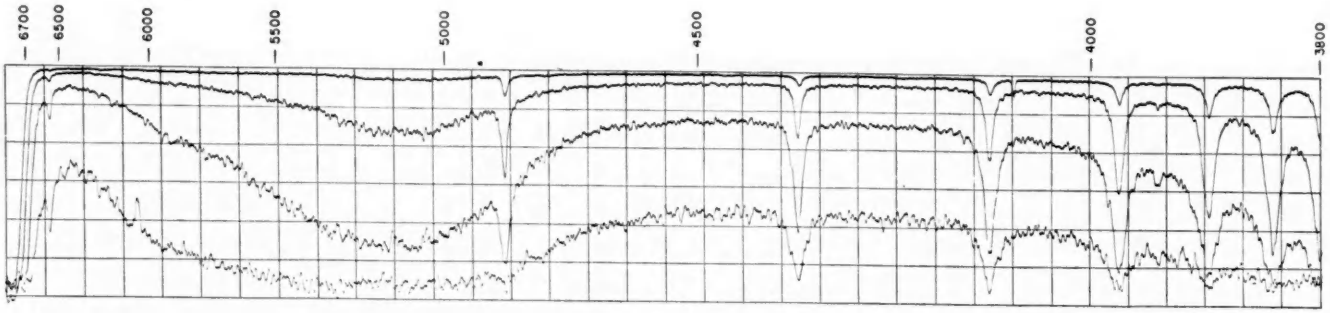

FIG. 1 — ζ Aquilae, spectral type B9n. Relative intensities: 100, 36, 14.5, 6.3. Spectrograph *f*, Agfa Supersensitive Panchromatic film

TABLE 1

OBSERVATIONS OF SUPERNOVA IC 4182

G.M.T.	Plate No.	Exposure	Instrument	Plate	Obs.*	Notes†	Fig. No.
1937		min.					
Aug. 30.130	D983	1	*a*	Eastman 33	H	1	2
30.133		2				1	3
30.136		4				1	4
30.140		3				2, 3	5
30.165	D984	10	*a*	Eastman Proc.	H	1	6
30.168		5					7
31.144	IS142	30	*f*	Agfa Supersens. Panchr.	M	1	8
31.156	C7115	76	*i*	Eastman 33	Me	1, 4	.....
Sept. 1.138	IS147	30	*f*	Agfa Supersens. Panchr.	M	1	9
5.137	IS152	40	*f*			1	10
8.135	IS157	42	*f*			5	.....
9.132	IS158	52	*f*			1	11
10.121	IS159	5	*j*	Imp. Ecl. Soft	M	1	.....
10.133		25					
11.126	IS160	40	*f*	Agfa Supersens. Panchr.	M	1	12
15.122	IS161	35	*f*			1	13
23.124	IS165	54	*e*			5	.....
Oct. 2.107	IS173	32	*e*			2	14
28.521	IS182	80	*e*			2	15
Nov. 3.522	D1004	20	*a*	Imp. Ecl. Soft	H	1	16
4.534	D1008	45	*b*	Eastman IF	M	2	....
9.476	D1011	222	*c*	Eastman *Ha*	M	2	17
Dec. 11.471	D1015	5	*a*	Imp. Ecl. Soft	H	1	...
11.494	D1016	20					...
13.535	IS199	120	*f*	Agfa Supersens. Panchr.	M	4, 5	...
17.534	IS200	120					18
1938							
Jan. 5.447	IS206	240	*f*	Agfa Supersens. Panchr.	M	2	19
27.436	IS219	360					20
Feb. 22.383	D1021	451	*c*	Eastman *Ha*	M	2	21
Mar. 24.328	D1022	640					22
Apr. 3.343	D1037	492	*b*	Eastman *Ha*	M	2	23
4.327		+525					
May 24.334	D1038	380	*d*	Agfa Superpan Press	M	2	24
25.340	D1039	390					...
June 28.260	D1040	241	*d*	Agfa Superpan Press	M	2	25
July 1.263		+195					
24.223	D1042	140	*d*	Agfa Superpan Press	M	2	26
25.220		+130					
27.218		+135					
28.216		+130					
29.215		+125					

* H, Humason; M, Minkowski; Me, Merrill.

† 1, wide; 2, narrow; 3, overexposed; 4, faint; 5, faint owing to bad seeing.

spectrograph to obtain spectrograms made with equal exposures to different intensities of light. Spectrograms of ζ Aquilae, visual magnitude 3.02 and spectral class B9n, were taken in this way on the same film as the supernova spectrum, to provide a calibration. Figure 1 shows tracings of such a set of spectra on Agfa Supersensitive Panchromatic film. The color sensitivity and the gradation are not very different from those of the other panchromatic emulsions which have been used. Figure 1 provides, therefore, a general idea of the distortion of the relative intensities caused by the properties of the photographic material.

THE SUPERNOVA IN IC 4182

Supernova IC 4182 reached its maximum on August 22, 1937. The first spectrograms were obtained on August 30 (all dates have been reduced to G.M.T.), the night following the announcement of the discovery by Zwicky. Because of the brightness and the high declination of the supernova, the observations could be continued, practically without interruption, through the conjunction with the sun in 1937, until July, 1938. Whether it will be possible to resume the observations after the conjunction with the sun in 1938 will depend on the development of the light-curve. Table 1 contains self-explanatory data relating to the spectrograms and, in the last column, the number of the figure in which the corresponding tracing is reproduced.

The nebular red shift for IC 4182 is unknown. As a dwarf system, it may be expected to have a value somewhere between 0 and +1500 km/sec.

The journal of comment on the individual spectrograms follows.

August 30, 1937, 8 Days after Maximum (Figs. 2–7)

The six spectrograms seem to indicate very rapid changes in the spectrum. Had they been obtained with the same exposure time and on the same kind of plate, there would be no doubt about the reality of these changes. The wave length at which the maximum of the most intense band appears is most likely affected by the differences in exposure time and in spectral sensitivity of the two plates, and its increase of about 100 A on the narrow and overexposed fourth spectrum is not conclusive proof of a real change. However, such variations as the later disappearance of the edge, which shows up clearly at λ 4025 in Figure 3, or the appearance of a fairly well-defined maximum at λ 4210, Figure 6, cannot

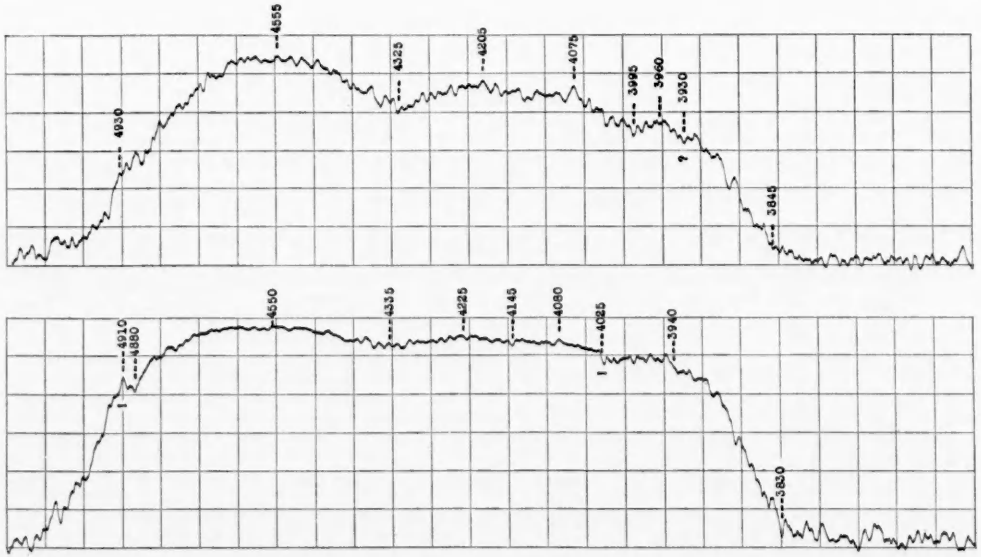

FIG. 2 (*above*).—IC 4182. August 30.130, 1937, 8 days after maximum. Spectrograph *a*, Eastman 33

FIG. 3 (*below*).—IC 4182. August 30.133, 1937, 8 days after maximum. Spectrograph *a*, Eastman 33

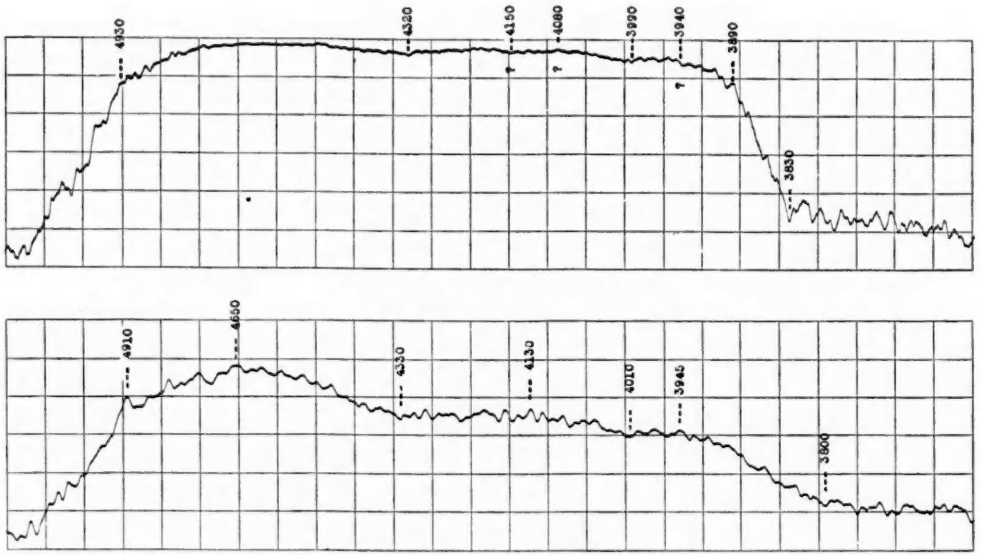

FIG. 4 (*above*).—IC 4182. August 30.136, 1937, 8 days after maximum. Spectrograph *a*, Eastman 33

FIG. 5 (*below*).—IC 4182. August 30.140, 1937, 8 days after maximum. Spectrograph *a*, Eastman 33

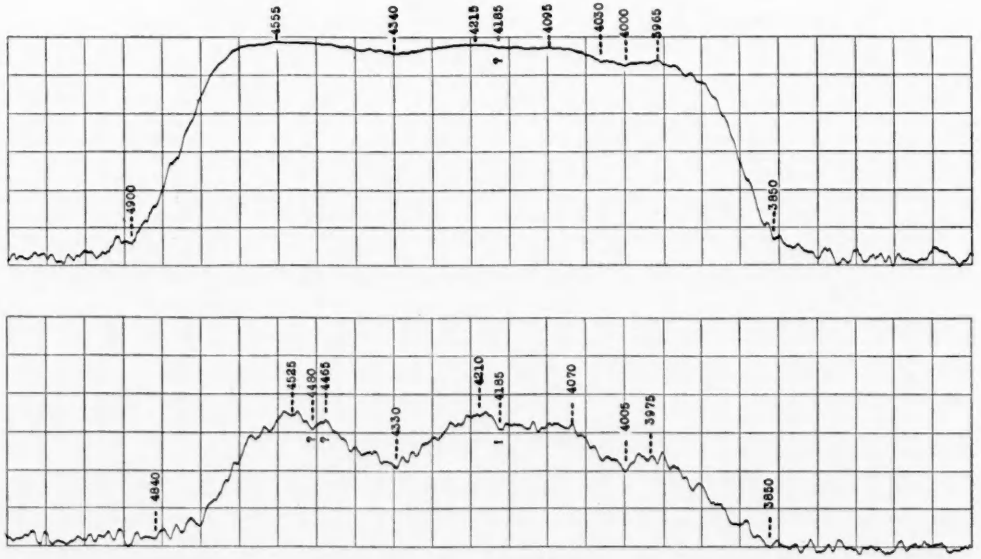

FIG. 6 (*above*).—IC 4182. August 30.165, 1937, 8 days after maximum. Spectrograph *a*, Eastman Process.

FIG. 7 (*below*).—IC 4182. August 30.168, 1937, 8 days after maximum. Spectrograph *a*, Eastman Process.

be so easily explained as spurious. The evidence is not at all conclusive, but it is strong enough to make it desirable to search for rapid changes in the spectra of future supernovae.

August 31, 1937, 9 Days after Maximum (Fig. 8)

The blue part of the spectrum has not changed much. Both plates obtained on this date agree perfectly in such details as the inflections at λλ 4885, 4485, and 4400. For shorter wave lengths, the record obtained with spectrograph *h* is too faint to be useful, owing to absorption in this spectrograph. Whether the spectrum ends in the red before the limit of the plate has been reached is hard to decide. The narrowest band, at λ 5425, has a width of about 100 A. The bands in the red are not flat-topped, as they appear on the tracings. They are greatly distorted by the varying color sensitivity of the photographic emulsion, as may be seen from Figure 1. The magnitude of these distortions can easily be recognized by a comparison with the tracings of spectra obtained by Popper[1] at the Lick Observatory.

September 1, 1937, 10 Days after Maximum (Fig. 9)

Only minor changes are noticeable. The band λλ 6160–5700 begins to break up. At λ 5700 a faint minimum has developed. The minimum at λ 5470 has disappeared. Distinct maxima have appeared at λλ 4910 and 4780. The inflections between λλ 4500 and 4350 have disappeared. The narrowest band, at λ 4910, has a width of the order of 100 A.

September 5, 1937, 14 Days after Maximum (Fig. 10)

The spectrum has changed considerably. The first band in the red begins to show structure; the step at λ 6325 is clearly visible on the plate. The band λλ 6160–5700 has divided into a relatively narrow band λλ 6150–6010 and a wider band λλ 6010–5705. This last band, or at least parts of it, is a permanent feature from now on for a considerable time. Between λλ 5700 and 5100 the spectrum has changed radically. The minimum at λ 5705 has become pronounced. The band λλ 5700–5495 has disappeared; and a very wide band, λλ 5705–5120, has been formed, which is possibly a blend of the band λλ 5290–5010 of September 1 (Fig. 9) and a band at about λ 5500, which emerges clearly on September 15 (Fig. 13). Details of the band λλ 5010–4390 have changed; most noticeable is the appearance of a shoulder at λ 4715 and the decrease in width of the flat top of the maximum. Instead of the maximum at λ 4195, a band with a flat top from λ 4320 to λ 4190 has appeared; this probably indicates the emergence of a maximum which appears at λ 4320 on September 9 (Fig. 11).

September 8, 1937, 17 Days after Maximum

The spectrogram shows only the strongest bands, without noticeable differences from those of September 9.

[1] *Pub. A.S.P.*, **49**, 283, 1937.

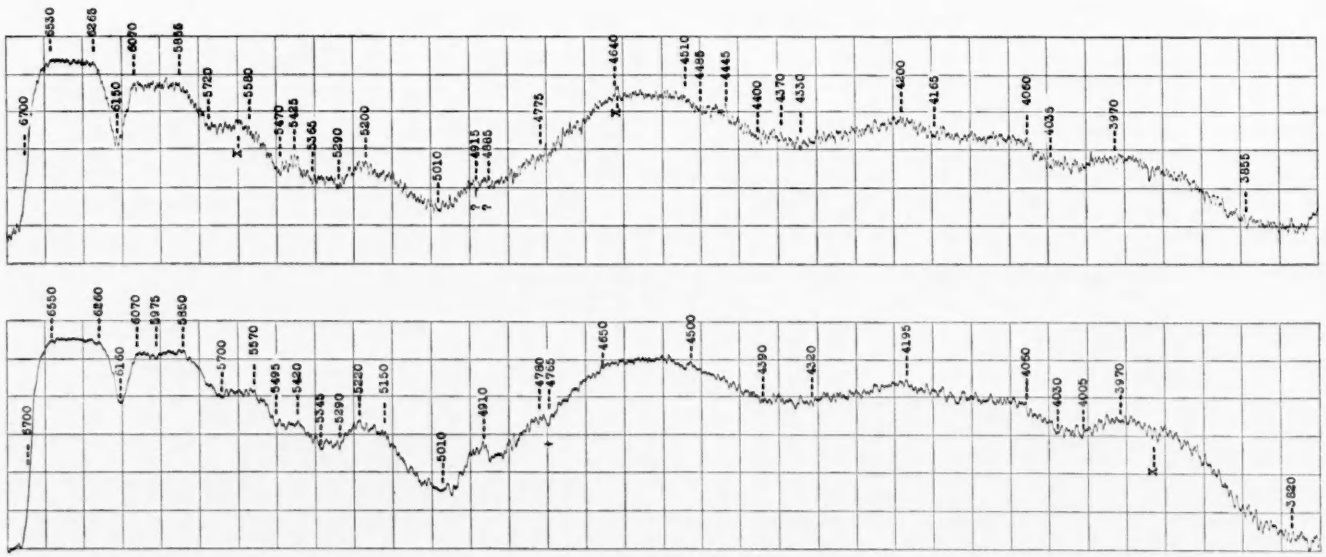

FIG. 8 (*above*).—IC 4182. August 31.144, 1937, 9 days after maximum. Spectrograph *f*, Agfa Supersensitive Panchromatic

FIG. 9 (*below*).—IC 4182. September 1.138, 1937, 10 days after maximum. Spectrograph *f*, Agfa Supersensitive Panchromatic

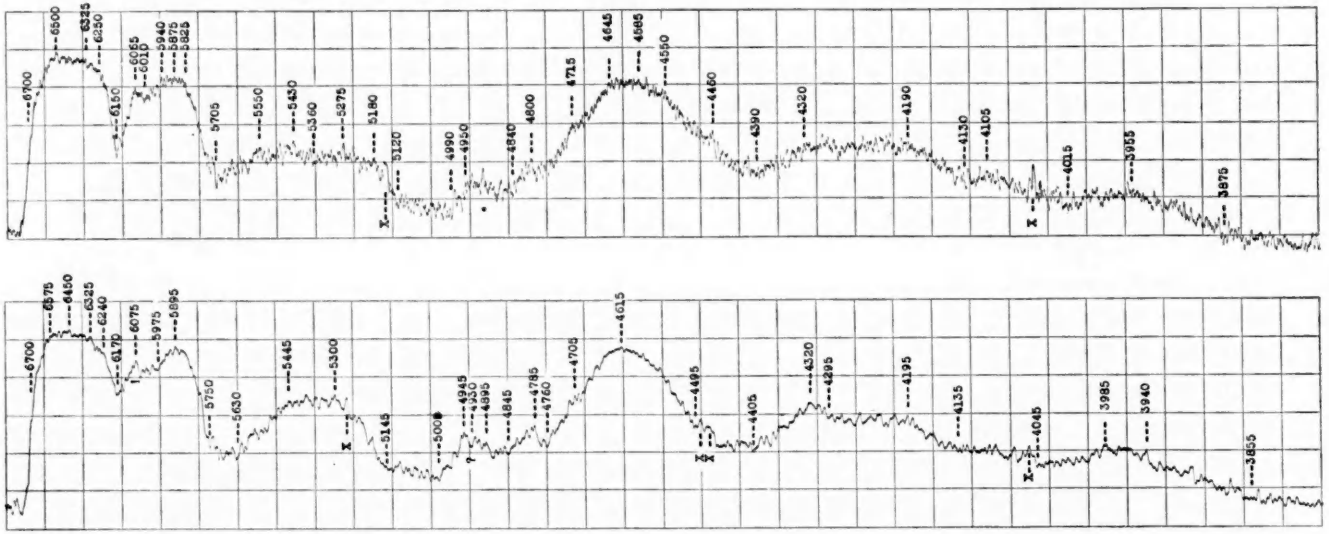

FIG. 10 (*above*).—IC 4182. September 5.137, 1937, 14 days after maximum. Spectrograph *f*, Agfa Supersensitive Panchromatic

FIG. 11 (*below*).—IC 4182. September 9.132, 1937, 18 days after maximum. Spectrograph *f*, Agfa Supersensitive Panchromatic

September 9, 1937, 18 Days after Maximum (Fig. 11)

The structure of the first band in the red has become more pronounced. The narrow band at λ 6075 and the wider one at λ 5895, which have developed from the band λλ 6150–5705, are quite distinct. The band λλ 5290–5010 of September 1 has apparently faded out, while a strong band with a flat top has emerged between λ 5630 and λ 5145. The flat top of the maximum at λ 4615 has disappeared. The maximum at λ 4320, whose appearance was first noted on September 5 (Fig. 10), has become clearly visible. The presence of the former maximum at λ 4195 is still indicated by a shoulder. The contour which has been formed in the blue part of the spectrum below λ 5000 shows no essential changes from now on, but the wave length at which the pattern appears varies.

September 10, 1937, 19 Days after Maximum

This spectrogram is so much overexposed that all details in the part of the spectrum observed with glass prisms have become almost entirely unrecognizable. A maximum at about λ 3700 can still be seen; this may be identical with the maximum at λ 3680 observed by Popper. Beyond λ 3600 the spectrum fades out rapidly without showing any pronounced maximum farther in the ultraviolet.

September 11, 1937, 20 Days after Maximum (Fig. 12)

The structure of the first band in the red, which has increased in intensity relative to the blue band and is overexposed, has apparently disappeared again. The band λλ 5710–5140 shows a minimum at λ 5340. The strongest band in the blue, with a maximum at about λ 4640, shows well-marked details which seem to indicate a band at λ 4530. On this spectrogram several narrow minima can be seen which suggest narrow absorption lines. Three of these are visible on the tracing at λλ 6040, 4870, and 4215. Two more, at λ 5230 and λ 4385, are obscured by the fluctuations of the tracings, which are due to the graininess of the plate. It seems impossible to decide whether these minima are spurious or not. At the most, they may be ephemeral details.

September 15, 1937, 24 Days after Maximum (Fig. 13)

The red again clearly shows structure. Its intensity, as well as that of all bands to the red of λ 5700, has increased considerably relative to the blue band. The band λλ 5700–5275 has developed from the band λλ 5710–5140 of September 11 (Fig. 12), apparently as a consequence of the fading-out of a band near λ 5300. The band at λ 4635 is distinctly unsymmetrical. The record below λ 4500 is too faint to decide with certainty whether the apparent differences from the spectrum of September 11 are real or not.

September 23, 1937, 32 Days after Maximum

On this underexposed spectrogram only the red band appears with sufficient intensity. It has its flat maximum between λ 6500 and λ 6420; its shape seems

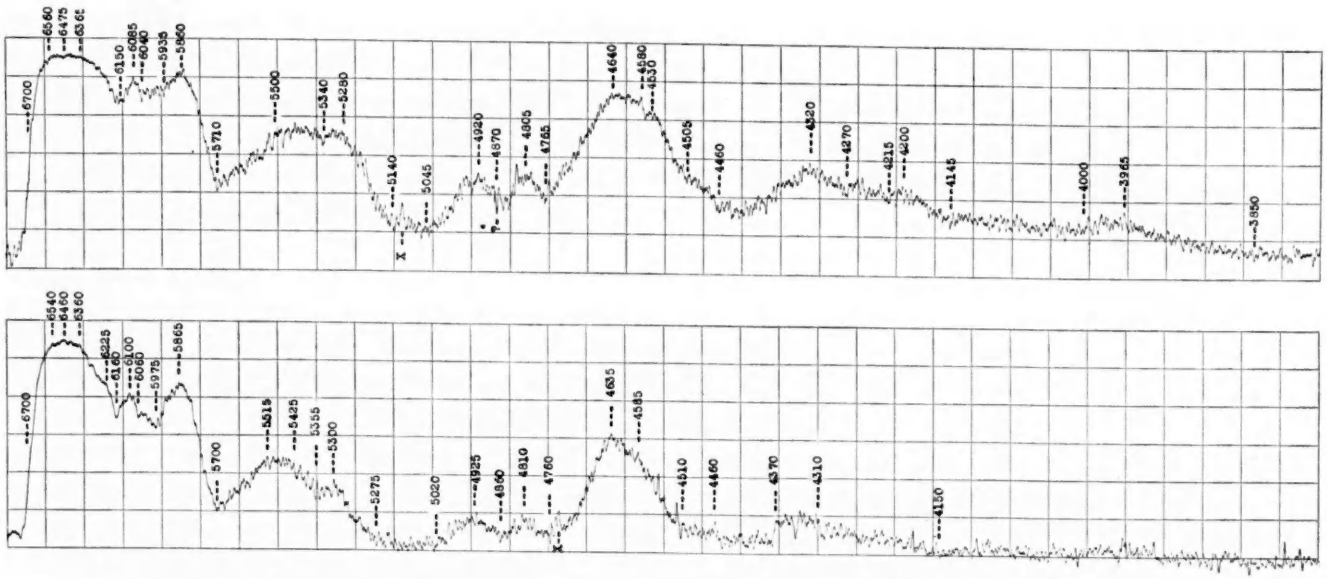

FIG. 12 (*above*).—IC 4182. September 11.126, 1937, 20 days after maximum. Spectrograph *f*, Agfa Supersensitive Panchromatic

FIG. 13 (*below*).—IC 4182. September 15.122, 1937, 24 days after maximum. Spectrograph *f*, Agfa Supersensitive Panchromatic

to be similar to that on September 15 (Fig. 13). The minimum at λ 6160 and the maximum at λ 6100 of September 15 are not visible. The bands λλ 5975–5700 and λλ 5700–5275 can be seen, but hardly measured; and the band at λ 4635 is barely noticeable.

October 2, 1937, 41 Days after Maximum (Fig. 14)

The bands in the red have become very intense; they have changed considerably. The first maximum has become narrower and shows some signs of structure on its red edge. A minimum at λ 6300 has been formed. The minimum at λ 6160 of September 15 (Fig. 13), which was most likely absent already on September 23, has disappeared, and a band between λ 6300 and λ 6035 has emerged. The band λλ 6035–5715 seems to show structure. The next band, which has a fairly well-defined maximum at λ 5565, seems to be the product of the continued activity between λ 5700 and λ 5100 since September 5. The blue band, which again shows structure, is recorded too faintly to decide whether its top is really flat.

October 28, 1937, 67 Days after Maximum (Fig. 15)

The intensity of the red part of the spectrum has decreased relative to that of the blue part. The minimum at λ 6325 has become well developed, and the band λλ 6325–6030 has a well-defined maximum at λ 6210 and a secondary maximum at λ 6095. The transformations between λ 5700 and λ 5100 continue. The maximum at λ 5530 may be identical with the maximum at λ 5565 of October 2 (Fig. 14). On its blue edge a new maximum λλ 5425–5090 has appeared, which seems to show some structure. The blue band at λ 4640 has apparently become much wider; its shape has reverted almost to that of September 5 (Fig. 10).

November 3, 1937, 73 Days after Maximum (Fig. 16)

This is the first well-exposed spectrogram of the blue part of the spectrum since that of September 11. The contour of the spectrum differs at the most in minor details, but the position of the bands has changed. The maxima which on September 11 (Fig. 12) appeared at λλ 4920, 4805, 4640–4580, 4320, 4200, and 3965 now appear at λλ 4950, 4855, 4630, 4340, 4240, and 4010, respectively.

November 4, 1937, 74 Days after Maximum

This exposure was made on an Eastman IF plate whose sensitivity in the red is smaller than that of the Agfa Supersensitive Panchromatic film previously used. Consequently, the record of the red region is faint. The next spectrogram was obtained only 5 days later, on a new plate, Eastman *Hα*, special emulsion 73213, which had just arrived. This emulsion has a color sensitivity very similar to that of the film but is faster if hypersensitized with ammonia. Since the blue portion shown on November 4 is the same as that of November 3, and the red part does not differ from that of November 9, the tracing for November 4 has not been reproduced.

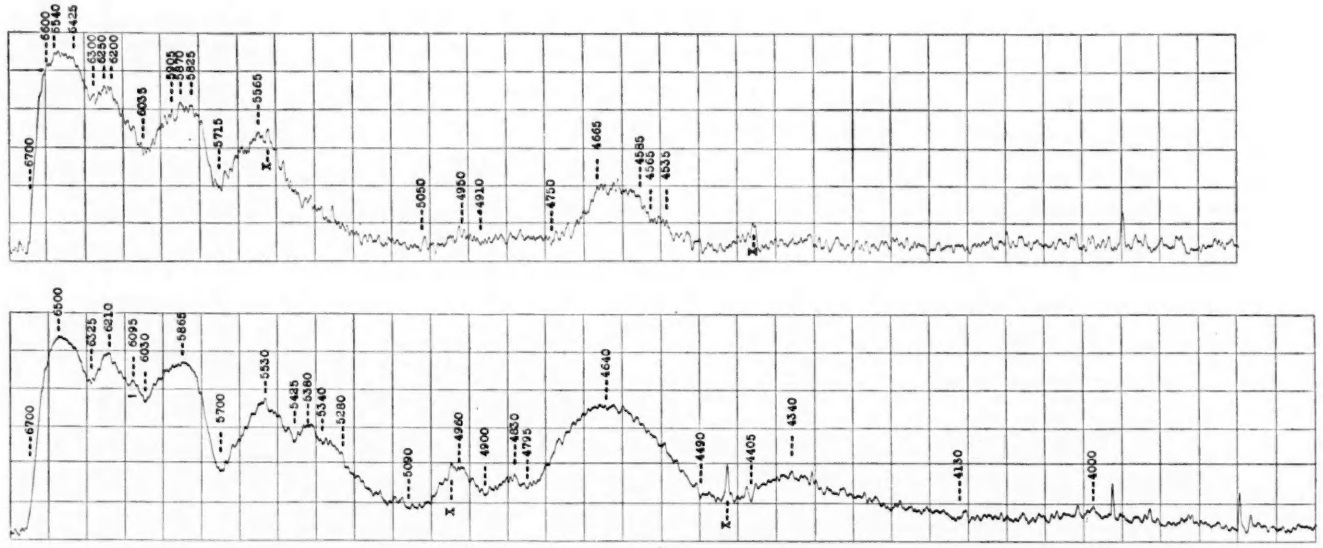

FIG. 14 (*above*).—IC 4182. October 2.107, 1937, 41 days after maximum. Spectrograph *f*, Agfa Supersensitive Panchromatic

FIG. 15 (*below*).—IC 4182. October 28.521, 1937, 67 days after maximum. Spectrograph *f*, Agfa Supersensitive Panchromatic

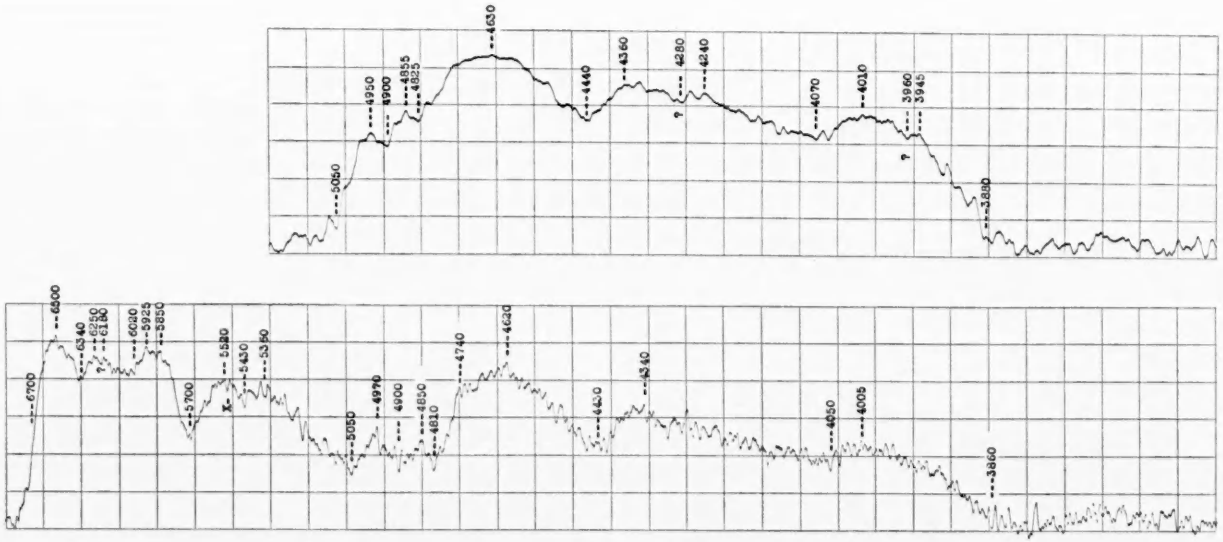

FIG. 16 (*above*).—IC 4182. November 3.522, 1937, 73 days after maximum. Spectrograph *a*, Imperial Eclipse Soft

FIG. 17 (*below*).—IC 4182. November 9.476, 1937, 79 days after maximum. Spectrograph *c*, Eastman *Hα* Special

November 9, 1937, 79 Days after Maximum (Fig. 17)

The relative intensities of the red and the blue parts of the spectrum are now again about the same as in the beginning. No pronounced changes have occurred since October 28 (Fig. 15). The maximum of the band λλ 6340–6020 has become less distinct, and the maximum at λ 5360 has reached about the same intensity as the maximum at λ 5520. The shape of the band λλ 4810–4430 has changed slightly since October 28, and the spectrum toward shorter wave lengths appears stronger; but the latter is most likely due to the use of different spectrographs.

December 11, 1937, 111 Days after Maximum

The spectrograms do not differ from the blue part of the record for December 17 (Fig. 18). The tracings are therefore not reproduced.

December 13, 1937, 113 Days after Maximum

The spectrogram, underexposed owing to bad seeing, shows only traces of the strongest bands.

December 17, 1937, 117 Days after Maximum (Fig. 18)

The intensity of the red part of the spectrum continues to decrease. The first band, λλ 6600–6300, has become narrower; the next, λλ 6300–6035, has reverted almost exactly to the shape on October 28 (Fig. 15); the maximum of the next band, at λ 5865, is apparently better defined; and λλ 5580–5425 is now fainter than the following band, which has developed a flat top from λ 5390 to λ 5310. No distinct maxima appear between λ 5070 and λ 4820; otherwise the blue part appears unchanged in outline, but the wave lengths of the maxima have continued to increase. The fog of the film is slightly higher at the violet end; the record of the spectrum ends, as usual, at about λ 3850.

January 5, 1938, 136 Days after Maximum (Fig. 19)

The first band, λλ 6650–6320, has decreased in intensity somewhat more rapidly than λλ 6320–6050, which has changed its structure slightly, and λλ 6050–5680. The minimum at λ 5680 is more pronounced. The maximum at λ 5495, presumably identical with λ 5510 of December 17 (Fig. 18), has not changed. The next band, which has a well-defined maximum at λ 5325, shows a very conspicuous increase in strength. The development of this band since October 2 (Fig. 14) seems to indicate that it is composed of two bands, one which appeared at λ 5380 on October 28 (Fig. 15) and one first suggested on December 17 (Fig. 18) by the formation of the flat top λλ 5390–5310; the latter has now become considerably stronger. Between λ 5080 and λ 4840 two maxima have reappeared at increased wave lengths. The maximum at λ 4985 is very strong. The strong maximum λλ 4840–4425 shows only minor changes, if any at all. From here on toward the violet end of the spectrum all maxima and minima appear more pronounced, a circumstance perhaps not wholly due to the stronger record obtained on this date.

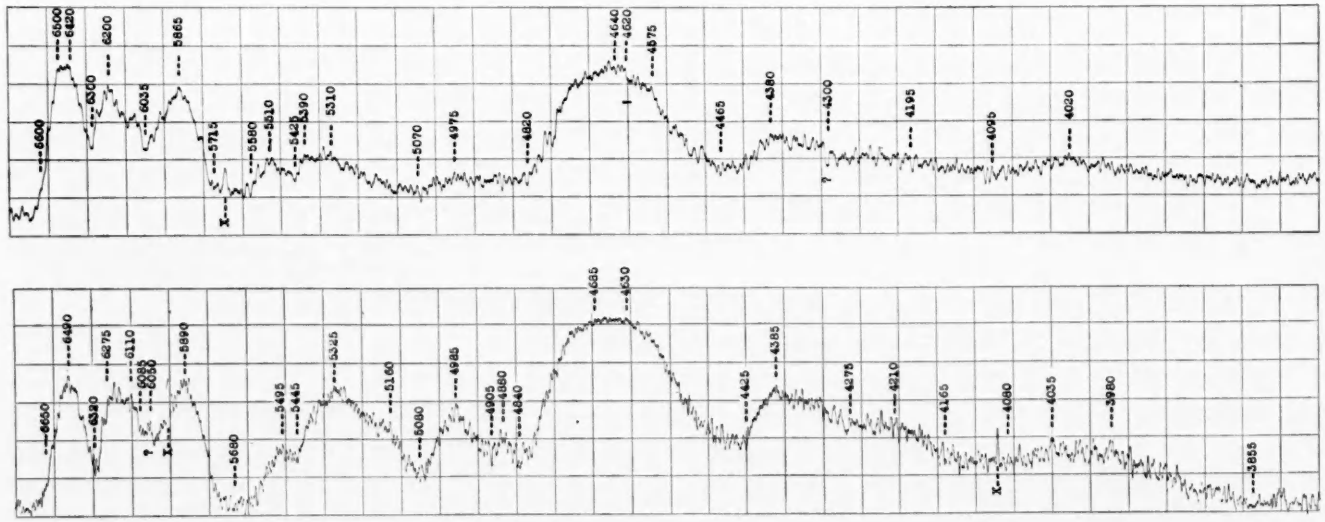

FIG. 18 (*above*).—IC 4182. December 17.534, 1937, 117 days after maximum. Spectrograph *f*, Agfa Supersensitive Panchromatic

FIG. 19 (*below*).—IC 4182. January 5.447, 1938, 136 days after maximum. Spectrograph *f*, Agfa Supersensitive Panchromatic

January 27, 1938, 158 Days after Maximum (Fig. 20)

The part of the spectrum from the red end to λ 5090 has become much fainter. All the bands present on January 5 (Fig. 19) can be seen, apparently without other change than that of intensity. The band λλ 5090–4905 may be fainter; its maximum appears flattened. The rest of the spectrum shows no changes in outline which cannot be ascribed to difference in the strength of the records.

February 22, 1938, 184 Days after Maximum (Fig. 21)

The red part of the spectrum has increased considerably in intensity. The contour of the blue region has not changed much above λ 4200, where a pronounced step has appeared. Another step appears at λ 4020, followed by a maximum at about λ 3960. The most essential and surprising change is the appearance of two narrow bands at λ 6296 and λ 6360. The stronger, λ 6296, could be measured on the plate with an error of ± 2 A.

March 24, 1938, 214 Days after Maximum (Fig. 22)

The intensity of the spectrum above λ 5700 begins again to decrease. The two narrow bands, however, have increased in intensity; both are now measurable on the plate. They appear shifted toward the red. Their measured width of about 40 A is only slightly greater than that of the lines of the comparison spectrum and is therefore not unaffected by the resolving-power of the spectrograph and the photographic plate, which for monochromatic lines in this part of the spectrum gives a width corresponding to about 25 A. The general structure of the spectrum shows no changes. The minimum at λ 4005, whose reality is not beyond doubt, may be a remnant of the step at λ 4020 on February 22 (Fig. 21).

April 3, 1938, 225 Days after Maximum (Fig. 23)

Only minor changes have occurred. The narrow bands appear slightly stronger and shifted toward the violet, to the same position as on February 22 (Fig. 21). From this plate on, the auroral [*O* I] line of the sky spectrum at λ 6300 appears faintly on both sides of the supernova spectrum. The plates themselves show clearly that the stronger of the two bands changes its position relative to this line. The step which appeared at about λ 4200 on February 22 and March 24 (Fig. 22) has been replaced by a more gradual decrease in intensity from λ 4275 to λ 4130.

May 24 and May 25, 1938, 275 and 276 Days after Maximum (Fig. 24)

With the exception of the two narrow bands, the red part of the spectrum has almost disappeared. Only the stronger of the two bands could be measured on these plates; the fainter is still visible on the tracing. No other changes are noticeable. The two plates agree in the inconspicuous details of the band λλ 4520–4125; both show the faint minimum at λ 4355 and the faint maximum at λ 4300.

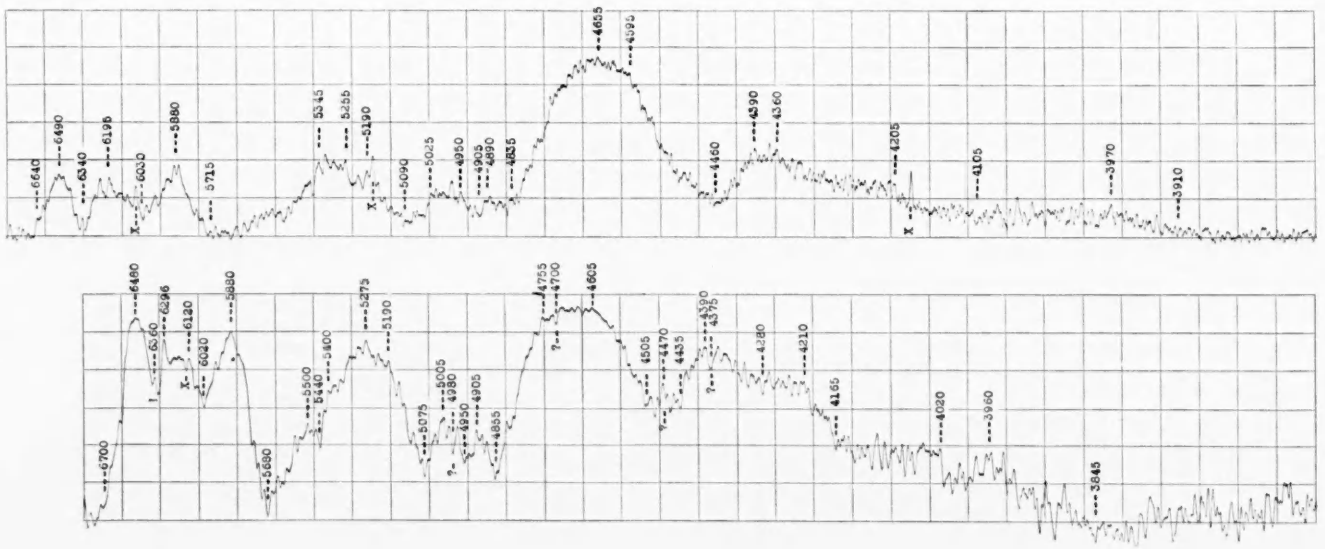

FIG. 20 (*above*).—IC 4182. January 27.436, 1938, 158 days after maximum. Spectrograph *f*, Agfa Supersensitive Panchromatic

FIG. 21 (*below*).—IC 4182. February 22.383, 1938, 184 days after maximum. Spectrograph *c*, Eastman $H\alpha$ Special

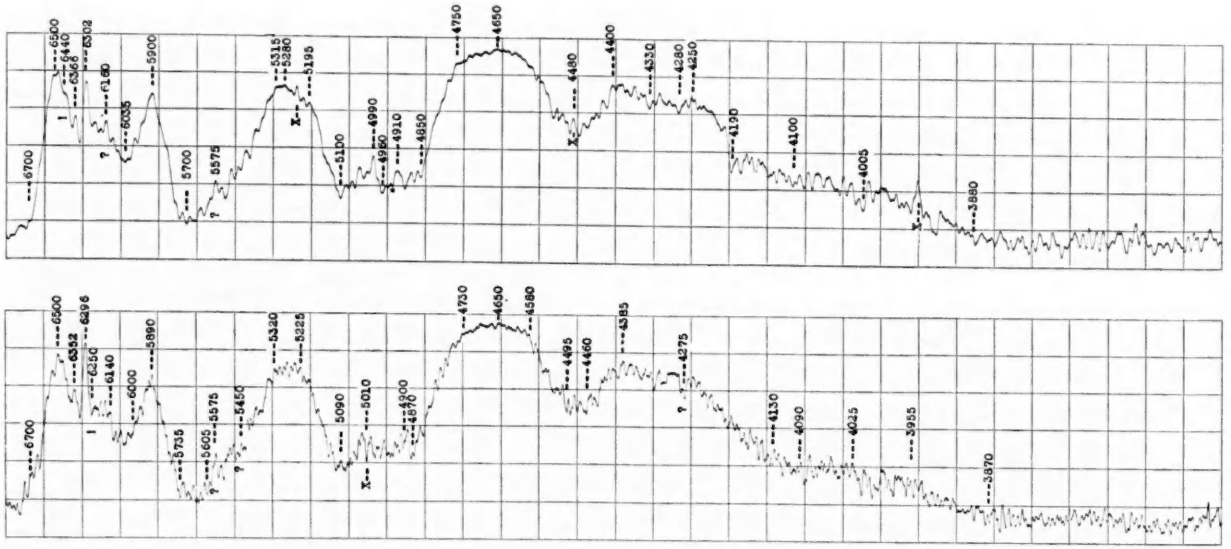

FIG. 22 (*above*).—IC 4182. March 24·334, 1938, 214 days after maximum. Spectrograph *c*, Eastman *Hα* Special

FIG. 23 (*below*).—IC 4182. April 3–4, 1938, 225 days after maximum. Spectrograph *b*, Eastman *Hα* Special

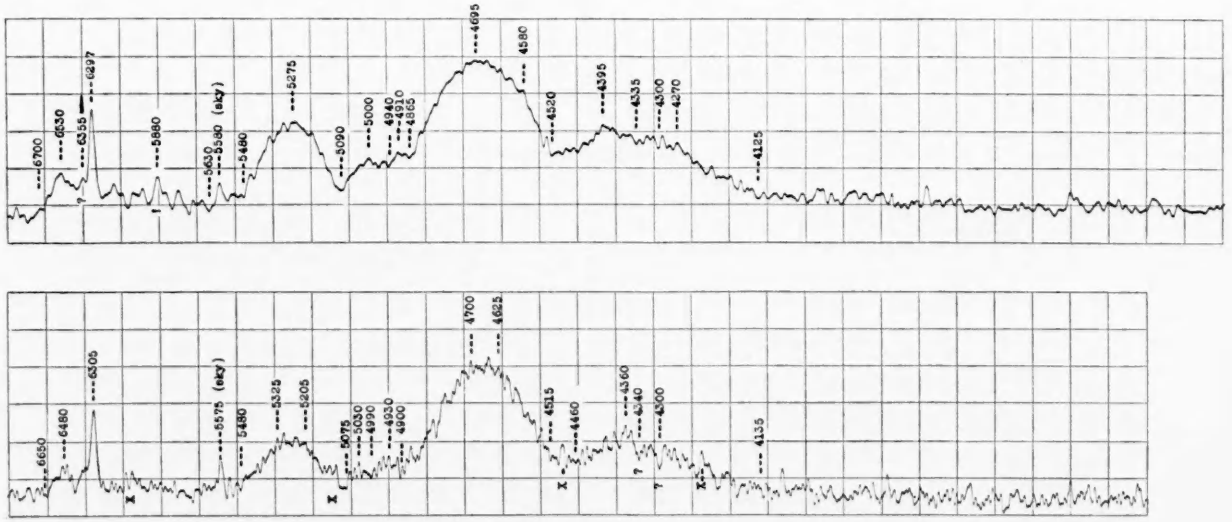

FIG. 24 (*above*).—IC 4182. May 24.334, 1938, 275 days after maximum. Spectrograph *d*, Agfa Superpan Press

FIG. 25 (*below*).—IC 4182. June 28–July 1, 1938, 312 days after maximum. Spectrograph *d*, Agfa Superpan Press

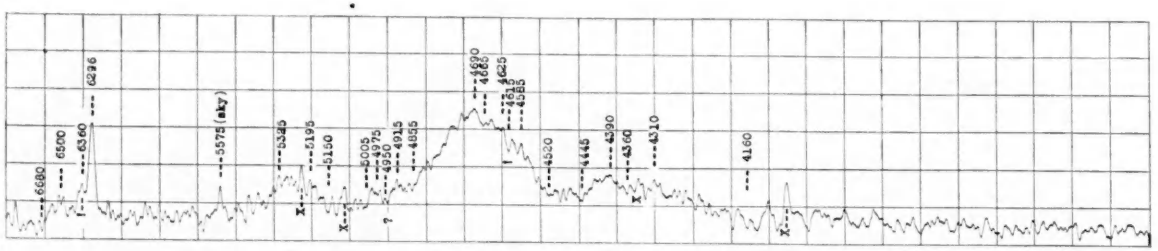

FIG. 26.—IC 4182. July 24–29, 1938, 339 days after maximum. Spectrograph *d*, Agfa Superpan Press

June 28–July 1, 1938, 312 (Mean) Days after Maximum (Fig. 25)

No changes of any importance are noticeable. The record is fainter than that of May 24 and May 25 (Fig. 24); consequently, the graininess of the film plays a more important role and makes it more difficult to decide on the reality of details.

July 24–July 29, 1938, 339 (Mean) Days after Maximum (Fig. 26)

The two narrow bands in the red have increased slightly in intensity; the fainter is again visible but is not measurable on the plate. The band λλ 4855–4520 once more reveals structure.

THE SUPERNOVA IN NGC 1003

Supernova NGC 1003 reached its maximum on September 14, 1937. The earliest spectrograms were obtained on September 12 and

TABLE 2

OBSERVATIONS OF SUPERNOVA NGC 1003

G.M.T.	Plate No.	Exposure	Instrument	Plate	Obs.*	Notes†	Fig. No.
1937		min.					
Sept. 12.444	D986	10	*a*	Imp. Ecl. Soft	H	1	27
12.473	D987	25				1	28
12.485		5				2, 3	29
15.298	IS163	120	*f*	Agfa Supersens. Panchr.	M	5	.....
15.428	IS164	260				4	30
16.413	γ21217	346	*g*	Imp. Ecl. Soft	A	4, 6	.....
17.419	γ21220	202	*h*		J	2	31
23.378	IS166	435	*e*	Agfa Supersens. Panchr.	M	1	32
Oct. 3.403	D991	26	*a*	Imp. Ecl. Soft	H	1	.....
6.512	D996	38				2	33
13.401	IS180	330	*e*	Agfa Supersens. Panchr.	M	6	34
28.290	IS181	470				1	35
Nov. 4.125	D1005	63	*a*	Imp. Ecl. Soft	H	6	.....
4.216	D1006	120				2	36
Dec. 7.726	D1013	80				2	37
Jan. 7.18	D1018	72				2, 4	.....

* H, Humason; M, Minkowski; A, Adams; J, Joy.

† 1, wide; 2, narrow; 3, overexposed; 4, faint; 5, very faint; 6, slightly widened.

give the first information on the spectrum of a supernova shortly before its maximum. The observations were continued until January 6, 1938. Table 2 contains the data relating to the spectrograms.

The nebular red shift for NGC 1003 is +475 km/sec.[2] The wave lengths in the spectrum of the supernova are probably affected by

[2] M. L. Humason, *Pub. A.S.P.*, **50**, 55, 1938.

rotation of the system, as well as by the general red shift. The wave lengths given are uncorrected values. The journal record follows.

September 12, 1937, About 2 Days before Maximum (Figs. 27–29)

The differences in exposure of the three spectrograms obtained on this date may explain the apparent differences in the spectra, which seem to indicate very rapid changes. The second spectrogram is much stronger than the first; the third is narrow and overexposed. The first shows a number of details which look like absorption lines; they are measurable on the plate and can be recognized on the tracings. Wave lengths for these details, measured by Humason, are given in Figure 27. The minima to which they correspond are indicated by dotted lines, while wave lengths read from the tracings are marked, as usual, by dashed lines. Most of these details cannot be seen on the other spectrograms. Whether any of these narrow minima are real is a difficult question. Some (e.g., λ 4646 and λ 4380) appear on the tracing so indistinctly that their spurious character is almost certain; others (e.g., λ 4450 and λ 4294) may easily be only the shallow minima which appear on the two other spectrograms; but there remain several which are so easily seen both on the plate and on the tracing that the possibility of their being absorption lines cannot be denied. Whether it is possible to identify these details and thereby obtain additional evidence for their reality will be discussed later. The third spectrogram shows a step between λ 4715 and λ 4680 and a flat top between λ 4680 and λ 4505, which cannot be seen on the other two spectrograms.

September 15, 1937, About 1 Day after Maximum (Fig. 30)

The two spectrograms obtained on this date show only faint records. The red band λλ 6700–6160 is by far the strongest feature of the spectrum. The blue region seems to show the greatest similarity to the last of the three spectra of September 12 (Fig. 29). The band λλ 4650–4490, however, is narrower than the band λλ 4680–4505 of September 12. The other differences may be due mainly, or even entirely, to the great differences in the strength of the exposures.

September 16, 1937, About 2 Days after Maximum

The record on the plate is faint, and the tracing is therefore not reproduced. This spectrogram of the region below λ 5000 is almost identical with that of the day before. It shows a band with a flat top from λ 4655 to λ 4490, a minimum at about λ 4440, a maximum at about λ 4405, followed by a wide and shallow minimum near λ 4270, and an indistinct maximum at approximately λ 4190. Besides, this plate shows a drop of intensity from λ 4095 to λ 4055, where the record ends.

September 17, 1937, About 3 Days after Maximum (Fig. 31)

The flat top of the main blue band has contracted to λλ 4630–4515. The minimum at λ 4315 and the maximum at λ 4220 seem to correspond to the minimum at λ 4270 and to the maximum at λ 4175 of September 15 (Fig. 30).

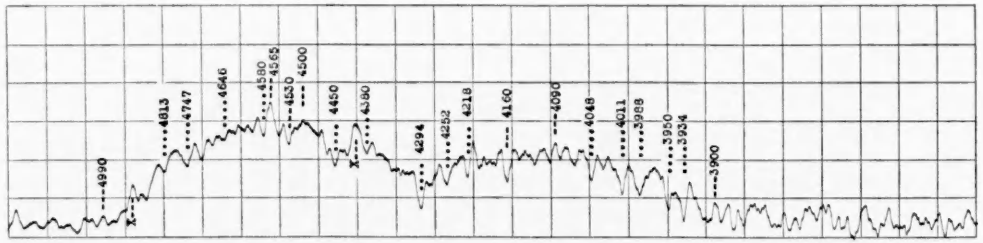

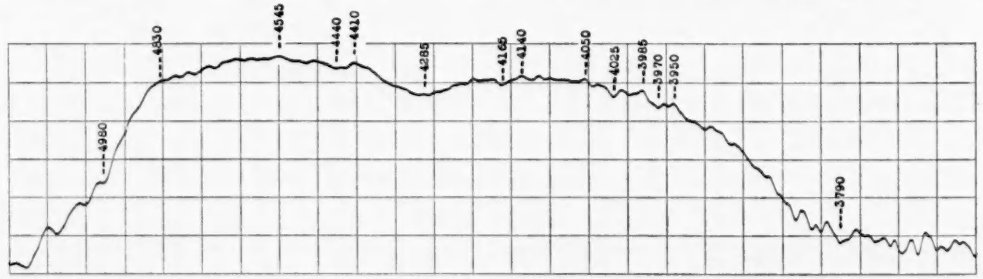

FIG. 27 (*above*).—NGC 1003. September 12.444, 1937, 2 days before maximum. Spectrograph *a*, Imperial Eclipse Soft.

FIG. 28 (*below*).—NGC 1003. September 12.473, 1937, 2 days before maximum. Spectrograph *a*, Imperial Eclipse Soft.

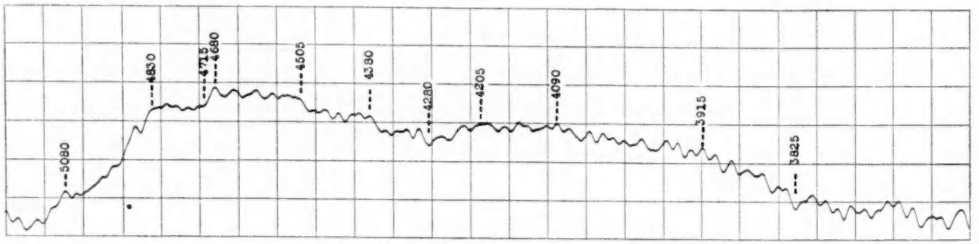

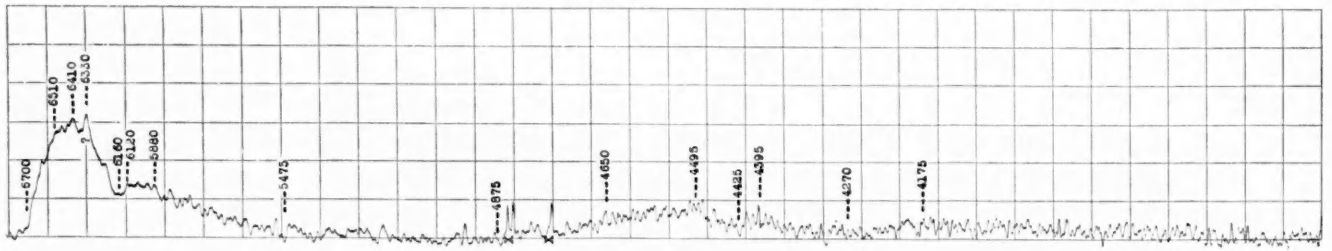

FIG. 29 (*above*).—NGC 1003. September 12.485, 1937, 2 days before maximum. Spectrograph *a*, Imperial Eclipse Soft

FIG. 30 (*below*).—NGC 1003. September 15.428, 1937, 1 day after maximum. Spectrograph *f*, Agfa Supersensitive Panchromatic

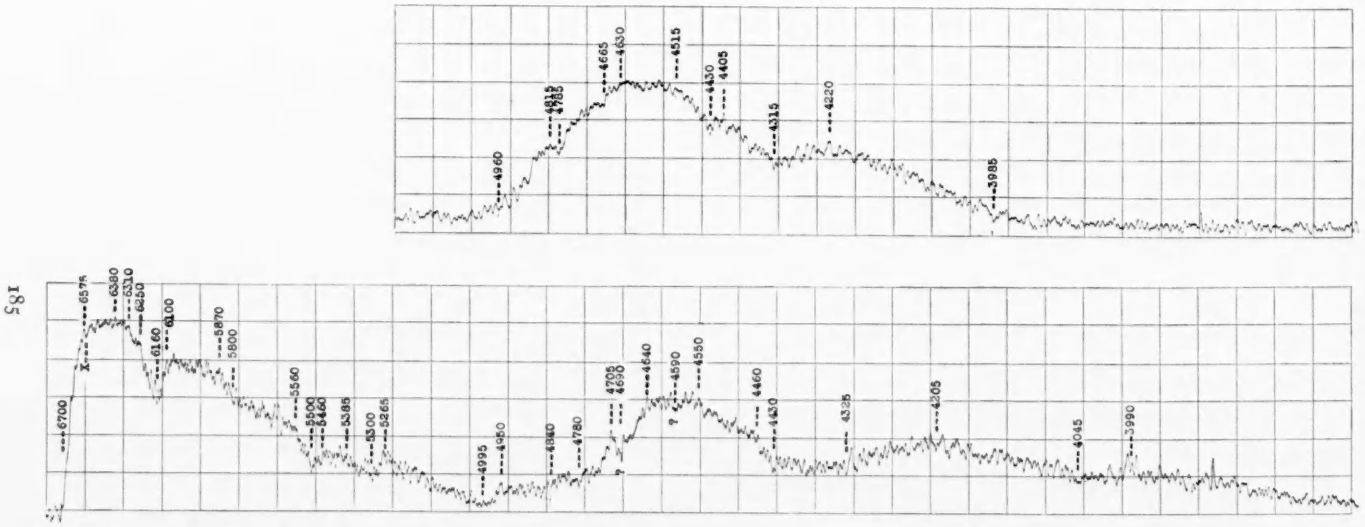

FIG. 31 (*above*).—NGC 1003. September 17.419, 1937, 3 days after maximum. Spectrograph *h*, Imperial Eclipse Soft

FIG. 32 (*below*).—NGC 1003. September 23.378, 1937, 9 days after maximum. Spectrograph *e*, Agfa Supersensitive Panchromatic

September 23, 1937, 9 Days after Maximum (Fig. 32)

As far as can be seen from the faint record of September 15 (Fig. 30), the spectrum above λ 4500 has remained unchanged. The flat top of the main blue band has further contracted to λλ 4640–4550. Whether the structure on its red edge has changed is doubtful; the minimum at λ 4690 may be spurious. The band at λ 4405 on September 16 has faded out, leaving a wide minimum between λ 4430 and λ 4325. From there on toward the violet end the differences may be due mainly to the use of different spectrographs. The spectrum is very similar to that of supernova IC 4182 on August 31, 1937 (Fig. 8).

October 3, 1937, 19 Days after Maximum

The spectrogram is virtually identical with that of October 6, which is of stronger exposure. The tracing has therefore been omitted.

October 6, 1937, 21 Days after Maximum (Fig. 33)

Two relatively narrow maxima have emerged at λ 4900 and λ 4820. The flat top of the main band has continued to contract, possibly owing to the fading-out of a band at about λ 4570. A new maximum has been formed at λ 4330, while the former maximum at λ 4205 has disappeared. The intensity is constant from λ 4190 to λ 3965, where the spectrum begins to fade out. The pattern thus formed in the blue part of the spectrum does not change much from now on, but all its features shift toward the red.

October 13, 1937, 29 Days after Maximum (Fig. 34)

The red part of the spectrum has greatly increased in intensity relative to the blue. The bands in the red have changed radically since September 23 (Fig. 32), a change corresponding in almost every detail to that in the spectrum of supernova IC 4182 from August 30 to October 2, 1937 (Figs. 7–14).

October 28, 1937, 44 Days after Maximum (Fig. 35)

No essential change has occurred since October 13 (Fig. 34). Minor differences may be due entirely to the intensity differences of the records.

November 4, 1937, 51 Days after Maximum (Fig. 36)

The outline of the spectrum is the same as on October 6 (Fig. 33). The maxima which then appeared at λλ 4900, 4820, 4660–4615, and 4330 now appear at λλ 4955, 4850, 4660, and 4340, respectively. Both plates obtained on this date agree in showing the very indistinct minimum at λ 4120, followed by an equally ill-defined maximum between λ 4120 and λ 3940.

December 7, 1937, 83 Days after Maximum (Fig. 37)

Virtually no change has occurred since November 4 (Fig. 36). The maximum at λ 4955 seems to be fainter; the difference in the strength of the exposures is not quite sufficient to explain its absence from this plate.

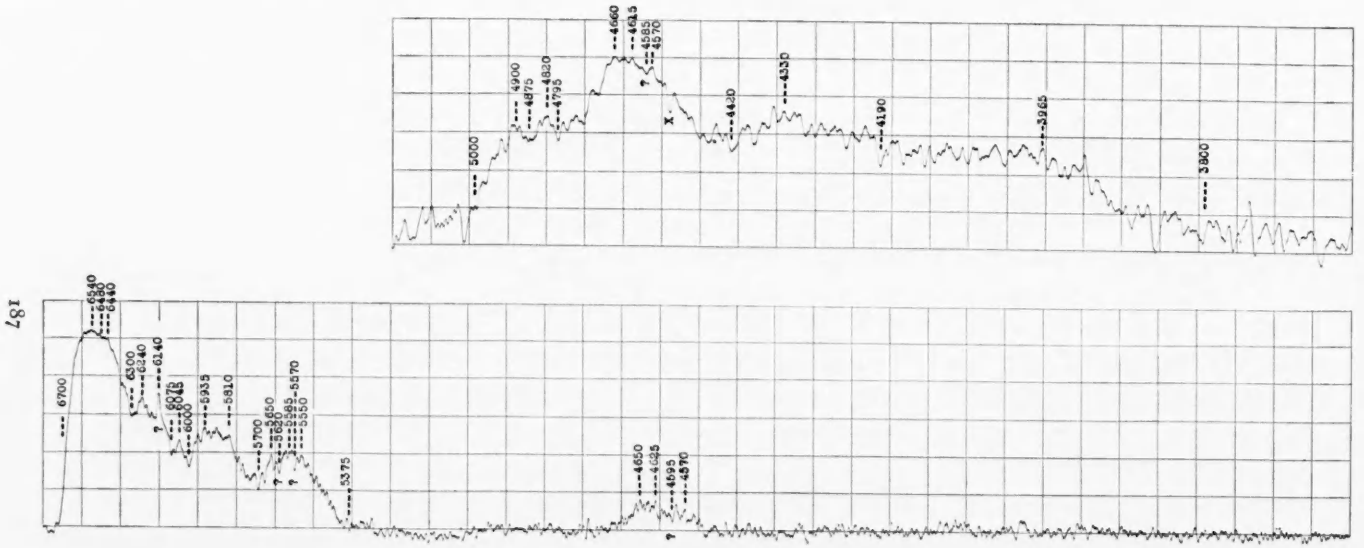

FIG. 33 (*above*).—NGC 1003. October 6.512, 1937, 22 days after maximum. Spectrograph *a*, Imperial Eclipse Soft

FIG. 34 (*below*).—NGC 1003. October 13.401, 1937, 29 days after maximum. Spectrograph *e*, Agfa Supersensitive Panchromatic

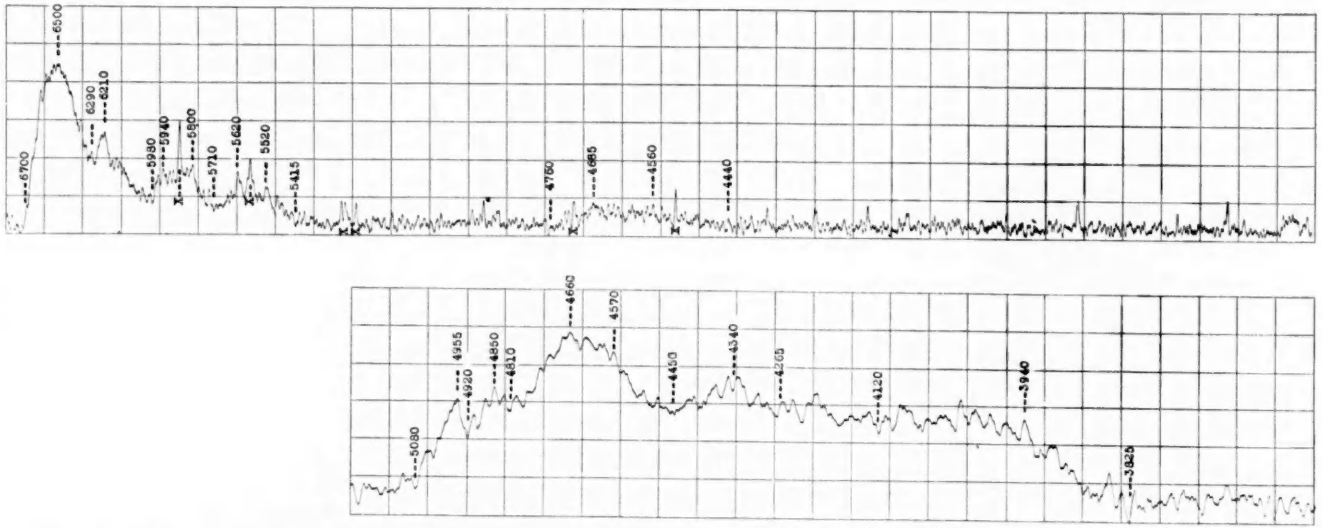

FIG. 35 (*above*).—NGC 1003. October 28.290, 1937, 44 days after maximum. Spectrograph *e*, Agfa Supersensitive Panchromatic

FIG. 36 (*below*).—NGC 1003. November 4.216, 1937, 51 days after maximum. Spectrograph *a*, Imperial Eclipse Soft

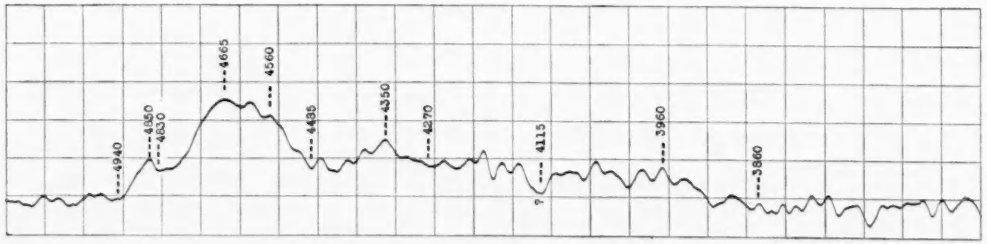

FIG. 37.—NGC 1003. January 7.118, 1938, 115 days after maximum. Spectrograph *a*, Imperial Eclipse Soft.

January 7, 1938, 115 Days after Maximum

The exposure was ended prematurely by clouds. The faint record shows no change since December 7 (Fig. 37).

COMPARISON OF THE SPECTRA OF DIFFERENT SUPERNOVAE

A comparison of the observational results for supernovae IC 4182 and NGC 1003 shows immediately the great similarity in the two series of spectra and in the changes which occur in them. The spectrum of supernova NGC 1003 on September 23, 9 days after maximum (Fig. 32), shows only minor differences from the spectrum of supernova IC 4182 on August 31, 9 days after maximum (Fig. 8). Again the spectra of supernova NGC 1003 on October 13, 29 days after maximum (Fig. 34), and on October 28, 44 days after maximum (Fig. 35), are closely similar to the spectrum of supernova IC 4182 on October 2, 41 days after maximum (Fig. 14).

Minor differences in the structure of the bands are apparently due to the fact that, while the time scale of the development in both supernovae is approximately the same, details appear not in quite the same order or at the same time after maximum. The shoulder on the violet edge of the first maximum in the red at about λ 6300 appears in the spectrum of supernova NGC 1003 on September 23, 9 days after maximum (Fig. 32), and in the spectrum of supernova IC 4182 on September 9, 18 days after maximum (Fig. 11). Another example of such differences is that, although the general outlines of the spectra of the two supernovae agree best 9 days after maximum, the structure of the strongest band in the blue of supernova NGC 1003 9 days after maximum is a better match with that of supernova IC 4182 14 days after maximum, i.e., on September 5 (Fig. 10). Apart from such differences the development of both spectra runs closely parallel not only for the more pronounced changes in the spectrum above λ 5000 but also for the gradual red shift of the permanent pattern below λ 5000, which will be discussed later.

This uniformity of development is not limited to these two supernovae. The following discussion of the spectra of former supernovae shows that, with the possible exception of S Andromedae, the spectra of all supernovae are similar and differ only in minor details.

NGC 224 (S Andromedae).—The visual observations of the spectra of S Andromedae have been collected and discussed by C. Payne Gaposchkin.[3] The descriptions of the spectrum by different observers do not lead to a very clear picture. Ten out of the twenty-four observations give only a very general statement—that the spectrum was continuous, with or without condensations; all these observations were made during the first three weeks after maximum. This result is quite consistent with the appearance of the spectra of supernovae IC 4182 and NGC 1003 during the corresponding interval; the bands were then so inconspicuous as to be unobservable under bad conditions. The remaining observations mention a band in the red twice, bands in the yellow ten times, and bands in the green also ten times. Twice a band near $H\beta$ is mentioned, and once a band near λ 4300. Only the one observation by Backhouse on September 16, 1885, can be interpreted as suggesting the existence of a band near λ 4600; while Vogel on September 1 and 2, 1885, observed a hazy dark minimum between λ 4861 and λ 4308.

To reconcile these observations with the existence of a strong band near λ 4600 is hardly possible, even if the difficulty of the visual observations be taken into account. Thus it seems likely that this band was absent from the spectrum of S Andromedae.

The frequent mention of bands in the green gives the impression that possibly one or more bands in this region may have appeared with greater intensity than in the spectra of the two recent supernovae. It may be significant in this connection that in these recent spectra, during the interval when the blue was relatively faint, about 40 days after maximum, a band near λ 5500 reached its maximum relative intensity. On the other hand, the prominence given to bands in the green and yellow may be due merely to the great sensitivity of the eye in these regions. In view of the difficulty of visual measurements in spectra of this type, the agreement of the wave lengths given for these bands by various observers with those of bands in the spectra of supernovae IC 4182 and NGC 1003 cannot be considered as strong evidence for identity of the bands.

That a band in the red has been mentioned only twice is clearly not due to lack of intensity in the red, as may safely be concluded

[3] *Ap. J.*, **83**, 245, 1936.

from the observations of the color of the star. Probably most observers interpreted the intensity in the red as due to a continuous background.

Thus it is not impossible that in the region above λ 5000 the spectrum of S Andromedae may have been similar to the spectra of supernovae IC 4182 and NGC 1003; the spectra below λ 5000 may have been different, however.

NGC 4273.—Several spectrograms of this supernova were obtained at Mount Wilson with spectrograph *a* and have been discussed by Humason[4] and Baade.[5] The pattern presented is essentially the same as that in the same region of the spectra of supernovae IC 4182 and NGC 1003. The first spectrogram, obtained by Sanford, on February 4, 1936, about 25 days after maximum, probably represents moonlight combined with light of the nova. If it can be assumed that the light of the nova dominated, the spectrum is to be regarded as showing some similarity to the spectrum of supernova IC 4182 on August 30, 1937, 8 days after maximum. If, however, a considerable part of the light was moonlight, the spectrum would be more nearly that of supernova IC 4182 on a later date.

The spectra obtained by Humason on February 20 and 24–26, 1936, about 45 days after maximum, are very similar to those of supernova NGC 1003 on November 4, 1938, 50 days after maximum. The main difference in the contour is that the maximum at λ 4235 and the band following toward the violet appear more distinctly than in supernova NGC 1003.

A spectrogram by Baade, on April 21–23, 1936, about 105 days after maximum, shows only the band at λ 4641, while mere traces of other bands are visible. This agrees well with the contours for both the recent supernovae at the same time after maximum, when the band around λ 4650 was by far the strongest feature in the blue region. The change in the wave length of this band from February to April is in good agreement with the gradual red shift of the permanent pattern below λ 5000 in the spectra of supernovae IC 4182 and NGC 1003 (cf. Fig. 38).

[4] *Pub. A.S.P.*, **48**, 110, 1936.

[5] *Ibid.*, p. 226.

NGC 4303.—Slitless spectrograms of supernova NGC 4303 were obtained by Shane[6] at the Lick Observatory on May 15, 1926, and by Duncan and Nicholson at Mount Wilson on May 17, 18, and 19, 1926, about 20 days after maximum. The spectrogram of May 19 is reproduced in Humason's paper on supernova NGC 4273.[4] The three Mount Wilson plates show no noticeable differences. They record the same bands as appear in the blue part of the spectra of super-

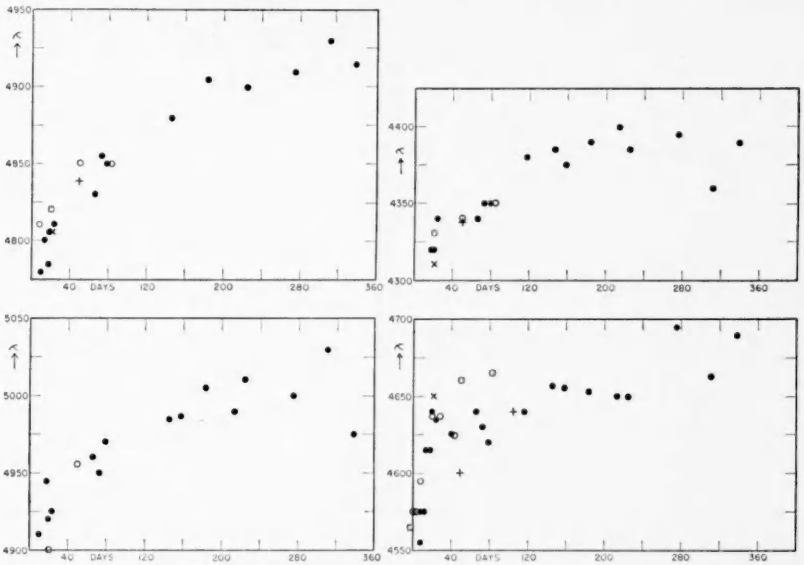

FIG. 38.—Wave lengths of maxima below λ 5000 and time after maximum. ●, IC 4182; ○, NGC 1003; +, NGC 4273; ×, Z Centauri.

novae IC 4182 and NGC 1003. The brightest of these bands, around λ 4600, seems, however, to be relatively fainter—not much more intense than the following band around λ 4300. This fact is of interest in connection with the observations of the spectra of S Andromedae, in which, as already noted, the band around λ 4600 was possibly fainter than the other bands in the blue, or even missing. Except for this possible difference, the spectrum is essentially the same as that of supernovae IC 4182 and NGC 1003.

Z Centauri.—The observations of Z Centauri fit perfectly into the series of spectrograms of supernova IC 4182. A discussion of the

[6] *Ibid.*, **38**, 182, 1926.

spectrum of Z Centauri by C. Payne Gaposchkin[7] is based on the tacit assumption, which at that time was not injudicious, that no radical changes take place in the later spectra of supernovae. In consequence, the observations seem to lead to contradictions, especially as the date of W. W. Campbell's latest observation, on February 8, 1896, has been omitted from the abbreviated report of his results. A rediscussion of the data is therefore necessary.

The first observation was obtained on July 18, 1895, between 10 and 35 days after maximum.[8] This slitless spectrogram was measured by Johnson,[9] and a tracing of it reproduced in Johnson's paper shows at once that the spectrum closely resembles that of supernova IC 4182 on September 15, 24 days after maximum, not only in outline but also in the wave lengths of the bands (cf. Fig. 38 and the discussion of the red shift on p. 195).

The Harvard visual observation of December 16, 1895, 161–186 days after maximum, showed that "the spectrum was monochromatic, and closely resembled that of the adjacent nebula." Since in the spectrum of supernova IC 4182 on January 27, 158 days after maximum, the band at λ 4655 exceeded all others in intensity, there can be hardly any doubt that this band was the only one seen at Harvard on December 16, 1895. The statement that the spectrum "closely resembled that of the adjacent nebula" may then be explained as already proposed by C. Payne Gaposchkin, namely, that "a low-dispersion spectrograph would have given that impression visually if the spectrum resembled the one that was earlier photographed." This would mean that the band at λ 4655 was identified with the lines at λ 5007 and λ 4862, which, according to Campbell,[10] appeared in the spectrum of the nebula with their usual relative intensities, while "the line near λ 4690 seemed to be present."

Campbell observed the spectrum of Z Centauri visually on December 22 and 29, 1895, 167–192 days and 174–199 days after maximum. He was "reasonably certain that the spectrum was continuous, but the seeing was too poor to permit a definite decision." The spectrogram of supernova IC 4182 on February 22, 1938, 184 days

[7] *Ap. J.*, **83**, 173, 1936.

[8] *Harvard Circ.*, No. 4, 1895; *Harvard Ann.*, **76**, 37 and Pl. 2, 1913.

[9] *Harvard Bull.*, No. 902, 1936.

[10] *Ap. J.*, **5**, 234, 1899.

after maximum, shows that the part above λ 5000 had reappeared with high intensity. With poor seeing, this spectrum could hardly lead to any other description than that given by Campbell for Z Centauri at the corresponding date.

Campbell's last visual observation, on February 8, 1896, 215–240 days after maximum, led him to a masterly description, which leaves no doubt that the spectrum was identical with that of supernova IC 4182 on April 3–4, 1938:

> The spectrum of the Harvard star was *continuous*, though very peculiar. The maximum visual intensity was in the yellow-green, the green-blue was very faint, while the blue was surprisingly strong. In fact, the blue was very much brighter visually than the green-blue. The spectrum was relatively very faint from about λ 5200 to λ 4600. There was no trace of the nebular lines visible, nor of the *Hβ* line. There was some evidence of bright lines or of irregularities in the brightest portions of the spectrum, but the light was too weak to enable me to decide.

In the light of the knowledge of supernovae IC 4182 and NGC 1003, it is clear that the seemingly conflicting spectroscopic observations of Z Centauri are due to the radical changes that the spectra of supernovae undergo, and that the spectra of Z Centauri and their time scale of changes resembled those of supernovae IC 4182 and NGC 1003 very closely indeed.

NGC 6946.—A slitless spectrogram of this supernova was obtained on August 16, 1917, by Pease and Ritchey, whose description reads: "The continuous spectrum is strong and is crossed by what appears to be a series of bright bands."[11] A comparison with the spectra of other supernovae leaves no doubt that the plate, although of poor quality, shows the typical supernova spectrum, with the λ 4600 band as the dominant feature; the bands at λ 4800 and λ 4300 can be recognized.

THE RED SHIFT

The spectral comparison of the five earlier supernovae with those in IC 4182 and NGC 1003 leads clearly to the conclusion that the spectra of six of the seven stars differ only in details which do not affect the general appearance of the spectrum. It is possible, but in view of the difficulties of visual observations not at all certain, that

[11] G. W. Ritchey, *Pub. A.S.P.*, **29**, 211, 1917.

the seventh, S Andromedae, presented a spectrum of the same type but with different features. This close relationship extends to the time scale of the major changes in the relative intensities of the red and the blue parts of the spectra and within the red part itself, and to the rate at which the permanent features in the blue change their wave lengths.

The wave lengths of the four most permanent bands in the blue are shown graphically in Figure 38 for four different supernovae as a function of the time after maximum. The values plotted are those of the maxima, or, when a band had a flat top, the wave length of the center of the flat top. For supernovae IC 4182 and NGC 1003 the data were taken from the tracings reproduced in Figures 2–26 and 27–37, respectively. For Z Centauri the tracing published by Johnson[9] was used. For supernova NGC 4273 values measured by Humason and by Baade have been used.

It is of interest to note that for the two faintest maxima, which appeared at about λ 4800 and λ 4900 shortly after the maximum, the points follow a smooth curve with not more scatter than might be expected from the operation of measuring the relatively ill-defined maxima. These two maxima are among the narrowest details in the spectra, and it is not unreasonable to assume that they represent single emission bands. The changes in the visibility of these bands may be due to fluctuations in the width and the intensity of the bands; it is not impossible, however, that the appearance and disappearance of underlying fainter bands are involved in the variations. The strongest band, which appeared at about λ 4575 shortly after maximum, shows almost continuous changes of structure, indicating that it is composed of several components of changing relative intensity whose fluctuations in different supernovae do not occur at exactly the same time after maximum. Consequently, the wave length of this band is subject to changes which are superposed on the red shift. The values of the wave lengths in Figure 38 indicate not only considerable scatter around a smooth curve but also systematic fluctuations. The changes in structure of the band which appeared at about λ 4300 shortly after maximum are less pronounced; and, as might be expected, the wave lengths in Figure 38 show less dispersion. The red shift for this band seems to show a maximum about

220 days after maximum; whether this is real or due to changes in the composition of the band or to uncertainty of measurement cannot be decided. The red shift develops in a very similar way for all four bands. Apparently it is not the same for all but seems to increase with the wave length of the band. However, the differences may be merely individual, either real or only apparent and due to changes in the composition of the bands. No systematic change in the width of the bands seems to accompany the shift.

The present evidence establishes the red shift as a common effect observable in the spectra of supernovae. Its size and rate of development in different supernovae appear to differ so little, if at all, that measurements of the wave lengths of the permanent bands in the blue seem to provide a means of determining when a supernova reached its maximum. It is hardly necessary to emphasize that this phenomenon has no counterpart in the spectra of ordinary novae. The red shift, together with the striking similarities in the red regions of the spectra of supernovae IC 4182 and NGC 1003 and the closely parallel changes in the relative intensity of the blue and the red for these supernovae and for Z Centauri, puts the spectra of supernovae in a class of their own.

Whether the bands in the red part of the spectrum participate in the red shift is difficult to decide. The early changes in this region are rapid, the bands are apparently complex, and all the variations in wave length may be due to changes in the composition of the bands. Two of these red bands in the spectrum of supernova IC 4182 are apparently permanent and show only small changes in structure after October 27, 1937, 66 days following maximum. One, at λ 6500 on this date, shows only a fluctuation in wave length, which drops to λ 6460 on December 17, 1937, and rises again slowly to λ 6500 on April 3–4, 1938. The other, at about λ 5865 on October 27, 1937, seems to shift slightly toward the red about 20 A until April 3–4, 1938. This change is much less than the shift of the bands in the blue during the same interval and may be due entirely to a change in the composition of the band, which at the same time became narrower. Although the evidence obtainable from the red part of the spectrum is not very conclusive, it suggests that the red shift is small or absent. This is not surprising; the transformations of the spec-

trum above λ 5000 and the variations in its intensity occur without any accompanying change in the permanent pattern below λ 5000. If the red shift above λ 5000 is small or absent, it only corroborates the independence of the two parts of the spectrum.

The earlier discussions of the spectra of supernovae have led to the conclusion that they are composed of very wide and partly overlapping emission bands. The basis for this opinion was the general appearance of the spectra and the close agreement of the most intensive band in the blue with the well-known *N* III lines near λ 4640. A reasonable identification for the strongest band in the photographic region appeared then to be provided. At the same time, a connection with the spectra of ordinary novae seemed to be established. The red shift in the blue invalidates this identification; it is not impossible that the strongest blue band includes the *N* III lines, but the merely temporary coincidence of wave lengths cannot be considered as convincing evidence. Indeed, no attempt at identification of the bands in the blue can give conclusive results so long as an explanation for the red shift is lacking. The assumption that the permanent features of the spectra are due to the emission of wide, overlapping bands thus rests entirely on the general aspect of the spectra. The question whether absorption plays no role at all or whether, especially near maximum, some of the features of the spectra are produced by absorption remains open.

The great similarity of the red shifts in the spectra of different supernovae rules out any explanation of the red shift as an incidental effect due to the fortuitous distribution of matter and its velocities in the neighborhood of the star. Nor can we satisfactorily assume that the shift is merely a fading-out of one band simultaneously with the appearance of another at a distance small compared with the width of the bands. To explain in this way the shift of the band in the spectrum of supernova IC 4182 from λ 6075 to λ 6100 between September 9 and September 15, 1937, is not objectionable; but that a pattern composed of a great number of individual bands which covers a considerable part of the spectrum should thus be shifted as a whole, without prominent changes in its structure, is extremely improbable.

Only Doppler effect and gravitational red shift seem to remain as

a basis for an interpretation of the red shift. It is evident that the closely similar behavior and amount of the red shift for different supernovae can be understood only with the aid of a general theory of supernovae. It is possible, however, to discuss to some extent the conditions under which an explanation of the red shift might be obtained. At present this discussion must remain incomplete; any attempt at explanation seems to necessitate assumptions so unusual that a final decision on the feasibility of the interpretation cannot be reached without a more complete study of the radiative equilibrium in the matter surrounding a supernova.

Even if the bands observed in the spectra of supernovae originate at a relatively great distance from the center of the star, the radiation density involved attains unusually high values. If the supernova outburst is accompanied by a collapse of the star, the radiation density will, in fact, become so high that the possibility of emission of relatively narrow bands becomes questionable. The photographic absolute magnitude M of a supernova is a measure of the average intensity emitted in the permanent bands between λ 4000 and λ 5000. If R is the distance from the center of the star, expressed in the sun's radius as unit, we obtain for the average radiation density $\rho(\nu)$ in the part of the spectrum where the red shift is observed

$$\rho(\nu) = 2 \cdot 10^{-12} \cdot \frac{10^{-0.4M}}{\epsilon^2 R^2}, \qquad (1)$$

in which the numerical factor $\epsilon < 1$ if the intensity of the emission varies between the center and the limb of the emitting layer, and is equal to 1 for a vanishing difference between center and limb.

The radiation densities derived from (1) may easily become so large that the natural width of the spectral lines is affected. To simplify the following discussion, it is convenient to assume that the lower level involved in the formation of the lines is the ground state of an atom or ion, that the upper level is the next higher one, and that the statistical weights of all levels are equal to unity; these assumptions do not affect the order of magnitude of the results.

For the natural width of a line, in units of $2\pi \times$ frequency, we then obtain

$$\Gamma = A_i + 2B_i\rho(\nu_i) + \sum_{k \neq i} B_k\rho(\nu_k) , \tag{2}$$

where A_i is the Einstein probability for spontaneous emission of the line with the frequency ν_i and B_i is the probability for induced emission and for absorption of this line. The sum on the right side of equation (2) is to be extended over all transitions from the upper and from the lower level, with the exception of those between the levels; but under the assumptions made, only upward transitions which have the probabilities B_k are possible. These transitions lead to absorption of lines with the frequencies ν_k. The probabilities B and A are connected by the relation

$$B_i = \frac{\lambda_i^3}{8\pi h} A_i . \tag{3}$$

If we consider first only the contribution to the natural width of the line produced by transitions within the line itself, leaving for later discussion the possible influence of other transitions included in the sum on the right of (2), we obtain

$$\Gamma = A_i \left(1 + \frac{10^{-12}\lambda_i^3}{2\pi h} \cdot \frac{10^{-0.4M}}{\epsilon^2 R^2}\right). \tag{4}$$

By substituting numerical values, we find for the mean wave length 4500 A

$$\Gamma = A_i \left(1 + 2.2 \cdot \frac{10^{-0.4M}}{\epsilon^2 R^2}\right). \tag{4a}$$

The structure of the permanent pattern in the blue indicates that the natural width of the lines is certainly less than 100 A. This leads to the condition

$$A_i \left(1 + 2.2 \cdot \frac{10^{-0.4M}}{\epsilon^2 R^2}\right) < 9.4 \cdot 10^{13} . \tag{5}$$

In the spectrum of supernova IC 4182 the permanent pattern was already well developed about two weeks after maximum; the abso-

lute magnitude was then $M = -15$. For strong permitted lines, A is of the order 10^8. Hence from (5) we obtain

$$R > 1.5\epsilon^{-1}. \tag{6}$$

Thus the observed lines can be strong permitted lines only if the radius of the emitting layer is larger than the radius of the sun, and the assumption of a much smaller radius entails the further assumption that the lines are forbidden lines.

An interpretation of the red shift proposed by Zwicky is that it is due to the increasing gravitational potential at the surface of a collapsing star.[12] It is evident that the lines participating in the red shift can then be only forbidden lines. An upper limit for their transition probability can be obtained. If Δ is the value of the red shift in angstroms and μ the mass of the star, the sun's mass being taken as unit, the radius of the emitting layer at which the red shift is observed becomes

$$R = 10^{-2}\frac{\mu}{\Delta}. \tag{7}$$

The values of R/μ following from (7) for supernova IC 4182 are given in the third column of Table 3. The corresponding values for the red shift in the second column are smoothed means obtained from the observed data for the four permanent bands, illustrated in Figure 38, on the assumption that the red shift started when the star reached its maximum. The fourth column of the table gives the photographic absolute magnitudes of the star,[13] and the fifth the values of $\rho(\nu)\epsilon^2\mu^2$ that follow from (1). The corresponding values of $F\epsilon^2\mu^2$ are in the sixth column, F being the total energy emitted between λ 4000 and λ 5000 per square centimeter of the surface into unit solid angle. On the assumption that the red shift is a gravitational effect, Table 3 shows that the radiation density reaches a maximum about 60 days after maximum. It may be significant that at about this time the bands in the red part of the spectrum reach their maximum intensity relative to those in the blue. The condition

[12] *Pub. A.S.P.*, **50**, 215, 1938; also Baade and Zwicky, *Mt. Wilson Comm.*, No. 114; *Proc. Nat. Acad.*, **20**, 254, 1934.

[13] Baade and Zwicky, *Mt. Wilson Contr.*, No. 601; *Ap. J.*, **88**, 411, 1938.

(5), which must be satisfied for maximum radiation density, then gives the upper limit for the transition probability, namely,

$$A_i < 13\epsilon^2\mu^2 . \tag{8}$$

From this upper limit of the transition probability a lower limit for the number of atoms in the upper levels of the permanent bands may be obtained by consideration of the emitted energy. The two different classes of transitions, spontaneous and induced, lead to

TABLE 3

RADIUS OF EMITTING LAYER AND RADIATION DENSITY FOR SUPERNOVA IC 4182 ON THE ASSUMPTION OF A GRAVITATIONAL RED SHIFT

Days after Maximum	Red Shift in A	$R/\mu \times 10^4$	M_{pg}	$\rho(\nu)\epsilon^2\mu^2$ in Erg Cm^{-3}	$F\epsilon^2\mu^2 \cdot 10^{-23}$ in Erg Cm^{-2} Sec^{-1}
20.....	15	6.7	−14.8	3.5	13
40.....	35	2.9	13.4	4.8	18
60.....	50	2.0	12.9	7.0	27
80.....	60	1.7	12.5	6.3	24
100.....	67	1.5	12.2	6.2	24
140.....	80	1.25	11.4	4.4	17
180.....	90	1.1	11.0	3.9	15
220.....	95	1.05	10.4	2.5	10
260.....	100	1.0	9.7	1.5	6
300.....	(105)	0.95	− 9.2	1.0	4

emission of different types. The spontaneous emission is isotropic, but the induced emission is directed and increases the intensity of the inducing radiation in the same way as absorption decreases it. The induced emission is therefore more appropriately designated as "negative absorption." The total absorption, which is the sum of the positive and the negative absorptions, depends on the difference of the numbers of atoms in the lower and in the upper levels of a line. In thermodynamical equilibrium the number of atoms N_i in the upper level can never be larger than the number N_i' in the lower level. Only for infinite temperature can N_i equal N_i' and the absorption disappear. In thermodynamical equilibrium, therefore, the intensity emitted can never exceed that produced by the spontaneous transitions.

Let N_i denote the total number of atoms in the upper level over 1 cm^2 of the surface. If $N_i' > N_i$, the maximum intensity emitted

by all bands of the permanent pattern in the blue is $h\Sigma N_i A_i \nu_i$, where the sum is to be extended over all transitions which lead to emission in this part of the spectrum. If $N = \Sigma N_i$ denote the total number of atoms in all upper levels, ν_0 the mean frequency, and $A = \Sigma N_i A_i \nu_i / N\nu_0$ the weighted mean of the transition probabilities, we obtain

$$NAh\nu \geqslant \pi F . \tag{9}$$

If the upper limit for A from (8) is substituted, (9) leads to the condition

$$N > 1.3 \cdot 10^{35} \epsilon^{-4} \mu^{-4} \tag{10}$$

for the maximum value of the intensity $F = 2.3 \cdot 10^{24} \epsilon^{-2} \mu^{-2}$, which occurs about 60 days after maximum. This is clearly impossible. The thickness of the layer in which the lines are emitted is not unlimited. The radial inhomogeneity of the gravitational field produces a contribution to the width of the lines which increases proportionally to the shift. As no effect of this kind is observed, this additional width must be small compared with the shift. Consequently, the thickness of the emitting layer cannot be much larger than $0.1R$. At the time of maximum intensity, R is $2 \cdot 10^{-4}\,\mu$. The corresponding thickness of the layer must be assumed smaller than $1.4 \cdot 10^{6} \mu$ cm, which leads to a density of excited atoms of $10^{29} \epsilon^{-4} \mu^{-5}$. This density is so high that, unless the mass of a supernova considerably exceeds that of ordinary stars, pressure effects would produce a width of lines irreconcilable with the observations. On the assumption of a gravitational effect in a star of ordinary mass, it must be concluded that the emission of the bands showing the red shift takes place under conditions which do not even approximate the thermodynamical equilibrium corresponding to any temperature.

This is no reason for rejecting the assumption of a gravitational effect. Deviations from thermodynamical equilibrium are indeed to be expected. In order to obtain a density which is not excessive, it is necessary to assume that these deviations are such that the number of atoms in the upper metastable level of the lines is larger than the number in the ground state. The negative absorption would then

exceed the positive absorption, and the observed emission lines would be really "negative absorption" lines. Conditions which lead to the formation of such lines can be realized only by some special mechanism of excitation, such as excitation of the metastable levels by collisions of slow electrons, which are produced by absorption in continuous spectra in the far ultraviolet; the process of excitation would then be qualitatively similar to that of forbidden lines in planetary nebulae. The accumulation of atoms in metastable levels would be possible even at fairly high density, since the ratio of the lifetime of the metastable states to that of other levels remains of the same order as that at low density, while the lifetime itself is greatly shortened by induced transitions.

If now we assume that the positive absorption is negligible, which means that the number of atoms in the lower level is small compared with that in the upper level, we obtain, instead of (9),

$$Nh\nu_0[A + B\rho(\nu_0)] \geqslant \pi F . \tag{11}$$

If B is replaced by A according to (3), the lower limit for the number of excited atoms becomes, instead of (10),

$$N > 3.8 \cdot 10^{22}\epsilon^{-2}\mu^{-2} . \tag{12}$$

The corresponding limit of the density of excited atoms is $3 \cdot 10^{16}\epsilon^{-2}\mu^{-3}$; this value is high but not excessive. The hypothesis of a gravitational effect can therefore be maintained if the bands are negative absorption lines.

The discussion of the transitions whose contribution to the natural width is represented by the sum on the right side of (2), which so far has been neglected, leads to restrictions of the possible structure of the term system of the emitting ions. If practically all the energy emitted by the supernova is contained in the observed part of the spectrum, the density of radiation which has the frequency ν_k of an absorption line formed by upward transitions from either the lower or the upper level of the observed lines ν_i will be small; the chance of a coincidence of ν_k with ν_i is small enough to be ignored. However, even if no energy is emitted in the unobserved parts of the spectrum, the scattering of the light emitted in the lines ν_i by other lines ν_k

cannot be disregarded. This scattering is due to the fact that the energy states of an atom are not sharply defined but show a probability distribution round a mean value. The process which leads to the scattering is a transition from the lower level of the line ν_k into the wing of its upper state, which brings about simultaneously the disappearance of a quantum $h\nu_i$ and the reappearance of a scattered quantum $h\nu_i$. Processes of this kind, negligible under ordinary conditions if ν_i is not very close to ν_k, become frequent at high radiation density. Their probability[14] is the sum of two parts, one proportional to the radiation density, the other proportional to the square of the radiation density. The latter prevails at high radiation density; and the probability of scattering becomes then, to a sufficient approximation,

$$W = \frac{27}{64\pi^4} \frac{e^4}{m^2c^4} \frac{\rho^2(\nu_i)\lambda_k^4}{h^2} \Gamma . \tag{13}$$

The oscillator strength of the line ν_k is here assumed to be unity. The condition that no additional width is produced by the scattering is

$$W < \Gamma . \tag{14}$$

This condition leads to an upper limit for λ_k. By substituting the values of the universal constants and of the maximum value of the radiation density from Table 3, we obtain

$$\lambda_k < 2 \cdot 10^{-7} \epsilon\mu . \tag{15}$$

The term system could then include no term below 600 V from which transitions into the ground state or into the metastable state at about 3 V are permissible. Conditions of this type might indeed be fulfilled in a very highly ionized atom. The metastable and the ground levels could be, for instance, the components of a multiplet ground term with a separation of about 3 V. A value of more than 600 V for the excitation potential of the next higher term would

[14] G. Placzek, in Marx, *Handbuch der Radiologie*, **6**, Part 2, 222, 1934. Equation (13) of the present text is an approximation obtained from the general formula given there, § 3, equation (11), which Dr. Placzek has kindly communicated to the author.

indicate an ionization potential of the order of 1000 V and would point to an eightfold or even more highly ionized atom.

The conditions which result, if now the assumption that the observed lines contain practically the total energy is no longer maintained, depend entirely on the distribution of intensity in the unobserved regions of the spectrum, especially in the far ultraviolet. It seems reasonable to assume as primary source of radiation a continuous spectrum emerging from the interior of the star with an intensity distribution which does not deviate essentially from that of a black body. Some part of the energy contained in this continuous spectrum will be converted into emission lines. Without knowledge of the mechanism of this conversion, it is not possible to derive a rational value for the energy remaining in the continuous spectrum in the layer of the atmosphere which radiates the emission bands showing the red shift. It might appear objectionable if, to avoid an excessive width of the lines, it were necessary to assume that more than a small part of the total energy has been converted into the emission bands between λ 4000 and λ 5000. If the total energy F emitted in these bands is a fraction η of the energy of the primary black-body radiation, with the temperature T_p, so that

$$F = \eta\sigma T_p^4 , \tag{16}$$

we obtain for the maximum value of F from Table 3 the value for the temperature

$$T_p = 1.5 \cdot 10^7 \eta^{-1/4} \epsilon^{-1/2} \mu^{-1/2} . \tag{17}$$

A lower limit for the wave length λ_k of a line corresponding to an upward transition from either of the levels involved in the formation of the forbidden line λ_i can now be obtained, and the comparison of this with the upper limit (15) leads to a lower limit for η. The resulting value λ_k will be large enough to obtain the radiation density $\rho_p(\nu_k)$ of the black-body radiation for this wave length from the Rayleigh-Jeans law. For the temperature (17) we find

$$\rho_p(\nu_k) = 1.7 \cdot 10^{-18} \lambda_k^{-2} \eta^{-1/4} \epsilon^{-1/2} \mu^{-1/2} . \tag{18}$$

By replacing A in (3) by the oscillator strength

$$f_k = \frac{mc^3}{8\pi^2 e^2 \nu_k^2} A_k , \tag{19}$$

and by substituting the numerical values, we have

$$B_k = 4.1 \cdot 10^{24} \lambda_k f_k . \tag{20}$$

For strong absorption lines, f_k is of the order of unity. From (18) and (20) we find the condition that the absorption of energy of the black-body radiation by the line λ_k does not increase the width of the forbidden line λ_i to be

$$B_k \rho_p(\nu_k) = 7 \cdot 10^6 f_k \lambda_k^{-1} \eta^{-1/4} \epsilon^{-1/2} \mu^{-1/2} < 9.4 \cdot 10^{13} , \tag{21}$$

or

$$\lambda_k > 7.4 \cdot 10^{-8} f_k \eta^{-1/4} \epsilon^{-1/2} \mu^{-1/2} . \tag{22}$$

The condition that (22) is compatible with (15) leads to

$$\eta > 2 \cdot 10^{-2} f_k^4 \epsilon^{-6} \mu^{-6} . \tag{23}$$

This limit indicates that the presence of a continuous spectrum of a considerable intensity does not affect the width of the forbidden lines; it is not necessary to assume that more than a small part of the energy is converted into the emission bands between λ 4000 and λ 5000.

Finally, the question remains whether emission and reabsorption of the permitted lines λ_k does not inevitably produce an excessive width of the forbidden lines λ_i. It seems reasonable to assume that the metastability of the upper level of the lines λ_i is in some way responsible for the excessive population of this level and that the number of atoms in the upper level of a line λ_k is not larger than that in the lower level of the forbidden line. The line λ_k will then be a true emission line with an intensity less than that of the negative absorption line λ_i, although its transition probability is much larger. At the same time, the natural width of the line λ_k, owing to its greater transition probability, will still be considerable. The radiation

density $\rho(\nu_k)$ can thus easily become so small that the contribution $B_i\rho(\nu_k)$ of the upward transitions in the line λ_k to the width of the line λ_i are negligible.

Zwicky's assumption that the observed red shift is caused by the increase of gravitational potential at the surface of a collapsing star thus leads to the picture that the lines showing the red shift are forbidden lines and that the conditions of excitation are such that the number of atoms in the metastable levels is larger than that in any other level. The bands which show the red shift are then really negative absorption bands. A survey of the conditions to be fulfilled, if the natural width of the bands remains less than the observed width, reveals no unsurmountable difficulties. Only if there should be a pronounced variation in the emitted intensity between the center and the limb of the emitting layer, resulting in a small value of ϵ, would it be necessary to assume that the mass of the star is larger than that of the sun; a very small value of ϵ would lead to conditions which would make it necessary to reject the gravitational hypothesis. A final decision can thus be reached only by an investigation of the radiative equilibrium on the surface of the star, which is beyond the scope of the present discussion.

If the red shift is to be explained as a Doppler effect, it cannot be the red shift which accompanies the expansion of a shell surrounding the star and which arises from the gradual emergence of that part of the envelope which in the beginning was hidden behind the star. In this case, the width of an emission line increases simultaneously with the shift by twice the amount of the shift. No effect of this kind occurred in the observed spectra. To explain the red shift as Doppler effect connected with the outward motion of matter is therefore possible only if it can be assumed that the main part of the observed intensity is emitted by a small part of the surface in the neighborhood of the center of the disk. The lines would then appear shifted toward the violet, and the red shift would really be a decreasing violet shift due to a decrease of the velocity. Decreasing velocities have frequently been observed in ordinary novae; the occurrence of a similar phenomenon in supernovae seems possible.

If V is the velocity, either of an expanding shell or of matter rushing outward through a spectroscopically active layer in the star's

atmosphere, and if φ is the angle between the line of sight and the direction from the center of the star to the edge of the emitting part of the surface, the contribution of the Doppler effect to the width of the line due to the outward flow of matter is $V(1 - \cos \varphi)$. A variation of V corresponding to the observed shift will then cause no appreciable change of the width if $\cos \varphi > 0.9$. If R is the radius of the emitting layer, the main part of the observed intensity will then be emitted inside a disk with a radius $< 0.44R$; ϵ is then < 0.44. From (6) we find that the lines which show the red shift may be strong permitted lines only if $R > 3.4$. If R is much smaller than this value, the same arguments as before force us to the assumption that the lines are forbidden lines; and, to avoid an excessive number of excited atoms, it becomes necessary again to assume that the lines are negative absorption lines.

If the lines are permitted, the restriction of the emitting area could be caused only by the presence of absorbing matter in or closely surrounding the emitting layer. Preliminary estimates indicate that the desired degree of a darkening toward the limb could be produced only by an amount of absorbing matter that must be considered as excessive. Furthermore, it is hard to understand how this absorbing matter could be kept close to the emitting layer; the absorbed part of the energy would be greater than the emitted part, and the radiation pressure would be very large. Unless a more detailed study of the radiative equilibrium shows a way of overcoming these difficulties, it will, apparently, be necessary to reject the possibility of such an exaggerated darkening toward the limb, and with it the possibility of explaining the red shift on the assumption that the bands are permitted emission lines.

The possibility still remains that the bands which show the red shift are negative absorption lines. This assumption was unavoidable in the case of a collapsed star. A study of the conditions under which a negative absorption line can be formed reveals, however, that the luminosity of supernovae is quite sufficient to allow the formation of negative absorption lines, even if the star is greatly expanded. Unlike the spontaneous emission, which is isotropic, the induced emission is anisotropic and follows strictly the direction of the incident light. Thus, if the conditions for the formation of a

negative absorption line (which will be discussed below) are fulfilled, the intensity of a beam of light increases with the optical depth, first exponentially, just as in a positive absorption line the intensity decreases, until the radiation density has become so high that the number of induced emission processes per second equals that of the processes which create the excited atoms. From this point on, the intensity will show a linear increase. If a negative absorption line is emitted in a layer of radius R surrounding a star of radius R_0, the observed negative absorption line will be formed only by the part of the layer which is in front of the star's disk, just as in the case of a positive absorption line. If the velocity of matter flowing outward is V, the range of observed velocities extends from V to $V \cdot \sqrt{1 - R_0^2/R^2}$. The condition that this range should be small enough to cause no observable change in the width of the lines with varying V is $R_0 < 0.44R$, or $\epsilon < 0.44$. Now, if V varies with the time, the negative absorption line, which corresponds to the positive absorption line on the violet edge of the emission bands of ordinary novae, will change its position without change of width.

To explain the observed red shift on this basis, it is necessary to assume that the negative absorption line, emitted from a disk with radius R_0, is more intense than the apparently unobserved emission band, emitted from a disk with the radius R, on the violet edge of which the negative absorption line appears. This gives the condition

$$\frac{B\rho(\nu_0)}{A} > \frac{R_0^2}{R^2}. \tag{24}$$

If B is replaced by A according to (3), we obtain from (23) and (1), for the mean wave length λ 4500,

$$R < 1.1 \cdot 10^{-0.2M}. \tag{25}$$

This condition admits a considerable expansion of the star at the time of maximum luminosity; later on, the condition becomes more stringent. It is clear that, if the star is assumed to be greatly expanded in the beginning, the permanence of the bands necessitates the assumption of a collapse with decreasing luminosity. The bands can therefore not be emitted in an expanding envelope. It must be

assumed that the negative absorption line is formed in a spectroscopically active layer which is not too far removed from the surface of the star. The decrease of the velocity with which matter flows through this layer then produces the red shift. Whether the observed lines are permitted or forbidden cannot be decided definitely. The formation of negative absorption lines occurs, as has been discussed earlier, if the number of atoms in the upper level of a line is higher than that in the lower level. Laboratory experiments have been performed in which a state of this kind has been produced for ordinary levels. It is not very likely, however, that the specialized conditions which lead to such an accumulation of atoms in an excited ordinary level are realized in a stellar atmosphere. Such an accumulation is much more probable for a metastable level. For this reason it appears preferable to assume that the bands are forbidden lines.

The final decision as to whether it is possible to accept the Doppler shift of a negative absorption line as a working hypothesis depends on a question which again can be answered only by a more detailed study of the radiative equilibrium. Spontaneous emission and scattering in the part of the layer which is not in front of the disk of the star give rise to induced emission in the direction of vision. Thus, instead of reabsorption effects in the emission band on the violet side of which the absorption line appears in the case of ordinary novae, we obtain negative reabsorption effects; and only if the intensity produced by these effects is small compared to that produced by the radiation from the stellar disk will the negative absorption line exceed the intensity of the emission band on the violet side of which it appears.

Two different explanations of the red shift, as either a gravitational effect or as a Doppler effect, thus appear possible. If a more detailed study of the radiative equilibrium does not lead to a rejection of one of these conceptions, a decision may be brought about by a theory of supernovae which explains the similarity of the red shift in different supernovae. Both explanations require the assumption that the bands which show the red shift are forbidden negative absorption lines. Such lines are emitted only under very unusual conditions, but the observations themselves present an equally unusual picture. It cannot be expected that the necessary conditions would

be satisfied for many lines, and this is in general agreement with the observed fact that only a few lines in a restricted part of the observed region of the spectrum stand out by their peculiar behavior.

THE PROBLEM OF IDENTIFICATIONS

In ordinary spectra, identifications of lines are based on the simultaneous coincidence of the wave lengths of several observed lines with those of known lines; the appearance of the spectrum leaves no doubt as to whether one has to deal with absorption or emission lines. In the spectra of supernovae practically all measurements of wave lengths are uncertain and affected by large errors due to the width and haziness of the features presented by these spectra.

For about 10 days after the star has reached its maximum, all details are indistinct and hazy. During this interval almost any line may be present. As already mentioned, the appearance of the spectrum is deceptive; the shape of the bands on the spectrograms is greatly affected by the varying color sensitivity of the photographic materials. In particular, the bands in the red are never really flat-topped, as may be seen by comparing tracings of the spectra with the calibration spectra in Figure 1. The true positions of the maxima, which, of course, are less affected later on when the details have become more distinct, can only be ascertained after the tracings have been reduced to true relative intensities. Before this has been done, attempts at identification are likely to lead to misinterpretation.

It seems certain that the lines of hydrogen, if present at all, are not among the stronger lines; $H\alpha$ may be included in the first band in the red, but no maxima are visible which indicate clearly the presence of any of the lines from $H\beta$ on. Similarly, it may be concluded that lines of helium are not among the more prominent features of the spectrum.

Details that may be faint absorption lines appear on several of the earlier spectrograms. In all these cases, the best example of which is the spectrum of supernova IC 4182 on September 11, 1937 (Fig. 12), the impossibility of duplicating the spectrograms prevents a decision as to whether the lines are real or spurious. Only the first spectrogram of supernova NGC 1003 (Fig. 27), obtained shortly before the star reached its maximum brightness, gives the appearance

of real absorption lines; but, as already noted, the reality of even these lines is doubtful because they are not visible on the following spectrogram, obtained only 40 minutes later.

Any attempt to identify these lines is difficult and may easily lead to an overinterpretation. Owing to the very low dispersion and the faintness of the details, the measures may be in error by several angstroms; and true absorption-line details may be shifted by an unknown amount toward the violet because of outward flow of matter in the atmosphere of the star. Suggested identifications, which are far from satisfactory, are given in Table 4. Two lines which might be expected, *He* II λ 4540 and *Si* IV λ 4075, cannot be identified with observed details; and the displacements which follow from the identifications scatter more than would be expected from the errors of the measures. On the other hand, the amount of the displacement, about 45 A, is in general agreement with the width of about 100 A shown by the narrowest emission bands in the early spectra. This displacement would indicate a radial velocity of about 3000 km/sec. Altogether, the identifications are hardly convincing enough to be considered as evidence for the reality of the suspected absorption lines.

The question may be raised whether the abrupt end of the spectrum in the ultraviolet is an indication of continuous absorption. The absence of strong emission bands in this region would warrant the assumption of continuous absorption only if identifications in other regions should lead us to expect the appearance of strong emission bands in the ultraviolet. The absence even of a continuous spectrum, however, deserves some discussion. The very strongly overexposed spectrogram of supernova IC 4182 obtained with a quartz spectrograph on September 10, 1937, shows no trace of a record below λ 3300. With the same instrument and exposure time, an early-type star of apparent photographic magnitude 12 would give a faint record in this region. Thus, one may conclude that, if only the continuous spectrum of the supernova were observed, the absolute photographic magnitude on this date would have been only −13 or fainter, instead of −16.2, as observed. The value −13 is an upper limit for the intensity of the continuous spectrum; and, on the assumption of black-body radiation, an upper limit for the tempera-

ture can be obtained for any value of the radius of the star. For a radius equal to that of the sun, we obtain $2.6 \cdot 10^9$ degrees as upper limit for the temperature, and, for smaller radii, values which increase with the inverse square of the radius. Temperatures of this order of magnitude would lead to the emission of an amount of energy which, integrated over the duration of the outburst, exceeds the equivalent of ordinary stellar masses converted into radiation.

TABLE 4

TENTATIVE IDENTIFICATIONS FOR SPECTRUM OF SUPERNOVA NGC 1003 ON SEPTEMBER 12.444, 1937

λ Obs.	Identification	Displacement
4813	4861 *Hβ*; 4859 *He* II	−47 A
4747	4798–4783 *O* IV	43
4646	4687 *He* II	41
4580*		
4530*		
4450		
4380		
4294	4340 *Hβ*; 4339 *He* II	46
4252		
4218	4262 *O* IV	44
4160	4190 *He* II	39
4048	4102 *H*; 4100 *He* II; (4089 *Si* II)	49
4011		
3988	4025 *He* II	37
3950	3995 *O* IV	45
3934	3975, 3977 *O* IV	−42

* Transitions $n = 5$ to $n = 6$ of *O* IV are to be expected in this region (cf. B. Edlén, *Zs. f. Ap.*, **7**, 383, 1933).

The actual temperature must have been lower; and if the radius of the star was not much larger than that of the sun, the absence of a continuous spectrum thus needs no explanation. For large values of the radius, on the other hand, the upper limit for the temperature decreases rapidly. Only if the star were greatly expanded would it be necessary, therefore, to explain the faintness of the continuous spectrum by continuous absorption in the ultraviolet.

From about two weeks on, after the star has reached its maximum brightness, the appearance of the spectrum leaves little doubt that the spectrum is composed essentially of wide and partially overlapping emission bands. These may be divided into three classes. The independence of the spectral regions below and above λ 5000, which

has already been discussed, can lead only to the conclusion that the permanent bands below λ 5000 differ in origin from the others. The variations in the relative intensities of the two parts of the spectrum indicate that the separation is complete in the sense that none of the strong original bands above λ 5000 is connected with the permanent bands below λ 5000. The two narrow bands which appeared in the red of supernova IC 4182 from February 21, 1938, on are of a different type from the other bands in the red; they increase in intensity while the others fade out.

The average wave lengths of the two narrow bands are λ 6299 and λ 6359. Within the errors of measurement they agree with the wave lengths of the [*O* I] lines λ 6300 and λ 6364. The relative intensities of the bands are also in good agreement with those of the [*O* I] lines. The fluctuations in the measured wave lengths of these only partially resolved bands are easily understood as due to variations in the intensity distribution, such as occur frequently in emission bands in ordinary novae. There can be hardly any doubt that these bands are to be identified as the nebular lines of [*O* I]. The absence of the auroral [*O* I] line λ 5577 may be taken as an indication that the lines are excited at extremely low pressure.[15] One difficulty presents itself, however. It is remarkable that only the two nebular lines of [*O* I] appear, unaccompanied by the lines of other origin which usually are seen with them. It is possible that this peculiarity may be explicable on the basis of the very small pressure, indicated by the absence of λ 5577, and the very small transition probability. Nevertheless, it is hard to understand how the lines can be excited without the appearance of other lines, unless the mechanism of the excitation is entirely different from that usually assumed for forbidden lines. With all reserve, the possibility of an increased abundance of oxygen as a result of nuclear reactions should, however, be mentioned.

The difficulties met in any attempt to identify the permanent bands below λ 5000 are obvious. The true wave lengths of these bands may be smaller than in the beginning or larger than in the latest spectra, depending on whether the explanation of the red shift is a real red shift or a decreasing violet shift. The discussion of the red

[15] I. S. Bowen, *Rev. of Modern Physics*, **8**, 72, 1936.

shift shows that these bands are probably emitted under conditions which are so peculiar that an identification with lines of known origin can hardly be expected. The merely temporary coincidence of one of the bands with a line of known origin cannot be considered as evidence. For this reason former identifications of these bands with lines of *N* III and *H* cannot be maintained. Besides, they are contradicted by the absence of lines above λ 5000, the presence of which should be expected; such lines should remain when the red part of the spectrum becomes faint. The invalidation of these identifications removes the only quantitative argument for the contention that the spectra of supernovae are similar to those of ordinary novae.

The red part of the spectrum is not subject to any considerable red shift. The main obstacle to identifications is thus missing. The fact that no lines below λ 5000 remain strong when the blue part of the spectrum becomes relatively faint, about 40 days after maximum, allows for bands above λ 5000 only such identifications as would not imply the presence of strong lines below λ 5000. Almost all known lines which could provide identifications for the strong and more permanent bands above λ 5000 are thus excluded. In particular, the hydrogen lines cannot be present; the assumption that *Hα* forms part of the first intensive band around λ 6500 is refuted by the absence of all other hydrogen lines. Similarly, the presence of *He* becomes at least extremely improbable; the band at about λ 5900 could be identified with *He* λ 5876, but all other *He* lines are certainly not present. The absence of *H* and *He* shows that the ionization in that part of the star's atmosphere in which the red lines appear is either very high or very low. The assumption of low ionization, which would permit an identification of the band at about λ 5900 with the *Na* D lines, is contradicted by the complete absence of other lines which would be expected to accompany the D lines, such as *Ca* I or *Ca* II, or numerous other lines in the observed range of the spectrum. We are thus led to the conception that the bands above λ 5000 are emitted by highly ionized atoms. The close coincidence, on September 11, 1938, of the two bands at λ 6085 and λ 5300 in supernova IC 4182, which emerged and disappeared simultaneously, with the forbidden lines of *Ca* V at λ 6086 and λ 5309 deserves mention in this connection as possible identifications. If the assump-

tion of very high ionization is justified, the failure to obtain identifications may be due merely to the incompleteness of our knowledge of the spectra of highly ionized atoms.

The conception that all bands in the spectra of supernovae are emitted under unique conditions of ionization and excitation possibly finds some support in the observations of the Crab nebula. It has become increasingly certain that the Crab nebula is the remnant of a former supernova.[16] If such is really the case, the final stage of a supernova does not differ from that of an ordinary nova. The Crab nebula shows the usual nebular spectrum,[17] developed by ordinary novae a few months after the outbreak; and the velocity of expansion of the nebula, about 1300 km/sec, is of the same order as that observed in ordinary novae. If the ejection of matter from a supernova coincides with the outbreak, as in ordinary novae, we might therefore expect the formation of a nebular spectrum only a few months after the maximum. The present observations show indisputably that this does not occur; at the most, the appearance of the [*O* I] lines may be the first step toward such a development. The absence of the nebular spectrum may be considered as a direct indication that, even a year after the supernova outbreak, the conditions of ionization and excitation are still widely different from those in ordinary novae.

CARNEGIE INSTITUTION OF WASHINGTON
MOUNT WILSON OBSERVATORY
October 1938

[16] W. Baade, *Mt. W. Contr.*, No. 600; *Ap. J.*, **88**, 285, 1938.

[17] N. U. Mayall, *Pub. A.S.P.*, **49**, 101, 1937.

THE ZERO POINT OF THE PERIOD-LUMINOSITY CURVE*

RALPH E. WILSON

ABSTRACT

From studies of radial velocities the group motion of 67 RR Lyrae variables has been found to be 119 ± 15 km/sec, and that of 157 Cepheids, 28.1 ± 1.4 km/sec. Their respective mean peculiar motions are 72 ± 5 and 14.0 ± 0.6 km/sec; and their rotational coefficients, 37 ± 20 and 27.4 ± 1.4, about a center in galactic longitude 326°.

Mean parallactic and peculiar motions in seconds of arc have been derived from the proper motions of 141 of these stars. Comparisons of these with the values in kilometers per second derived from the radial velocities give mean parallaxes of the proper-motion stars. Assuming Joy's value of the rotational constant, A = 20.9 km/sec per kiloparsec, the rotational coefficients give measures of the mean distances of the radial-velocity stars. The two sets of parallaxes, in combination with the corresponding sets of mean photographic magnitudes, determine two sets of absolute magnitudes which are in fair accord. The weighted means of the two determinations indicate corrections to the photographic period-luminosity curve amounting to ±0.00 ± 0.2 for the short-period variables, and −0.14 ± 0.2 for those of longer period, if we correct for galactic absorption of 0.85 mag. (photographic) per kiloparsec. When the data are further subdivided into period groups, the computed absolute magnitudes are in good agreement with those derived from the curve.

The conclusion is that the radial-velocity and proper-motion data now available confirm both the zero point and shape of the photographic period-luminosity curve.

Because the period-luminosity curve is a most effective yardstick for the measurement of cosmic distances, its zero point, the fundamental basis of the scale of distance, has been the subject of several investigations since Shapley[1] based his original determination upon the parallactic motions of but eleven of the brighter Cepheids. Studies by Gerasimovič,[2] Lundmark,[3] Oort,[4] Bok and Boyd,[5] and the writer,[6] among others, have indicated corrections to the zero point covering a range of approximately 1.5 mag. (absolute). This value is best determined through the relations between the mean parallactic and peculiar motions derived from proper motions and from radial velocities. The difficulty has been, and to a lesser extent still is, that we have had neither radial velocities nor good proper motions in sufficient numbers to warrant a great deal of confidence

* *Contributions from the Mount Wilson Observatory, Carnegie Institution of Washington*, No. 604.

[1] *Mt. W. Contr.*, No. 151; *Ap. J.*, **48**, 89, 1918.

[2] *A.J.*, **41**, 17, 1931.

[3] *Lund Medd.*, Ser. 2, **6** (No. 60), 1931.

[4] *B.A.N.*, **4**, 92, 1927.

[5] *Harvard Bull.*, No. 893, 1933.

[6] *A.J.*, **35**, 35, 1923.

in the result. The best determinations of mean parallactic and peculiar motions in kilometers per second, for instance, were based upon radial velocities of but 26 RR Lyrae variables and 37 Cepheids.[7] The strongest determinations in seconds of arc depend upon proper motions of but 47 and 51 variables, respectively.

Justification for further study at the present time of the mean absolute magnitudes of these variables is based upon three considerations: (1) the greatly increased number of radial velocities now available through observations at the Mount Wilson Observatory; (2) an appreciable increase in the quality and quantity of the proper motions of the Cepheids; and (3) knowledge of the effect of galactic absorption upon both the photometric data and the rotational constant. Furthermore, pending the completion of the programs for determining photographically the proper motions of these stars now under way at the Mount Wilson and McCormick observatories, there appears little prospect of an effective increase in the amount of data for some time to come.

I. DATA

Radial velocities.—Recent publications by Joy[8, 9] have given us the radial velocities of 67 RR Lyrae variables and 155 Cepheids. To the latter have been added the velocity of α UMi from Moore's *General Catalogue of Radial Velocities*[10] and an unpublished Mount Wilson value for V 383 Cyg. All have been used with equal weight.

Proper motions.—The faintness of the RR Lyrae variables in general precludes the determination of the proper motions of any considerable number of them from meridian observations of position. We are forced to rely almost exclusively upon the photographic determinations of Luyten, Mrs. Bok, and Miss Boyd at Harvard. To these we have added three based on meridian observations and one weak determination by Kapteyn and van Rhijn.[11] Several have been modified by combining two or three independent determinations with weights proportional to the quoted probable errors. The 55 proper motions of these stars are listed in Table 1.

[7] *Mt. W. Contr.*, No. 293; *Ap. J.*, **61**, 371, 1925.

[8] *Pub. A.S.P.*, **50**, 303, 1938.

[9] *Mt. W. Contr.*, No. 578; *Ap. J.*, **86**, 363, 1937.

[10] *Lick Obs. Pub.*, **18**, 10, 1932.

[11] *B.A.N.*, **1**, 40, 1922.

TABLE 1

PROPER MOTIONS OF RR LYRAE VARIABLES

Star	α_{1900}	δ_{1900}	m_{pg}	Per.	μ_α	μ_δ	Auth.*
SW And...	0^h18^m0	+28° 51′	9.3	0.44	+0″.003± 5	−0″.016± 5	H2, W
RR Cet....	1 27.0	+ 0 50	8.6	.55	+ .014 4	− .064 4	H2, K
U Tri....	1 49.7	+33 17	11.6	.45	+ .019 5	− .022 5	H2, K
TU Per....	3 1.8	+52 48	11.7	.61	+ .018 8	− .042 8	H2
X Ari....	3 3.1	+10 4	9.4	.65	+ .049 7	− .078 7	H2
SS Tau....	3 31.4	+ 5 2	12.2	.37	+ .026 8	+ .032 8	H2
RX Eri....	4 45.2	−15 54	9.2	.59	+ .011 6	+ .001 6	H2, W
U Lep....	4 52.0	−21 22	9.5	.58	+ .047 7	− .049 7	H2
RZ Cam...	6 23.6	+67 6	12.0	.48	+ .019 12	− .008 12	H1
TZ Aur....	7 4.6	+40 56	11.6	.39	+ .015 20	− .001 20	H1
RR Gem...	7 15.2	+31 4	10.2	.40	− .007 12	+ .025 12	H1
AI Vel....	8 11.3	−44 20	7.0	.11	+ .036 9	+ .054 9	B
RW Cnc....	9 13.2	+29 29	11.7	.55	+ .014 9	− .051 9	H2
X LMi...	10 0.1	+39 51	12.0	.68	+ .031 7	− .014 7	H2
RR Leo....	10 2.1	+24 29	9.4	.45	+ .007 10	− .004 10	H1
V LMi...	10 19.8	+29 8	10.7	.54	− .001 14	+ .016 14	H1
RX Leo....	11 18.7	+27 10	12.2	.65	+ .026 7	− .006 7	H2
SS Leo....	11 28.8	+ 0 31	11.1	.63	− .008 18	− .006 18	H1
SU Dra....	11 32.2	+67 53	9.2	.66	− .034 5	− .074 5	H2, W
UU Vir....	12 3.6	+ 0 6	10.3	.48	+ .001 20	− .005 20	H1
SW Dra....	12 13.1	+70 4	10.0	.57	− .020 7	− .006 7	H2
RR CVn...	12 24.2	+35 12	11.0	.56	− .004 8	+ .008 8	H2
SV Hya...	12 26.2	−25 37	10.9	.48	− .005 8	+ .014 8	H2
S Com...	12 27.8	+27 35	10.9	.59	− .021 12	+ .047 12	H1
U Com...	12 35.1	+28 3	11.8	.29	− .043 8	− .016 8	H2
Z CVn...	12 45.1	+44 19	10.2	.65	+ .006 11	− .020 11	H1
SX UMa..	13 22.3	+56 47	9.8	.31	− .038 8	+ .002 8	H2
RV UMa..	13 29.4	+54 30	9.8	.47	+ .017 8	− .018 8	H2
RU CVn...	13 55.1	+32 7	11.1	.57	− .025 5	.000 5	H2, K
W CVn...	14 2.2	+38 18	10.3	.55	− .039 4	− .012 4	H2, K, W
ST Vir....	14 22.5	− 0 27	10.8	.41	+ .005 4	− .020 4	H1, K
SW Boo....	14 23.4	+36 30	10.8	.51	− .057 8	+ .009 8	H2
RS Boo....	14 29.3	+32 12	10.3	.38	+ .002 4	+ .005 4	H2, K
SZ Boo....	14 37.9	+28 38	11.6	.52	.000 7	− .007 7	H2
ST Boo....	15 26.8	+36 8	10.8	.62	− .013 7	+ .014 7	H2
RW CrB...	15 35.2	+29 56	10.2	.73	− .014 7	− .008 6	W
RV CrB...	16 15.5	+29 57	11.5	.33	− .009 7	− .004 7	H2
VX Her....	16 26.2	+18 36	10.4	.46	+ .017 9	− .023 9	H2
RW Dra....	16 33.7	+58 3	10.4	.44	− .006 7	− .002 7	H2
VZ Her....	17 8.8	+36 6	11.5	0.44	−0.026 7	−0.032 7	H2

* Authorities: B, Boss; H1, Harvard, Luyten; H2, Harvard, Bok and Boyd; K, Kapteyn and van Rhijn; W, Wilson.

TABLE 1—*Continued*

Star	α_{1900}	δ_{1900}	m_{pg}	Per.	μ_α	μ_δ	Auth.*
ST Oph...	$17^h28^m.8$	− 1° 1′	11.6	0.45	−0″.005± 4	+0″.001± 4	H2, K
TW Her....	17 50.7	+30 26	11.5	.40	+ .003 7	− .029 7	H2
S Ara....	17 51.5	−49 25	10.0	.45	− .015 13	− .010 13	H1
Y Lyr....	18 34.2	+43 52	11.8	.50	− .006 8	− .001 8	H2
RZ Lyr....	18 39.9	+32 42	10.4	.51	+ .004 8	+ .033 8	H2
RR Lyr....	19 22.3	+42 36	7.6	.57	− .122 1	− .193 1	W
XZ Cyg....	19 30.4	+56 10	9.7	.47	+ .081 7	− .027 6	H2, W
XX Cyg....	20 1.3	+58 40	11.8	.13	− .001 8	− .015 8	H2
AA Aql....	20 33.1	− 3 14	12.0	.36	− .007 7	− .002 7	H2
UY Cyg....	20 52.3	+30 3	10.0	.56	− .001 7	+ .016 7	H2
RV Cap....	20 55.9	−15 37	10.0	.45	+ .035 6	− .118 6	H2
SW Aqr....	21 10.2	− 0 20	10.4	.46	− .054 4	− .045 4	H2, K
SX Aqr....	21 31.1	+ 2 47	11.8	.54	− .005 4	− .030 4	H2, K
VV Peg....	22 8.3	+17 46	11.2	.49	+ .001 8	+ .031 8	H2
RZ Cep....	22 35.7	+64 20	9.5	0.31	+0.082 14	+0.179 14	K

The improvement in the proper-motion situation, in so far as the Cepheids are concerned, is not so much in the number now available as in their accuracy from the standpoint of both systematic and accidental error. A good many of these stars appear in the *Boss General Catalogue*.[12] All variables brighter than 8.0 visual magnitude at maximum were placed on the observational program leading up to the formation of this catalogue, and special efforts were made to determine their positions. Likewise, special programs at other observatories—notably Lund, Bergedorf, and Lyon—have emphasized determinations of positions of variable stars. Only those lists which were included in the more general catalogues of position, with sufficient observations of fundamental stars to tie them to the standard system, were used in the *General Catalogue*. The completion of this catalogue, however, afforded the opportunity to derive from the variables themselves approximate values of systematic corrections which would reduce the observations in the various special lists to the *G.C.* system. This reduction has been made by the writer; the positions and proper motions of the *G.C.* have been revised in all cases in which the added material warranted a revision; and some four hundred new proper motions have been determined. Among

[12] *Carnegie Inst. of Washington Pub.*, No. 468, 1938.

these are a number of Cepheids. We have also added a few determinations by Gerasimovič[2] where it was apparent that he had used observations of position as yet unpublished, or at least not listed in current references to published positions. The proper motions of 86 of these stars are listed in Table 2.

The wide range in the accuracy of the proper motions forces the adoption of a system of weights. If the data were abundant, it would be advisable to reject all proper motions with probable errors exceeding 0".010 and to use the balance without weights. The scarcity of data, however, compels the use of the weaker proper motions. For the RR Lyrae variables we have used all the Harvard data with quoted probable errors up to 0".020. In view of the minuteness of the average motions of the Cepheids, approximating, as they do, the size of the probable errors involved, we have rejected all proper motions of these stars with probable errors exceeding 0".015. The following system of weights was then adopted.

P.E.	Weight
0".001–0".005	1.5
.006– .010	1.0
.011– .012	0.7
.013–0.014	0.5
0.015–	0.3

II. THE APEX AND THE GALACTIC ROTATION

The relations which lead to the determination of the solar motion are based upon the assumption of at least approximate uniformity of distribution of the reference stars over the sky. Unfortunately, neither the RR Lyrae variables nor the Cepheids whose motions are known are so distributed, nor are their respective distributions at all similar. The former, though fairly uniformly distributed in galactic latitude, are strongly concentrated in longitudes 0°–180°, 70 per cent of them lying on one side of the direction toward the solar apex referred to the stars in general. The latter, on the other hand, show a good distribution in galactic longitude but are overwhelmingly concentrated within a few degrees of the galactic plane, only 6 of the 157 having galactic latitudes in excess of 20°. Nor are the motions of the two classes of stars at all similar. The radial velocities of the RR Lyrae variables range from 0 to 390 km/sec with a high median

TABLE 2

PROPER MOTIONS OF δ CEPHEI VARIABLES

Star	α_{1900}	δ_{1900}	m_{pg}	Per.	μ_α	μ_δ	Auth.*
TU Cas...	0^h20^m9	+50° 44′	8.3	2.14	−0″.020 ± 5	−0″.009 ± 6	W
UZ Cas...	1 6.4	+60 41	11.9	4.26	− .007 7	.000 7	H
α UMi..	1 22.6	+88 46	3.3	3.97	+ .058 1	− .004 1	B
VX Per....	2 0.8	+57 58	10.0	10.90	− .035 15	− .040 13	G
SU Cas...	2 43.0	+68 28	6.8	1.95	+ .009 2	− .007 2	B
RW Cam..	3 46.2	+58 22	9.4	16.41	− .029 12	− .014 10	W
RX Cam..	3 56.7	+58 23	8.7	7.92	− .021 10	− .009 9	W
SZ Tau...	4 31.4	+18 20	7.0	3.15	− .014 8	− .007 8	B
SV Per....	4 42.8	+42 7	9.3	11.13	− .007 10	− .005 10	G, K, W
RX Aur...	4 54.5	+39 49	8.3	11.62	− .004 7	− .007 6	W
Y Aur...	5 21.5	+42 21	9.7	3.86	+ .011 12	− .010 12	W
β Dor...	5 32.8	−62 33	5.0	9.84	− .007 3	+ .004 3	B
ST Tau...	5 39.4	+13 32	8.7	4.03	+ .001 9	+ .002 8	W
SV Mon..	6 16.1	+ 6 31	9.4	15.23	− .039 12	− .027 11	W
RS Ori....	6 16.5	+14 44	9.2	7.57	− .004 14	− .021 11	W
T Mon..	6 19.8	+ 7 8	7.3	27.01	+ .012 7	.000 5	W
RT Aur...	6 22.1	+30 33	6.0	3.73	+ .005 2	− .016 2	B
W Gem..	6 29.2	+15 24	7.4	7.91	+ .013 6	− .007 7	W
ζ Gem..	6 58.2	+20 43	4.5	10.15	− .004 1	− .003 1	B
X Pup...	7 28.5	−20 42	9.4	25.96	+ .014 12	+ .001 12	W
AH Vel....	8 9.8	−46 24	6.4	4.23	− .010 5	+ .004 5	B
V Car...	8 26.7	−59 47	8.8	6.70	− .004 8	− .016 6	B
RZ Vel....	8 33.6	−43 46	7.6	20.40	− .021 8	.000 6	B
SW Vel....	8 40.4	−47 3	8.7	23.51	− .042 11	− .009 8	B
SX Vel....	8 41.5	−45 58	9.0	9.55	− .011 11	− .006 8	B
V Vel....	9 19.2	−55 32	7.6	4.37	− .009 13	− .025 12	W
l Car...	9 42.5	−62 3	4.8	35.52	− .015 3	+ .007 3	B
UX Car...	10 25.4	−57 6	9.8	3.68	− .021 15	− .027 14	W
Y Car...	10 29.4	−57 59	8.7	3.64	− .023 14	+ .012 12	G
VY Car...	10 40.6	−57 2	8.6	18.98	+ .045 14	− .045 13	W
U Car...	10 53.7	−59 12	8.6	38.72	+ .011 8	+ .006 6	B
ER Car...	11 5.4	−58 18	8.0	7.72	+ .002 8	− .024 6	B
S Mus...	12 7.4	−69 36	6.9	9.66	− .010 8	− .021 7	B
T Cru...	12 15.9	−61 44	8.2	6.73	− .005 8	.000 6	B
R Cru...	12 18.1	−61 4	8.3	5.83	+ .012 9	− .023 7	B
AG Cen...	12 35.7	−59 14	8.8	3.84	+ .018 14	− .010 13	W
R Mus...	12 36.0	−68 52	7.7	7.51	+ .006 8	− .014 6	B
S Cru...	12 48.4	−57 53	7.9	4.69	− .013 9	− .014 7	B
W Vir....	13 20.9	− 2 52	10.4	17.27	+ .009 12	+ .005 9	B
XX Cen...	13 33.8	−57 6	7.6	10.96	−0.012 9	−0.031 8	B

* Authorities: B, Boss; G, Gerasimovič; H, Harvard; W, Wilson.

TABLE 2—*Continued*

Star	α_{1900}	δ_{1900}	m_{pg}	Per.	μ_α	μ_δ	Auth.*
V381 Cen...	13^h44^m0	−57° 5′	8.3	5.08	−0″.033 ± 12	0″.000 ± 10	B
V Cen...	14 25.4	−56 27	8.1	5.49	− .024 9	− .021 7	B
R TrA...	15 10.8	−66 8	7.1	3.39	− .004 7	− .027 6	B
S TrA...	15 52.2	−63 30	6.9	6.32	− .005 9	− .011 7	B
U TrA...	15 58.4	−62 38	8.8	2.57	+ .026 15	− .024 13	B
S Nor...	16 10.6	−57 37	7.1	9.75	+ .002 6	− .008 5	B
RV Sco...	16 51.8	−33 27	7.6	6.06	− .005 15	− .036 14	B, G
BF Oph...	16 59.9	−26 27	8.2	4.07	− .001 6	+ .003 5	B
X Sgr....	17 41.3	−27 48	5.1	7.01	− .003 2	− .014 2	B
RY Sco...	17 44.3	−33 40	8.9	20.31	+ .024 9	+ .021 9	B
Y Oph...	17 47.3	− 6 7	7.3	17.12	+ .003 5	− .015 5	W
W Sgr....	17 58.6	−29 35	5.2	7.59	+ .010 3	− .006 3	B
AP Sgr....	18 7.0	−23 9	7.7	5.06	− .008 7	− .010 6	B
WZ Sgr....	18 11.1	−19 6	9.0	21.85	+ .013 8	− .008 6	W
Y Sgr....	18 15.5	−18 54	6.2	5.77	+ .010 5	− .013 5	B
XX Sgr....	18 19.0	−16 51	9.5	6.42	− .013 12	− .002 11	W
U Sgr....	18 26.0	−19 12	7.9	6.74	− .009 4	− .005 4	W
RU Sct...	18 36.7	− 4 13	10.6	19.70	− .028 12	+ .021 12	W
SS Sct....	18 38.3	− 7 50	8.4	3.67	− .012 7	+ .023 6	W
V350 Sgr....	18 39.3	−20 45	8.0	5.15	+ .004 11	− .035 12	W
YZ Sgr....	18 43.7	−16 50	8.0	9.55	− .001 5	− .005 4	W
BB Sgr....	18 45.1	−20 24	7.6	6.64	+ .008 5	− .033 6	W
κ Pav...	18 46.6	−67 21	5.1	9.11	− .006 4	+ .009 3	B
FF Aql...	18 53.8	+17 14	6.0	4.47	− .009 3	− .011 4	B
SZ Aql...	18 59.6	+ 1 9	10.4	17.14	− .014 9	+ .026 9	W
TT Aql...	19 3.2	+ 1 9	8.3	13.75	− .015 4	− .012 4	W
U Aql...	19 24.0	− 7 15	7.3	7.02	+ .031 6	− .013 5	W
U Vul...	19 32.3	+29 7	8.2	7.99	− .007 4	− .028 4	W
SU Cyg...	19 40.8	+29 1	7.3	3.85	+ .004 8	− .009 6	W
SV Vul...	19 46.8	+27 12	8.8	45.13	− .012 6	− .004 5	W
η Aql...	19 47.4	+ 0 45	5.0	7.18	+ .007 1	− .008 1	B
S Sge...	19 51.5	+16 22	6.3	8.38	− .001 2	− .007 2	B
X Vul...	19 53.3	+26 17	9.2	6.32	− .009 8	+ .012 7	W
CD Cyg...	20 0.6	+33 50	9.8	17.07	− .007 9	+ .022 10	G
SZ Cyg...	20 29.6	+46 16	10.3	15.11	− .013 13	− .001 12	W
X Cyg...	20 39.5	+35 14	7.4	16.39	− .017 4	+ .001 3	W
T Vul...	20 47.2	+27 52	6.4	4.44	− .003 3	− .003 2	W
VX Cyg...	20 53.6	+39 48	10.4	20.12	+ .002 14	+ .025 15	W
DT Cyg...	21 2.3	+30 47	5.9	2.50	− .005 3	− .003 3	B
VZ Cyg...	21 47.7	+42 41	9.5	4.86	− .017 13	+ .012 12	W
Y Lac...	22 5.2	+50 33	8.6	4.32	+ .014 11	+ .002 15	G, W
δ Cep...	22 25.4	+57 54	4.2	5.37	+ .012 1	+ .002 1	B
Z Lac...	22 36.9	+56 9	9.1	10.89	− .018 14	− .010 12	G, W
RR Lac...	22 37.5	+55 55	9.3	6.42	− .001 12	− .025 11	W
V Lac...	22 44.6	+55 48	9.3	4.98	− .019 11	+ .017 10	W
X Lac...	22 45.0	+55 54	9.1	5.44	+0.017 14	−0.024 12	G

value; those of the Cepheids range from 0 to 93 km/sec. But, as Joy has shown,[13] the greater part of the latter range is due to rotation effects. The mean proper motions of the former are likewise known to be large relative to the latter. We are thus forced to treat the two sets of stars separately, hereafter designating the RR Lyrae variables as "group I" and the Cepheids as "group II." Since the two groups have widely differing distributions and motions, and since the radial velocities and proper motions are affected differently by the anomalous distributions, it would hardly be reasonable to expect that the four sets of data would give even approximately the same values for the direction of the solar apex. Before we adopt a value for the apex, however, it is desirable that we find out what the data do indicate.

Radial velocities.—The radial velocities have been analyzed by means of the well-known relation

$$V = K + X \cos b \cos l + Y \cos b \sin l + Z \sin b + du + ev ,$$

in which K denotes the K term; X, Y, and Z, the components of the solar motion in galactic co-ordinates; and l and b, the galactic longitude and latitude. Also

$$u = \bar{r}A \cos 2l_0 , \qquad d = \sin 2l \cos^2 b ,$$

$$v = \bar{r}A \sin 2l_0 , \qquad e = -\cos 2l \cos^2 b ,$$

where A is the constant of galactic rotation, $\bar{r}$ the mean distance in kiloparsecs, and l_0 the longitude of the center of rotation. Finally we denote the mean of the peculiar motions taken without regard to sign by θ. The results of these analyses are given in Table 3.

In view of the large probable errors and the peculiar distribution of the stars involved, the results from group I are not disconcerting. The determinations of K and the rotational terms are seriously affected by the distribution and in turn produce large uncertainties in the derived position of the apex.

In group II the geometrical problem is somewhat different, for there we have good distribution in longitude but very high galactic concentration. As a result we should get a good determination of

[13] *Mt. W. Contr.*, No. 607; *Ap. J.*, **89**, 1939; in press.

galactic rotation, a fair determination of the longitude of the apex, but a poor determination of its latitude. We actually get from the rotational terms a direction of the galactic center in excellent agreement with the best modern results and a value of $\bar{r}A$ in good agreement with Joy's results[13] based upon the assumed apex ($A_0 = 271°$, $D_0 \infty +28°$). The longitude of the apex, however, comes out about 15° greater than the conventional position, while the latitude, affected by four times the probable error attached to the longitude, comes very close to the standard position.

TABLE 3

RESULTS FROM RADIAL-VELOCITY SOLUTIONS

	Group I ($P<1$ Day)	Group II ($P>1$ Day)
K	+ 10 ± 8 km/sec	− 1.7 ± 0.9 km/sec
X	− 86 15 km/sec	− 20.7 1.2 km/sec
Y	−118 19 km/sec	− 17.7 1.6 km/sec
Z	− 34 14 km/sec	− 10.0 6.0 km/sec
u	+ 67 22 km/sec	+ 10.4 1.4 km/sec
v	+ 2 ±21 km/sec	− 23.4 ± 1.5 km/sec
V_0	150 ±16 km/sec	29.0 ± 2.9 km/sec
l_a	54° 6°	40°.5 3°.0
b_a	+ 13° 6°	+ 20°.2 12°.2
$\bar{r}A$	67 22 km/sec	25.6 1.5 km/sec
l_0	1° 18°	326°.9 2°.8
θ	72 ± 5 km/sec	14.0 ± 1.0 km/sec
No.	67	157

The most surprising result of this solution is, however, that through the quadrupling of the data and the consideration of rotation effects the value of the deduced solar speed is much greater than that resulting from previous investigations. From 37 radial velocities Strömberg[7] derived in 1923 a solar speed of but 11.5 km/sec. After the discovery of galactic rotation Oort[4] showed that its effect would increase Strömberg's value to more nearly the conventional speed of 20 km/sec. The value here derived, in conjunction with the still higher value referred to the RR Lyrae variables, would suggest that, as we go farther out into space, the group motions of the stars, and consequently the reflected solar motions, tend to increase.

Proper motions.—The corrections to the Newcomb precessions derived by Wilson and Raymond[14] were applied to the proper motions in Table 2. In order to attempt the determination of possible rotational effects, all the proper motions were transformed to proper motions relative to the galaxy in the form $\mu_l \cos b$ and μ_b. These quantities were then analyzed by means of the relations

$$\mu_l \cos b = X \sin l - Y \cos l + Q \cos b + C \cos 2l \cos b + S \sin 2l \cos b ,$$

$$\mu_b = X \cos l \sin b + Y \sin l \sin b - Z \cos b - \frac{C}{2} (\sin 2l \sin 2b) + \frac{S}{2} (\cos 2l \sin 2b) ,$$

where X, Y, Z, l, and b have the same significance as in the radial-velocity equations and Q, S, and C are the rotational constants.

$$Q = \frac{B}{4.74} , \qquad C = \frac{A}{4.74} \cos 2l_0 , \qquad S = \frac{A}{4.74} \sin 2l_0 .$$

The results of these analyses are given in Table 4.

TABLE 4

RESULTS FROM PROPER-MOTION SOLUTIONS

	Group I (Unit, 0".01)	Group II (Unit, 0".01)
X	+0.79 ±0.31	+0.22 ±0.15
Y	+1.33 .30	+ .43 .16
Z	−0.26 .35	+ .56 .11
Q	+0.62 .42	− .06 .12
C	−1.21 .50	− .01 .16
S	−1.11 ±0.48	0.00 ±0.17
$q = h/\rho$	1.57 ±0.32	0.74 ±0.14
l_a	59° 12°	63° 17°
b_a	− 10° 12°	+ 49° 11°
$P = A/4.74$	1.64 0.49	0.01 ±0.17
l_0	291° ± 17°	.....
No.	55	86
Solar motion only:		
q	2.10 ±0.32	0.75 ±0.14
l_a	53° 12°	63° 17°
l_b	+ 10° ± 12°	+ 48° ± 11°

[14] *A.J.*, **47**, 57, 1938.

In confirmation of the results of Gerasimović's investigation we find here no evidence of rotation effects in the proper motions of group II. The proper motions of group I, on the other hand, give indications of a very large but also extremely uncertain rotation about a center 70° distant from that given by their radial velocities. The mean of the two discordant values of the longitude of the rotational center is 326°, a purely fortuitous agreement with that derived from the radial velocities of group II.

The results for the position of the apex given in Tables 3 and 4 show neither accord between the two types of variables nor accord between the results based upon radial velocities and proper motions within each type. We believe that this lack of agreement is primarily due to distribution, the anomalies of which are not only different in the two types but operate differently upon the two sets of data. It is evident, therefore, that in order to reduce the distances to be derived by comparison of the data to a common basis, we must adopt a position of the solar apex. The only consistency in the positions derived above is that all the solutions give an unexpectedly large longitude and hence a high declination for the apex. This is partly due to distribution, but there may be other contributing factors. For example, there is evidence from analyses of both proper motions and radial velocities of stars of all types which indicates an increase in longitude, and hence in declination, of the solar apex with decrease in brightness. Wilson and Raymond[15] have recently shown, also, that the stars of small proper motions and presumably greater mean distance give relatively high apical declinations. So, since the Cepheids themselves give a very uncertain declination of over $+50°$ and the conventional declination, $+30°$, appears to be somewhat low for stars similar in magnitude and proper motion to the Cepheids, we have adopted as co-ordinates of our standard apex, $A_0 = 270°, D_0 = +36°$. A_0 has its conventional value, and D_0 is taken from the determination of Wilson and Raymond referred to 26,978 stars with proper motions $< 10''$ per century. We adopt for the direction of the galactic center the value given by the Cepheids themselves, $l_0 = 326°$.

[15] *Ibid.*, p. 65.

III. THE MEAN PARALLACTIC AND PECULIAR MOTIONS

Radial velocities.—The directions of the apex and the rotational center having been fixed, least-squares solutions were made to determine new values of K, V_0, $\bar{r}A$, and θ by means of the relation

$$V = K + V_0 \cos \lambda + \bar{r}A \sin 2(l - 326^\circ) \cos^2 b ,$$

the only new symbol introduced being λ, the distance of the star from the adopted apex. The results are given in Table 5.

TABLE 5

RESULTS OF RADIAL-VELOCITY ANALYSES
(Apex and Galactic Center Assumed)

	Group I	Group II
	km/sec	km/sec
K	− 3± 8	− 3.0±1.0
V_0	119 15	28.1 1.4
$\bar{r}A$	+ 37 20	+27.4 1.4
θ	72± 5	14.0±0.6

In group II the adoption of a standard apex has produced rather insignificant changes in the unknowns. The changes produced in group I are much larger, but so also are the probable errors. In this case the use of the five largest radial velocities (>240 km/sec) in the determination of $\bar{r}A$ was questionable. The value derived was +45 km/sec. We preferred to give them no more than half-weight in the determination of this quantity, and the resulting value is that given in the table.

The most significant result of these solutions is the lack of any change in the values of the mean peculiar motions θ, in spite of the adoption of an apex somewhat different from that indicated by the data. Although the apex is practically indeterminate, we feel that the mean peculiar motions are fairly well determined. It should be stated that the mean peculiar motion of group II was determined in two ways. Use of the mean value of $\bar{r}A$ in Table 5 gives $\theta = 14.2$. Using Joy's value of A (20.9 km/sec/kpc) out to about 2 kpc, as determined from the period-luminosity curve, and beyond that

point a flat value of 40 km/sec (also from Joy's work), we get $\theta = 13.8$. The mean is given in Table 5.

Proper motions.—The components of the proper motions in the direction of the solar apex, v, and at right angles to it, τ, were computed. For group I they were reduced to the mean photographic magnitude, 10.5. In group II no such reduction is necessary or desirable; the proper motions of the brighter stars are small, and reduction to a mean magnitude would produce large unbalanced errors in

TABLE 6

PROPER-MOTION DATA

(Unit, 0".01)

	Group I	Group II
$\overline{\log P}$	−0.32	+0.89
$\bar{m}_{pg}$	10.50	7.96
No.	55	86
μ_{med}	2.75	1.60
$\bar{\mu}$	3.62	1.79
Wt.	56.2	85.0
$\bar{\tau}$	−0.08±0.28	−0.03±0.08
$\bar{v}$	+1.39±0.26	+0.59±0.10
τ_{med}	1.40	0.85
τ_{av}	2.27±0.30	1.04±0.09
$\bar{\rho}$	0.70	0.67
ρ_0	0.82	0.78
q	1.92±0.34	0.79±0.13

the resulting motions of the fainter stars. Mean, median, and average values of the data in the two groups are given in Table 6. Here $q = \Sigma v \sin \lambda / \Sigma \sin^2 \lambda$ is the mean parallactic motion in seconds of arc per century, τ_{med} and τ_{av} are the median and mean values of τ taken without regard to sign, and $\bar{\rho}$ is the mean of the quoted probable errors of the determinations of proper motion. The values of τ_{med} and τ_{av} are not the true values of the peculiar motions. In using proper motions with relatively large probable errors we artificially increase the mean or median τ as computed from individually properly weighted τ's taken without regard to sign, an error which is largely compensated for in the mean parallactic motion derived from the algebraic mean.

Kapteyn[16] has shown that the observed and true means of proper

[16] *Groningen Pub.*, No. 30, p. 52, 1920.

motions, taken without regard to sign, are quite approximately related in the form

$$\mu_0^2 = \bar{\mu}^2 - \kappa\bar{\rho}^2 ,$$

where μ_0 is the true mean; $\bar{\mu}$, the observed mean; $\bar{\rho}$, the probable error of unit weight; and κ, a factor determined empirically. The values of τ may be treated in the same manner. Thus we have

$$\tau_0^2 = \tau_{av}^2 - \kappa\bar{\rho}^2 .$$

This is equivalent to the well-known relation

$$\tau_0^2 = \tau_{av}^2 - \eta^2 ,$$

where η denotes average error in place of probable error. If the data are sufficient, the equation in the form given by Kapteyn has the distinct advantage of taking account empirically of underestimation of probable error.

TABLE 7

DEPENDENCE OF τ_{av} ON PROBABLE ERROR

(Unit, 0".01)

GROUP I				GROUP II			
$\bar{\rho}$	τ_{av}	τ_{med}	No.	$\bar{\rho}$	τ_{av}	τ_{med}	No.
0.41	2.18	1.70	12	0.21	0.50	0.50	13
0.69	1.89	1.20	17	0.44	0.86	0.80	9
0.83	2.54	1.65	16	0.65	1.01	0.70	13
1.20	2.78	1.70	5	0.84	1.02	0.80	19
1.72	3.10	1.40	5	1.05	1.37	1.30	6
				1.22	1.68	1.40	13
				1.44	2.15	1.90	12

The correlations between τ_{av}, τ_{med}, and $\bar{\rho}$, in which $\bar{\rho}$ is derived from the quoted probable errors, are shown in Table 7. Least-squares solutions of these data for κ and τ_0 give:

	Group I	Group II	
κ_1	1.9	1.9	Average
κ_2	0	1.2	Median
τ_{01}	2.06	0.40	Average
τ_{02}	1.40	0.40	Median

The large values of κ_1 in both groups indicate that the probable errors have been underestimated by about 17 per cent. For both groups the true values, ρ_0, are 1.17 times the values of $\bar{\rho}$ quoted in Table 6, or 0.82 and 0.78; the true values of the average errors, η, thus become 0.97 and 0.92, respectively. The difference between the values of the true τ_{01} and τ_{02} in group I is largely due to four apparently abnormal reduced proper motions: SS Tau (12^m2), $\mu_r = 9''.2$; RW Cnc (11^m7), $9''.5$; RV Cap (10^m0), $9''.8$; and RZ Cep (9^m5), $12''.4$. The radial velocities are not abnormal ($+5$, -85, -80, and 0 km/sec, respectively). The omission of these four stars would reduce τ_{av} to $1''.97$, τ_{01} to $1''.71$, and τ_{02} to $1''.35$. The median value, τ_{02}, probably represents better than τ_{01} the mean peculiar motion of group I.

IV. THE MEAN PARALLAXES

From the parallactic and peculiar motions derived above we get the mean parallaxes of the two classes of stars through the relations

$$\pi_q = \frac{kq}{V_0} \quad \text{and} \quad \pi_\tau = \frac{k\tau_0}{\theta},$$

in which $k = 0.04737$, since q and τ_0 were derived in seconds of arc per century. They are, in units of $0''.001$:

	Group I	Group II	
π_q	$0.73 \pm .13$ $0.76 \pm .13$	$1.27 \pm .24$ $1.40 \pm .22$	From Table 4* From Table 6
π_τ	1.36 0.92 $\pm .20$	1.35 1.35 $\pm .30$	From τ_{01} From τ_{02}

* Mean of two values of q used.

The agreement between the values of π_q and π_τ in group II is eminently satisfactory. The accord in group I is not so good. The large value of π_τ is due partly to the four stars with abnormal proper motions mentioned above. If we leave these out, π_τ from the average τ_{01} reduces to 1.13 and that from the median τ_{02} to 0.89; and there still remains a considerable difference between π_q and π_τ for

this group. It is desirable, therefore, to check the mean parallaxes derived above by other methods.

In *Mt. W. Contr.* No. 558,[17] Strömberg summarizes various methods of using proper-motion and radial-velocity data to secure values of mean parallaxes. Let us apply his formula (13),

$$\bar{\pi} = \frac{\Sigma(A\mu_1 + B\mu_2)}{p\Sigma(A^2 + B^2)} = \frac{k\Sigma\mu \sin\lambda}{pV_0\Sigma \sin^2\lambda},$$

in which μ_1 and μ_2 are the proper motions in arc in right ascension and declination, respectively, and A and B are functions of V_0 and the position of the apex. If the group motion projected on an axis toward the standard apex is numerically equal to the standard velocity, p is equal to unity and the formula is equivalent to $\pi_q = kq/V_0$, the formula used above. Inasmuch as we are using the velocity given by the groups under discussion and an apex which apparently represents the data as well as any, presumably we might assume $p = 1$ without introducing any appreciable error. We have, however, computed values of p as a check and find that the assumption is permissible. The first part of formula (13) presents the distinct advantage of deriving a value of $\bar{\pi}$ directly from the proper motions without computing the τ- and v-components. From it we find

$$\pi_q = 0.77 \text{ (I)}, \qquad 1.38 \text{ (II)} \qquad \text{(unit, 0''.001)}.$$

Since we have already computed the v-components of the proper motions, we may also use formula (15) of the same article,

$$\bar{\pi} = \frac{\Sigma v}{p\Sigma\sqrt{A^2 + B^2}} = \frac{k\Sigma v}{pV_0\Sigma \sin\lambda}.$$

From the first part of this formula we find

$$\pi_q = 0.80 \text{ (I)}, \qquad 1.43 \text{ (II)} \qquad \text{(unit, 0''.001)}.$$

The stars of group II being strongly concentrated near the galactic plane, we get still another determination of π_q from the projection

[17] *Ap. J.*, **84**, 555, 1936.

of the proper motions on the galactic plane. Using equations (34) of Strömberg's paper in the form

$$\bar{\pi} = \frac{\Sigma A_l \mu_l}{p \Sigma A_l^2},$$

we find

$$\pi_q = 1.11 \text{ (II)} \qquad \text{(unit, } 0''.001).$$

The values of π_q derived by different methods are, therefore, in satisfactory agreement.

For the peculiar motions we have the relations derived from Strömberg's formulae (11),

$$\bar{\epsilon} = \overline{\eta + \frac{\pi\theta}{k}} = \tfrac{1}{2}[\overline{\mu_1 - pA\pi} + \overline{\mu_2 - pB\pi}],$$

all means being taken without regard to sign. To solve this equation, we must know an approximate value of $\bar{\pi}$. This we have from the values of π_q. $\bar{\epsilon}$ is then determined from the last term in the equation, and we have

$$\bar{\epsilon}_{\text{av}} = 2''.30 \text{ (I)}, \qquad 1''.06 \text{ (II)},$$
$$\bar{\epsilon}_{\text{med}} = 1''.90 \text{ (I)}, \qquad 0''.90 \text{ (II)}.$$

Values of π_r are then determined by the relation (16) of Strömberg,

$$\bar{\pi} = \frac{k}{\theta} \sqrt{\bar{\epsilon}^2 - \bar{\eta}^2},$$

$\bar{\eta}$ being the average error previously determined. The treatment of the median values of $\bar{\epsilon}$ in order to secure true values is not so simple. The assumption that the same relation holds between median values and probable errors as between average values and average errors will, however, give comparable results. It should be pointed out that, even if the parallax assumed in determining $\bar{\epsilon}$ is essentially correct, $\bar{\epsilon}_{\text{av}}$ will in general be larger than τ_{av}, and the parallax derived from it will be too large. This is due to two factors. First, $\bar{\epsilon}$ is the average of the peculiar motions in right ascension and declina-

tion and thus is equivalent to the combination of the average τ with the average residual resulting from correction for parallactic motion. Second, the statistical effect of the use of a constant value π for the solution of equations determining the values of residual v or of $\bar{\epsilon}$ is such as to produce values of these quantities that are too large, and hence mean parallaxes based upon them that are also too large. In dealing with stars with large dispersion in distance, therefore, this method should be used with caution. In taking the means to determine π_τ we have given it half-weight. The values of π_τ derived through $\bar{\epsilon}$ are

π_τ =	1.38 (I), 1.76 (II)	average	
	1.10	4 rejections	(unit, 0".001)
	1.13 1.72	median	

From the well-known relation

$$\pi_\tau = \frac{k}{\theta}\sqrt{\tau_{\mathrm{uv}}^2 - \bar{\eta}^2}\,,$$

which is not subject to the foregoing criticism, we find

π_τ =	1.35 (I), 1.62 (II)	average	
	1.13	4 rejections	(unit, 0".001)
	0.75 1.12	median	

It is clear from these results that the differences between the mean parallaxes derived from the parallactic and the peculiar motions, as well as the range in the latter, arise from weakness in the proper-motion data rather than from the methods of treatment. Moreover, we are dealing with very small parallaxes, and the results are probably carried beyond a point justified by the data. The straight means of each set of determinations certainly give a fair representation of mean parallax. The various determinations are summarized in Table 8.

In determining $\bar{\pi}_m$ from the values of π_q and π_τ for group I a proper weighting is important, in view of the apparently systematic difference between them. From the probable errors of q and τ de-

rived from the solutions the relative weights would be $\pi_q:\pi_r::$ 2.4:1 (I) and 1.7:1 (II). From Russell's criterion[18] they would be 1.2:1 and 1.4:1, respectively. It has been shown, however, that the effects of the weaker determinations of proper motion enter systematically into the determinations of π_r, whereas they tend to eliminate each other in the determination of π_q. Although we have attempted to take account of this correlation in various ways, the

TABLE 8

MEAN PARALLAXES

(Unit, 0".001)

Method	π_q		Method	π_r	
	Group I	Group II		Group I	Group II
Table 4	0.73	1.27	Kapteyn	1.13	1.35
Table 6	.76	1.40	$\bar{\tau}$-comp.	1.05	1.37
(13)	.77	1.38	ϵ-comp.	1.20	1.74
(15)	0.80	1.43	(wt., $\frac{1}{2}$)		
(34)	.....	1.11			
Mean	0.76	1.30	Mean	1.11	1.44

dependence of the results for π_r upon assumptions as to errors and their effects is such that we certainly cannot place as much reliance upon π_r as upon π_q. We therefore have adopted the relative weights $\pi_q:\pi_r::3:1$ (I) and 2:1 (II). Combining with these weights, we find as the mean parallaxes of the RR Lyrae variables and the Cepheids, the proper motions of which are given in Tables 1 and 2,

$$\bar{\pi} = 0''.00085 \text{ (I)}, \qquad 0''.00135 \text{ (II)}.$$

V. THE ABSOLUTE PHOTOGRAPHIC MAGNITUDES

The mean parallaxes and mean apparent photographic magnitudes being known (see Table 6), the mean absolute photographic magnitudes are determined by the relation

$$\bar{M}_c = \bar{m} + 5 + 5 \log \bar{\pi}.$$

[18] *Ibid.*, **54**, 140, 1921.

Hence,

$$\overline{M}_c = +0.15\ (\mathrm{I}),\ -1.39\ (\mathrm{II})\,.$$

These, however, are not true values; they must be corrected first for dispersion in absolute magnitude. Also, since the δ Cephei stars are strongly concentrated near the galactic plane, their mean apparent magnitude is presumably estimated too faintly, owing to galactic absorption, and must be corrected for this effect. Strömberg has shown[17] that if $\overline{M}$ denotes the true and $\overline{M}_c$ the computed mean absolute magnitude and if σ is the dispersion,

$$\overline{M} = \overline{M}_c - 5 \log C\,,$$

where C is defined by the relation

$$\sigma^2 = 21.71 \log C\,.$$

Hence,

$$\overline{M} = \overline{M}_c - 0.23\sigma^2\,.$$

Since the proper motions of group I were reduced to the same apparent magnitude and among them there is very little dispersion in period and therefore in absolute magnitude, it may be assumed that for this group, $\sigma = 0$, approximately. From comparisons with the period-luminosity curve we find for group II, $\sigma = 0.54$. With these values we have

$$\overline{M} = \overline{M}_c\ (\mathrm{I}), \qquad \overline{M}_c - 0.07\ (\mathrm{II})\,.$$

For the additional correction to the mean absolute magnitude of group II, we use an absorption of 0.85 mag. (photographic) per kiloparsec, which Joy has found to satisfy the rotation factors for these stars. At the distance derived for these stars this correction amounts to −0.63. The true absolute magnitudes are therefore

$$\overline{M} = +0.15\ (\mathrm{I}), \qquad -2.09\ (\mathrm{II})\,.$$

With the values of log P in Table 6, we find from the period-luminosity curve

$$M_{\mathrm{curve}} = -0.03\ (\mathrm{I}), \qquad -1.70\ (\mathrm{II})\,.$$

The corrections to the curve resulting from this analysis are therefore

$$\Delta M = \overline{M} - M_{\text{curve}} = +0.18 \pm 0.23 \text{ (I)}, \qquad -0.38 \pm 0.22 \text{ (II)}.$$

The mean errors are estimated by means of Schlesinger's formula[19]

$$\text{m.e.} = \frac{R}{2n}\sqrt{\frac{(n+1)(n+2)}{3(n-1)}},$$

where R is the range in the absolute magnitudes derived from the various mean parallaxes given in Section IV and n the number of determinations.

Approximate values of the mean absolute magnitudes may be derived from the radial velocities without recourse to the proper motions through consideration of the rotation factors $\bar{r}A$. The degree of approximation which can be attained depends not only upon the accuracy with which $\bar{r}A$ and A may be determined but also upon the relation of $\bar{\pi}$ to $\bar{r}$. For A we adopt Joy's determination, 20.9 km/sec per kiloparsec.[12] Since from our radial velocity solutions

$$\bar{r}A = 37 \pm 20 \text{ (I)}, \qquad 27.4 \pm 1.4 \text{ (II)},$$

it follows that

$$r = 1.77 \pm 0.96 \text{ kpc (I)}, \qquad 1.31 \pm 0.07 \text{ kpc (II)}.$$

It is known that

$$\bar{\pi} \cdot \bar{r} = e^{(0.46\sigma)^2},$$

where σ is again the dispersion in absolute magnitude. By means of this relation we find

$$\bar{\pi} = 0''.00057 \text{ (I)}, \qquad 0''.00088 \text{ (II)}.$$

The mean photographic magnitudes of the stars with measured radial velocities are

$$\bar{m}_{\text{pg}} = 10.84 \text{ (I)}, \qquad 9.85 \text{ (II)}.$$

[19] *A.J.*, **46**, 161, 1937.

Therefore,

$$\overline{M}_c = -0.38\ (\mathrm{I}), \qquad -0.43\ (\mathrm{II}).$$

Correcting for dispersion in absolute magnitude and, in group II, for galactic absorption, we have

$$\overline{M} = -0.38\ (\mathrm{I}) \qquad -1.47\ (\mathrm{II}).$$

Since for these stars

$$\overline{\log P} = -0.32\ (\mathrm{I}), \qquad +0.97\ (\mathrm{II}),$$

we find

$$M_{\mathrm{curve}} = -0.03\ (\mathrm{I}), \qquad -1.84\ (\mathrm{II}).$$

Hence the corrections to the period-luminosity curve derived from the rotational coefficients are

$$\Delta M = -0.35\ (\mathrm{I}), \qquad +0.37\ (\mathrm{II}).$$

Though subject to considerable uncertainty, these results are quite comparable, quantitatively, with those derived in the previous analysis. If we combine the two sets of results, giving half-weight to the latter, we have

$$\overline{\Delta M} = 0.00\ (\mathrm{I}), \qquad -0.14\ (\mathrm{II}),$$

with a probable error of about 0.2 in each case. It would appear, therefore, that the zero point of the period-luminosity curve, as given in Shapley's *Star Clusters*, is essentially correct. Certainly there is no evidence in the radial-velocity and proper-motion data now available that would justify a change.

VI. THE SHAPE OF THE CURVE

The shape of the period-luminosity curve is based upon the magnitudes and periods of variables in the Magellanic Clouds, globular clusters, and extragalactic nebulae. The fact that the corrections to the zero point derived in the preceding section from two groups of stars with quite different periods are essentially equal is in itself

some confirmation of the general shape. The criticism by Schilt[20] that there is a break in the continuity of the curve at a period of 10 days and that the Cepheids of longer period are absolutely fainter than those having periods from 2 to 10 days was perhaps satisfactorily answered by Gerasimovič.[2] There can be little doubt that some, at least, of the anomalies which produced the criticism were due to the scarcity and poor quality of the data at that time available. It seemed desirable, therefore, to see what evidence of continuity might come out of the data recently accumulated. Group II has therefore been broken down into three subgroups with log $P < 0.75$, $= 0.75-1.00$, and > 1.00, the maximum value being 1.65. It would have been desirable to make two groups of those stars for which log $P > 1.00$, but the proper-motion data are not good enough to permit it. The proper-motion data are exhibited in Table 9, following the general form of Table 6.

TABLE 9

PROPER-MOTION DATA

(Unit, 0".01)

	log P		
	<0.75	0.75−1.00	>1.00
$\overline{\log P}$	0.60	0.88	1.26
m_{pg}	7.75	7.50	8.67
No.	32	27	27
μ_{med}	1.70	1.37	1.80
μ_{av}	1.83	1.53	2.05
Wt.	30.2	29.7	25.1
$\bar{\tau}$	−0.01 ± .13	−0.13 ± .14	+0.06 ± .18
$\bar{v}$	+0.93 ± .16	+0.59 ± .12	+0.14 ± .20
τ_{av}	0.95 ± .13	0.97 ± .13	1.24 ± .19
$\bar{\rho}$	0.66	0.61	0.79
η	0.78	0.72	0.93
q	1.23 ± .21	0.76 ± .16	0.31 ± .26

While the decrease in v and q with increasing $\overline{\log P}$ is evidence of increase in absolute magnitude with period, the trend in τ_{av} would appear to be in the opposite direction. Unfortunately, we cannot assume that the correlation between τ and ρ is the same in each sub-

[20] *Ap. J.*, **64**, 149, 1926; *A.J.*, **38**, 197, 1928.

division as in the group as a whole. Investigation shows that it is not, κ being small in the first two groups and large in the last; but the data in the subgroups are not sufficient to give determinate values of κ. We cannot, therefore, use Kapteyn's formula. We can, however, determine η from the quoted probable errors and apply the formulae correlating $\bar{\pi}$ and $\bar{\epsilon}$ and $\bar{\pi}$ and τ_{av}, used in Section IV. We must assume that the group motion of each of the subgroups is the same as that of the whole group. Fortunately, this can be approximately verified through the mean peculiar motions. We find θ = 14.4, 14.0, and 14.0 km/sec. Their group motions along the direction of the apex must therefore be approximately the same.

TABLE 10

π_q AND π_τ FROM SUBGROUPS

π_q			π_τ		
q	(13)	Mean	τ_{av}	$\bar{\epsilon}$	Mean
0".0021	0".0022	0".0021	0".0017	0".0029	0".0021
.0013	.0013	.0013	.0022	.0024	.0023
0.0005	0.0003	0.0004	0.0028	0.0009	0.0022

From the values of q and V_0 and from the application of Strömberg's formula (13) we get two sets of values of π_q. Likewise, from the τ_{av} values corrected for the average errors η and from the values of $\bar{\epsilon}$, also corrected for average error, we get two sets of values of π_τ. These are shown in Table 10. The values of π_q and the values of π_τ derived from the $\bar{\epsilon}$'s show the same trend. In view of the equality in the peculiar motions θ, the opposite trend in π_τ, as determined from the τ-components, must be attributed to the weakness of the data. We take the straight means of the two sets of values to determine π_q, and give the value of π_τ based on $\bar{\epsilon}$ half-weight in the determination of $\bar{\pi}_\tau$, as in Section IV. Combining these mean values with the relative weights, 2:1, assigned in the same section, we have the values of $\bar{\pi}$ given in the first column of Table 11. With these and the apparent magnitudes in Table 9, we compute $\overline{M}_c$, which, corrected for dispersion and absorption as in Section V, gives us $\overline{M}$. Comparison with the period-luminosity curve

shows the differences in the last column of the table. The projection on the period-luminosity curve of the various values of $\overline{M}$ derived in this and the preceding sections is shown in Figure 1. There is in them no evidence of discontinuity in the curve.

TABLE 11

MEAN ABSOLUTE MAGNITUDES FROM SUBGROUPS

$\overline{\pi}$	$\overline{M}_c$	$\overline{M}$	M_{curve}	ΔM
0".00210	−0.64	−1.05	−1.22	+0.17
.00163	1.44	1.96	1.66	− .30
0.00100	−1.33	−2.18	−2.24	+0.06

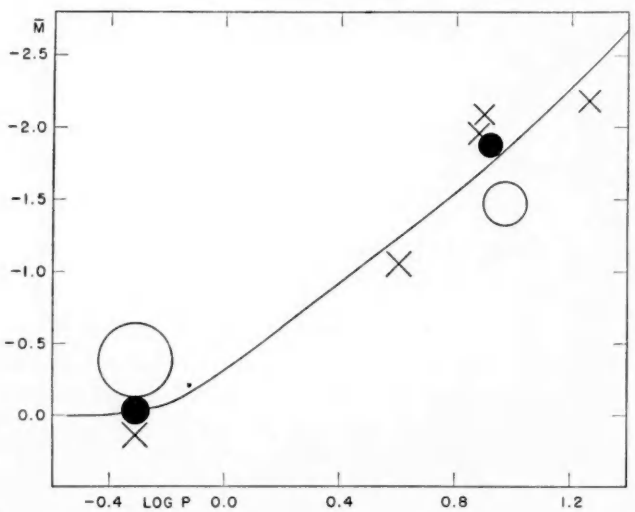

FIG. 1.—The curve represents the photographic period-luminosity relation (Shapley, *Star Clusters*, p. 135, 1930); crosses denote $\overline{M}$ derived from parallactic and peculiar motions; open circles, $\overline{M}$ derived from rotation factors; and filled circles, the concluded mean values.

Since reduced total proper motion should be a direct index of absolute magnitude, we should find evidence of a correlation between period and proper motion. The earlier proper motions gave very little evidence of such a dependence and tended to cast some doubt about the correlation of period and luminosity among the galactic Cepheids. Most investigators have felt that this was

largely due to the weakness of the proper-motion data. The mean parallactic motion of these stars is only 0".008, and the peculiar motions are known to be small. It is obvious, therefore, that in the means of small numbers of proper motions with large probable errors, small changes, such as those to be expected from the period-luminosity relation, may be completely hidden, whereas better data might reveal them. Of the 86 stars listed in Table 2, 52 have proper motions with probable errors $\leq$0".008. Their mean magnitude is 6.5. Their proper motions, reduced to this magnitude, show a small but definite decrease with period, as shown in columns 1 and 2 of Table 12.

TABLE 12

THE PERIOD–PROPER-MOTION DEPENDENCE FROM THE BEST PROPER MOTIONS

$\overline{\log P}$	$\overline{\mu}$	$\overline{\pi}$	$\overline{M}_{6.5}$	$\overline{M}_{8.0}$	M_{curve}	ΔM	ΔM_1
0.56.....	0".0192	0".00168	−2.85	−1.38	−1.16	−0.22	−0.02
0.84.....	.0157	.00138	3.41	1.91	1.60	.31	−0.11
1.23.....	0.0134	0.00118	−3.86	−2.36	−2.32	−0.04	+0.16
0.86.....	0.0162	0.00142	−3.34	−1.84	−1.64	−0.20	0.00

We may go farther and compare this dependence with the period-luminosity curve. From all the stars in Table 2 we have found that for $\overline{m} = 8.0$ and $\overline{\log P} = 0.89$, μ_r = 0".0154 and $\overline{\pi}$ = 0".00135. If we assume that the ratio $\overline{\pi}/\mu_r$, here found, holds in the groups of Table 12, we get the values of $\overline{\pi}$ in column 3 and the values of $\overline{M}_{6.5}$ and $\overline{M}_{8.0}$, corrected for absorption, in the succeeding columns. The small values of ΔM in the last two columns show definitely that the observed decrease in μ_r derived from the best-determined proper motions follows the period-luminosity curve.

The conclusion is reached, therefore, that the radial-velocity and proper-motion data now available confirm both the zero point and the shape of the photographic period-luminosity correlation for the Cepheid variables.

CARNEGIE INSTITUTION OF WASHINGTON
MOUNT WILSON OBSERVATORY
November 1938

THE SHELL-SOURCE STELLAR MODEL

C. L. CRITCHFIELD AND G. GAMOW

ABSTRACT

The evolutionary behavior of a shell-source model for stars is calculated, with the result that changes in luminosity and radius with decreasing hydrogen-content do not essentially differ from the corresponding changes of a point-source model. A qualified mass-luminosity relation is obtained and is indicative of a weaker dependence of luminosity on mass than that found for the point-source model.

INTRODUCTION

It is generally accepted at present that the main source of stellar radiation energy is in thermo-nuclear reactions taking place in the central regions of stars. For ordinary thermo-nuclear reactions the rate of energy production increases exponentially with the temperature; thus, it must be concluded that almost all the energy is liberated near the center of a star and that the so-called "point-source model" may be used for the calculation of the properties of such stars.

It was indicated, however, by one of us[1] that the presence of a resonance effect for one of the reactions which can occur in stellar interiors must lead to a rather different model. In fact, as soon as the temperature at the center approaches the resonance value, the rate of such a reaction must increase very rapidly by a large factor and begin to decrease again for higher temperatures. The presence of the Maxwell distribution of thermal velocities will smooth out the sharp resonance maximum somewhat, and it can be shown[2] that thermo-nuclear energy production undergoes a rapid increase near the resonance temperature but falls down slowly with higher temperatures. Since the temperature increases toward the center of a star, the maximum energy production should then be expected not at the center of the star but at a certain distance from the center, thus forming a "shell source" of energy. The slow decrease of energy production with temperatures higher than that at the maximum

[1] G. Gamow, *Ap. J.*, **87**, 206, 1938; *Phys. Rev.*, **53**, 595, 1938, quoted later as "*I*."

[2] G. Gamow and E. Teller, *Phys. Rev.*, **53**, 608, 1938.

would prevent the realization of a very narrow region in which the total energy source of a star model could be considered as concentrated. Since, however, a star model with a sharply defined and narrow energy-producing shell might be expected to behave similarly to that with the broader selective temperature source, and since it is mathematically much simpler, we have undertaken to calculate some of the features of the simpler model in order to compare them with those of the point-source model. It will be also accepted, for simplicity, that the stellar material represent the mixture of hydrogen with the "Russell mixture" of heavy elements.

At present there seems to be no necessity for considering possible selective temperature effects in order to explain observations on stars of the main sequence,[3] because the difficulty in obtaining a definite mass-luminosity relation can be solved for those stars by taking into account the statistical character of such a relation.[4] However, it seems that the very heavy stars (Trumpler stars and red giants) in the Hertzsprung-Russell (H-R) diagram still present serious difficulties from the point of view of the point-source model. In particular, for the Trumpler stars the ordinary mass-luminosity relation breaks down, and their luminosity seems to be independent on their mass. The investigations of Chandrasekhar[5] have also shown that these stars possess much smaller central condensations than one should expect from the ordinary point-source model. It is therefore interesting to see what regularities must exist for stars constructed according to the shell model and, in particular, how the position of such a star will change on the H-R diagram as its hydrogen content decreases in the process of evolution.

CALCULATIONS FOR A NARROW SHELL

The temperature at which energy production due to a certain nuclear reaction takes place at the greatest rate will be designated by T^*. It will be assumed that no appreciable contribution to the total energy production arises in those parts of the model at a temperature higher than $T^* + \frac{1}{2}\Delta T$ and lower than $T^* - \frac{1}{2}\Delta T$.

[3] As proposed in *I*.

[4] Gamow, *Phys. Rev.*, **53**, 907, 1938.

[5] Chandrasekhar, *Introduction to the Study of Stellar Structure*, University of Chicago Press, 1939.

The energy of the model will then be produced in the region lying between two radii, $R^* - \frac{1}{2}\Delta R$ and $R^* + \frac{1}{2}\Delta R$. At radii larger than $R^* + \frac{1}{2}\Delta R$ the same equations and solutions apply as for a similar model with a central point source. At radii smaller than $R^* - \frac{1}{2}\Delta R$ the gas should be at constant temperature, $T^* + \frac{1}{2}\Delta T$. The detailed variation of temperature, pressure, and density in the energy-producing shell depends upon the particular reaction considered.

It is not our purpose to consider a particular reaction, but rather to make calculations for a simplified model showing selective-temperature effects which should serve as the leading term in any detailed solution expanded in powers of $\Delta R/R^*$. The direct applicability of our results is therefore dependent upon the condition

$$\Delta R << R^* . \tag{1}$$

As pointed out in the Introduction, in reality a very narrow region would not be expected to be possible because of the breadth of the Maxwellian distribution. Nevertheless, conclusions based on equation (1) may be qualitative indications of what may be expected from models of this general type.

In consequence of (1) we may consider the temperature inside the region $R^* \pm \frac{1}{2}\Delta R$ to be T^* everywhere, the density to be ρ^*, etc. The luminosity, L, of the star model is presumed to be governed by the penetration of hydrogen into nonhydrogen nuclei (hydrogen into hydrogen does not show appreciable resonance effects).[6] The rate of production of energy is other than zero only in this region, where it is taken to be constant throughout. If X is the fraction of hydrogen present (by weight),

$$L = 4\pi R^{*2}\Delta R X(1 - X)\rho^{*2}\epsilon , \tag{2}$$

where ϵ is the energy production per gram. In addition to (2) there is the equation connecting the flow of energy with the gradient of temperature, which may be written

$$\frac{dT}{dr} = -\frac{3}{4}\frac{\kappa_0}{\sigma c}\rho^2 T^{-6.5}\frac{L}{4\pi r^2} . \tag{3}$$

[6] H. A. Bethe and C. L. Critchfield, *ibid.*, **54**, 253, 1938.

κ_0 is the coefficient of opacity given below in (5). Under condition (1) we may solve for the average value of L in the interval ΔR, $\bar{L}$,

$$\bar{L} = -\left(\frac{4\sigma c}{3\kappa_0}\right)\rho^{*-2}T^{*6.5}4\pi R^{*2}\left(\frac{\Delta T}{\Delta R}\right). \tag{4}$$

We assume $L = 2\bar{L}$, and eliminate ΔR by taking the square root of the product of (2) and (4):

$$\left.\begin{aligned} L &= f_0\kappa_0^{-1/2}X^{1/2}(1-X)^{1/2}R^{*2}\,, \\ f_0 &= (\tfrac{8}{3}\pi^2\sigma c T^{*6.5}\epsilon\Delta T)^{1/2}\,, \\ \kappa_0 &= 3.9\times 10^{25}\,(1-X^2)\,. \end{aligned}\right\} \tag{5}$$

Relations (5) show that in this approximation the luminosity of a shell source varies with composition and R^* only, when the energy is presumed to arise from the penetration of hydrogen into heavier nuclei.

Definite, numerical information about a star model is obtained by integrating the equations of equilibrium. If, as in the present discussion, equilibrium in the static sense is assumed to exist, these equations are

$$\left.\begin{aligned} \frac{dP}{dr} &= -\frac{GM_r\rho}{r^2}\,, & \frac{d(\sigma T^4)}{dr} &= -\frac{3\kappa\rho L_r}{4\pi c r^2}\,, \\ \frac{dM_r}{dr} &= 4\pi r^2\rho\,, & \frac{dL_r}{dr} &= 4\pi r^2\rho^2\epsilon X(1-X)\,, \\ P &= \frac{k\rho T}{\beta\mu m_h}\,, & P_R &= P(1-\beta) = \frac{\sigma T^4}{3}\,, \\ & & \kappa &= \kappa_0\rho T^{-3.5}\,, \end{aligned}\right\} \tag{6}$$

where μ is the molecular weight, m_h the mass of the proton, k Boltzmann's constant, and P_R the radiation pressure. For the shell-source model, L_r = constant = L in the region $r > R^* + \frac{1}{2}\Delta R$. Inside $R^* - \frac{1}{2}\Delta R$, $L_r = 0$, T is constant and the pressure is proportional to the density. At $r = 0$, $dP/dr = 0$, and in the immediate neighborhood $M_r = 4\pi r^3\rho_0/3$, where ρ_0 is the central density. More

exactly, by differentiating (6), power series for M_r and ρ can be found with coefficients depending on ρ_0:

$$\left.\begin{aligned} M_r &= \frac{4\pi\rho_0}{3} r^3 - \frac{8\pi^2\beta\mu m_h G\rho_0^2}{15kT} r^5 + \cdots, \\ \rho &= \rho_0 - \frac{2\pi\beta\mu m_h G\rho_0^2}{3kT} r^2 + \cdots. \end{aligned}\right\} \tag{7}$$

M_r may then be expressed as a function of ρ:

$$M_r = \frac{4\pi\rho}{3} r^3 \left(1 + \frac{4\pi\beta\mu m_h \rho G}{15kT} r^2\right), \tag{8}$$

under the condition

$$\eta \equiv \frac{4\pi\beta\mu m_h \rho G r^2}{15kT} << 1. \tag{9}$$

Numerical integrations of equations (6) for the mass, radius, and luminosity of the sun (with $\mu = 1$), pertaining to the point-source model, were made available to us by Dr. B. Strömgren. Those solutions which came to the total mass (integrating from the surface) before reaching the center were fitted to spheres of constant density and of the correct mass to account for that of the sun. The radius at which the junction takes place is an estimate of R^*. The density of the isothermal interior was taken to be the same as that of the point-source solution at the junction. Values of R^*, T^*, ρ^*, and the estimated error in R^* ($\delta R^*/R^* = \eta/3$), obtained from these calculations, are shown in Table 1. A typical solution (that for log

TABLE 1

$\log \kappa_0$	R^*/R	T^*	ρ^*	$\delta R^*/R^*$	$(R^*/R)_{cor}$
24.692.....	0.139	17.4×10^6	39	0.048	0.146
24.592.....	.212	13.9	28	.100	.233
24.492.....	.238	12.5	24	.120	.267
24.392.....	0.270	10.8	20	0.150	0.310

$\kappa_0 = 24.392$) is shown in Figure 1. It is evident that the leading term in (8), which is the curve shown in the graph, gives an under-

estimate of R^*. The corrected values of R^*/R shown in the last column of Table 1 will be used in the remainder of the discussion.

As is well known, detailed solutions of (6) for any mass, luminosity, molecular weight, and opacity can be derived from that for the sun with $\mu = 1$ by changing the scale of units in accordance with (6).

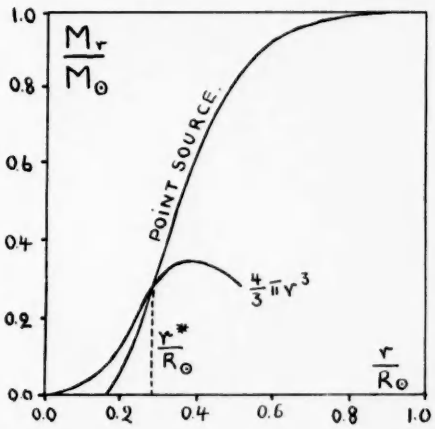

FIG. 1.—Graphical representation of the method of estimating R^*. Point-source integrations which run out of mass before reaching $r = 0$ satisfy equilibrium conditions outside the shell, whereas inside the model has almost constant density. Choosing R^* at the intersection guarantees that the total mass is that of the sun.

This homology transformation for the point-source model may be written

$$\left.\begin{aligned} \bar{M} &= aM, & \bar{\rho} &= a^{-32}b^{-45}c^{6}d^{6}\rho\,, \\ \bar{\mu} &= b\mu\,, & \bar{T} &= a^{-10}b^{-14}c^{2}d^{2}T\,, \\ \bar{\kappa}_0 &= c\kappa_0, & \bar{r} &= a^{11}b^{15}c^{-2}d^{-2}r\,, \\ \bar{L} &= dL, & \bar{T}_{\text{eff}} &= a^{-11/2}b^{-15/2}cd^{5/4}T_{\text{eff}}\,. \end{aligned}\right\} \tag{10}$$

Since the same relations hold for $L = 0$, (10) may be used to bring the results in Table 1 to a common resonance temperature. No experimental value is known for T^*, so we make an arbitrary choice of $T^* = 25 \times 10^6$ degrees. Without changing the mass, radius, or luminosity the transformation to be applied is then

$$a = 1, \quad d = 1, \quad b^{15}c^{-2} = 1, \quad \bar{T} = bT, \quad \bar{\mu} = b\mu, \quad \bar{\kappa}_0 = c\kappa_0\,, \tag{11}$$

when b is adjusted for each solution to bring T^* to 25×10^6. The result of this transformation is shown in Table 2. According to the usual theory of opacity, the maximum value of log κ_0 is 25.591 ($\kappa_0 = 3.9 \times 10^{25}$), so that $T^* = 25 \times 10^6$ is hardly suited to the sun; and indeed, as mentioned above, there is no need to suppose that resonance plays an important part in the energy production of ordinary stars. We therefore transform Table 2 to apply to a star of $M = 10M_\odot$, $L = 49{,}000L_\odot$, keeping T constant, of course, since T^* must remain at R^*. This transformation is the same for each solu-

TABLE 2

$M = M_\odot$, $R = R_\odot$, $L = L_\odot$

R^*/R	T^*	μ	log κ_0
0.146	25×10^6	1.44	25.872
.233	25	1.80	26.504
.267	25	2.00	26.750
0.310	25	2.31	27.126

tion in Table 2 and may be written $a = 10$, $b = 0.541$, $c = 0.028$, and $d = 49{,}000$. It is readily verified that $\bar{T} = T$. These particular values were chosen so that if the star model is considered as composed of hydrogen ($\mu = \frac{1}{2}$) and elements heavier than helium ($\mu = 2$) alone, $R^*/R = 0.310$ becomes a solution consistent with the relations

$$\mu = \frac{2}{1 + 3X}, \qquad \kappa_0 = 3.9 \times 10^{25} (1 - X^2), \tag{12}$$

with $X = 0.20$. The results of the transformation are shown in Table 3. Of the four solutions shown in Table 3, $R^*/R = 0.31$ is the only one for which (12) is satisfied. Relations (12) can be satisfied for larger values of X, however, if L and R are changed by homology transformations; and in this way a correlation between hydrogen content, as well as R^*/R and luminosity, can be obtained. An evolutionary track may then be plotted on the H-R diagram, the course of time being indicated not only by decreasing hydrogen content but also by changing R^*/R.

Restrictions on the transformations suggested in the preceding paragraph are as follows: the mass and the temperature are unchanged, and the luminosity must transform in accordance with (5).

TABLE 3

$M = 10M_\odot$, $L = 49{,}000L_\odot$, $R = 5.4R_\odot$, $T^* = 25 \times 10^6$

R^*/R	μ	$\log \kappa_0$
0.146	0.78	24.319
.233	0.97	24.951
.267	1.08	25.197
0.310	1.25	25.573

If we write the ratio of a given R^*/R to 0.310 as q, equations (5) and (10) require

$$d = \sqrt{\frac{X(1-X)}{X_0(1-X_0)}}\, c^{-1/2} b^2 q^2 \tag{13}$$

for constant temperature and mass, where X_0 in this case is just 0.20. X is the hydrogen content which satisfies (12). Constant temperature requires

$$d = b^7 c^{-1}, \tag{14}$$

so that, eliminating d,

$$1 = \frac{\sqrt{X(1-X)}}{.40}\, c^{1/2} b^{-5} q^2 . \tag{15}$$

Now, b and c are given in each case by

$$b = \frac{2}{\mu(1+3X)}, \qquad c = \frac{3.9 \times 10^{25}(1-X^2)}{\kappa_0}, \tag{16}$$

where μ and κ_0 are the values shown in Table 3. If we substitute (16) in (15), square and separate knowns and unknowns, we get

$$\left.\begin{aligned} F(X) &= 0.16 q^{-4} \frac{\kappa_0}{3.9 \times 10^{25}} \left(\frac{2}{\mu}\right)^{10}, \\ F(X) &\equiv X(1-X)(1-X^2)(1+3X)^{10} . \end{aligned}\right\} \tag{17}$$

Solutions of (17) for each R^*/R are shown in Table 4 under "X." Luminosities, radii, and effective temperatures are also tabulated

TABLE 4

R^*/R	X	$R/R_\odot$	log $(L/L_\odot)$	log $(T_{\text{eff}}/T_{\text{eff}\odot})$
0.146	0.46	5.8	3.75	0.56
.233	.32	5.7	4.24	.69
.267	.26	5.6	4.45	.74
0.310	0.20	5.4	4.69	0.81

for each shell, and from them the evolutionary track plotted in Figure 2 is derived. The path on the H-R diagram described by a star having a shell source is evidently parallel to the main sequence for a large portion of its life and is, in that respect, the same as that found in (*I*) for the point-source model. Although this has been demonstrated for only one particular example, a more extensive study is hardly justifiable in the light of the artificiality of condition (1) and the arbitrariness of T^*. It may, however, be conjectured that no striking change in the predicted course of stars (from point-source arguments) is forthcoming in case selective temperature effects play an important part in the energy source.

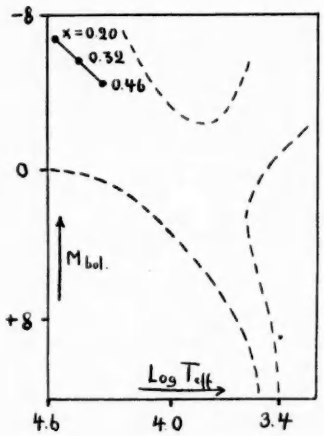

FIG. 2.—Evolutionary track, on a Hertzsprung-Russell diagram, of a shell-source model of ten solar masses composed only of heavy elements ($\mu = 2$) and hydrogen, the latter varying from 46 to 20 per cent.

MASS-LUMINOSITY RELATION

Relations (10) may be used to compare star models of different masses and luminosities but with the same R^*/R. In this way a qualified mass-luminosity relation is obtained. Let the hydrogen contents of two models be X_1 and X_2; then, from (5),

$$d = \sqrt{\frac{X_2(1 - X_2)}{X_1(1 - X_1)}}\, b^2 a^2 c^{-1/2}\,, \tag{18}$$

assuming, of course, that $\bar{T}^* = T^*$. The condition of constant temperature gives also

$$d = a^5 b^7 c^{-1} . \tag{19}$$

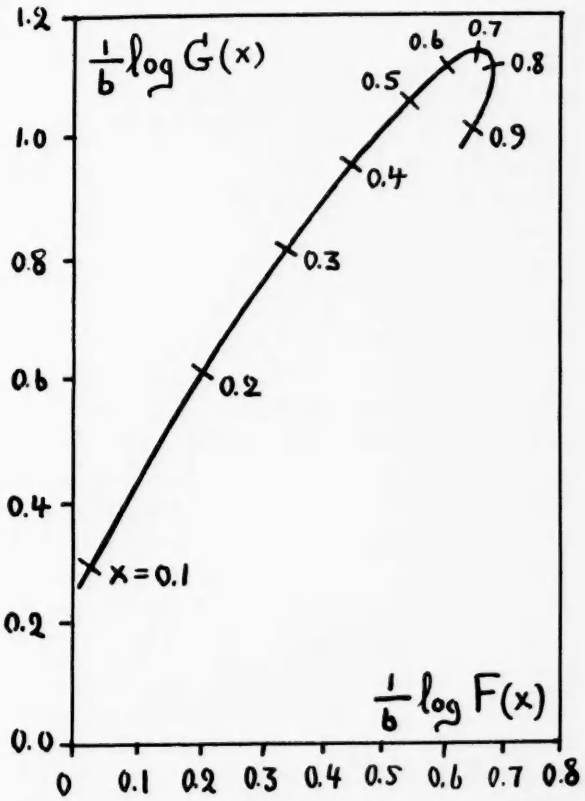

FIG. 3.—Plot of $\frac{1}{6}\log G(X)$ against $\frac{1}{6}\log F(X)$ for shell models of the same R^*/R and containing only heavy elements and hydrogen. The fraction of the latter is indicated by the numbers along the curve. For two star models of hydrogen contents X_1 and X_2 the difference in ordinates of these X-values gives the logarithm of the factor by which L differs, and the difference in abscissas that by which M differs.

Substituting b and c from (12) and eliminating d from (18) and (19),

$$a = \left[\frac{F(X_2)}{F(X_1)}\right]^{1/6} . \tag{20}$$

Similarly, eliminating a,

$$\left.\begin{aligned} d &= \left[\frac{G(X_2)}{G(X_1)}\right]^{1/6}, \\ G(X) &\equiv X^5(1-X)^5(1+3X)^8(1-X^2)^{-1}. \end{aligned}\right\} \tag{21}$$

A plot of $\frac{1}{6}\log G(X)$ against $\frac{1}{6}\log F(X)$ gives the relation between mass and luminosity. Such a plot showing the hydrogen contents at various points is shown in Figure 3. From that plot it is readily seen that models of hydrogen content between 0.1 and 0.7 and the same R^*/R approximately obey the relation $\log d = 1.5 \log a$. The usefulness of this relation is, of course, rather restricted, but it may be said with some confidence that stars which depend upon selective temperature effects in their energy production will show a dependence of luminosity on mass which is lower than that found for point-source models, i.e., $\log d \cong 5 \log a$.

It is interesting to note in this connection that observational evidence[7] indicates that, whereas for stars in the central regions of the main sequence (from 0.5 to 3 solar masses) the mass-luminosity relation corresponds to the fifth power, for very heavy stars (as, for example, Trumpler stars) the increase of luminosity with mass is much slower.

In conclusion, the authors wish to express their thanks to Dr. B. Strömgren for access to his unpublished tables and to Dr. E. Teller for many helpful discussions.

GEORGE WASHINGTON UNIVERSITY
WASHINGTON, D.C.

[7] G. P. Kuiper, *Ap. J.*, **88**, 472, 1938.

THE SPECTRUM OF γ CASSIOPEIAE IN THE PHOTOGRAPHIC REGION

SECOND PAPER

RALPH B. BALDWIN

ABSTRACT

The changes of structure and intensity in the emission and absorption lines of *H*, *He* I, *Fe* II, *Si* II, and *Mg* II are discussed for the interval of March 23, 1935, to October 24, 1938. These spectral variations are correlated with the changes in color temperature and the light-curve. A changing effective photosphere is suggested to explain the correlation between the light- and the temperature-curve.

It is shown that no hypothesis heretofore advanced to interpret Be variations can explain all the changes through which γ Cassiopeiae has recently passed.

The present investigation is a supplement to one published previously in the *Astrophysical Journal*.[1] The earlier paper gave a list of identifications of all emission lines measured during the single-line stage. This paper traces the behavior of five of these elements, *H*, *He* I, *Fe* II, *Si* II, and *Mg* II, throughout their changes of radial velocity, V/R, and absorption intensity.

The results are based on a series of 70 spectrograms taken with the one-prism spectrograph on the $37\frac{1}{2}$-inch reflector of the University of Michigan Observatory between March 23, 1935, and October 24, 1938. They constitute a temporal extension of Cleminshaw's paper,[2] and carry through the period of extreme change in 1937 and 1938.

McLaughlin[3] has published a reconnaissance of the first twelve plates, but the data of the present paper are based on my own measures, and consequently differ slightly from those of McLaughlin.

The dispersion is 19 A/mm at $H\omega$, 40 A/mm at $H\gamma$, and 62 A/mm at $H\beta$.

During the single-line stage all visible features were measured. On the rest of the plates measures were limited to (1) the Balmer series of hydrogen out to, and including, $H\omega$ wherever possible;

[1] Baldwin, *Ap. J.*, **87**, 573, 1938.

[2] *Ibid.*, **83**, 495, 1936. [3] *Ibid.*, **84**, 235, 1936.

(2) the *He* I lines 3820, 3889, 3965, 4026, and 4472, and occasionally 4388 and 4713; (3) the *Fe* II lines 4173, 4179, 4233, 4303, 4352, 4385, 4417, 4489, 4491, 4508, 4515, 4520, 4522, 4549, 4556, 4584, and 4629. On most plates only a fraction of these could be utilized, as blends, grain effects, and general faintness operated to distort the lines. V/R estimates were often made on lines of this group which could not be measured. (4) The five lines of *Si* II, 3854, 3856, 3863, 4128, and 4131, and (5) *Mg* II 4481, completed the list. No interstellar calcium lines were present at any stage.

The probable errors of the measured velocities as derived from the residuals from the smooth curves drawn through the points are: ± 2.00 km/sec for hydrogen, ± 2.78 km/sec for *He* I, ± 2.75 km/sec for *Si* II, ± 4.43 km/sec for *Fe* II, and ± 4.56 km/sec for *Mg* II. Some of the deviations from the smooth curves may represent actual velocity changes. This is almost certainly the case for hydrogen, and thus the probable errors may be too large.

THE HYDROGEN LINES

During the stages immediately subsequent to those studied by Cleminshaw, about JD 2428000, the hydrogen spectrum was represented by relatively few Balmer lines, each composed of two emission components, widely separated, with a rather sharp, strong absorption line nearly in the center. Underlying the whole configuration was a broad, shallow absorption approximately 600 km/sec wide. $H\beta$ was prominent, while lines beyond $H\eta$ were very weak. No line was as intense as it became later. The red component of each emission line was decidedly stronger than the violet.

From JD 2427885 to JD 2428200 the two components of the emission gradually separated (Fig. 1), the violet component changing position more than the red. The maximum separation occurred about the latter date. The red component, however, had reached a maximum positive velocity 150 days earlier and had then begun to show a smaller velocity of recession. After the date of maximum width both components gradually approached one another more or less smoothly except for an oscillation on the velocity-curve of the red component around JD 2428500. This fluctuation was real and was shown with differing degrees of strength by the corresponding

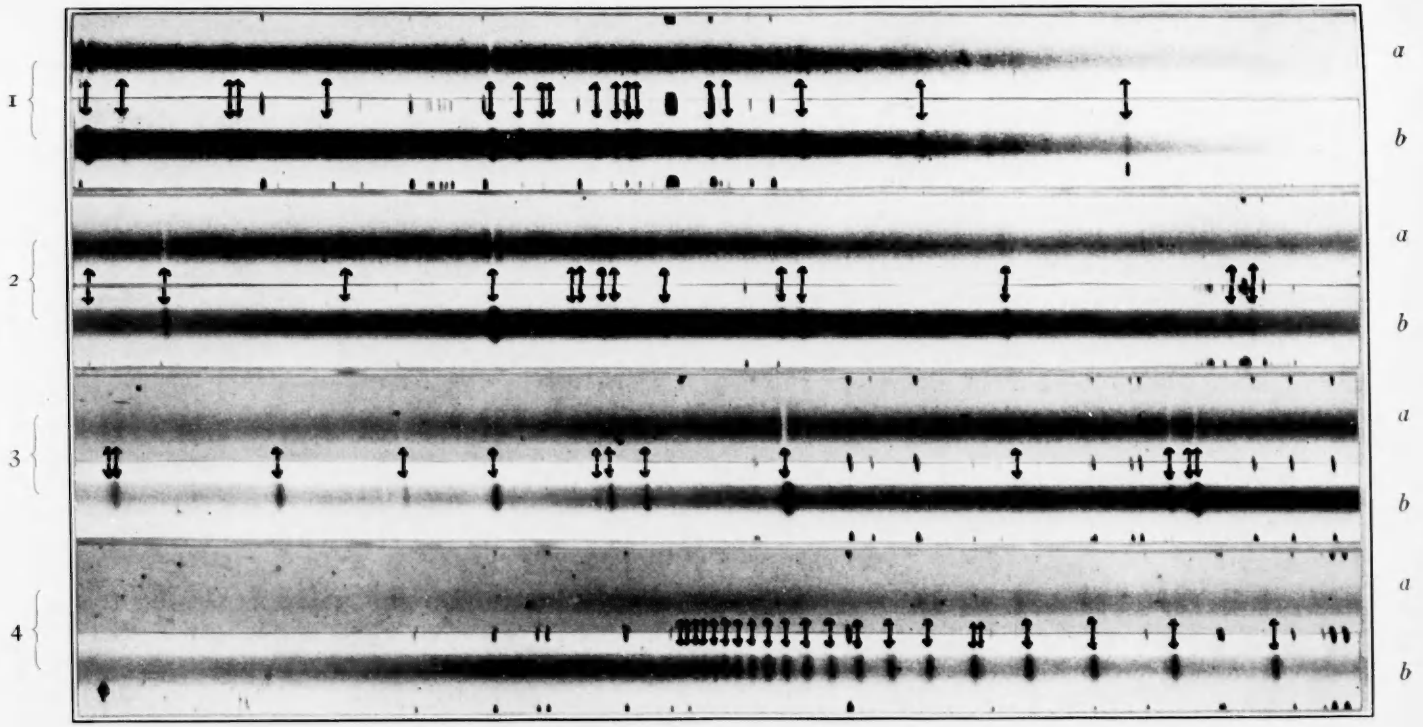

THE SPECTRUM OF γ CASSIOPEIAE

The lines in the four sections are, from right to left:

a) March 28, 1936; *b*) September 22, 1937.

SECTION 1: *He* I 4713, *Fe* II 4629, *Fe* II 4584, *Fe* II 4556, *Fe* II 4549, *Fe* II 4522, *Fe* II 4520, *Fe* II 4515, *Fe* II 4508, *Fe* II 4491, *Fe* II 4489, *Mg* II 4481, *He* I 4472, *Fe* II 4417, *He* I 4388, *Fe* II 4385, *Fe* II 4352, *Hγ*

SEC. 2: *Fe* II 4303, *Fe* II 4297, *Fe* II 4233, *Fe* II 4179, *Fe* II 4173, *He* I 4144, *Si* II 4131, *Si* II 4128, *Fe* II 4123, *He* I 4121, *Hδ*, *Ni* II 4067, *He* I 4026, *He* I 4009

SEC. 3: *Hε*, *Ca* II 3968, *He* I 3965, *Ca* II 3933, *Hζ*–*He* I 3889, *Si* II 3863, *Si* II 3856, *Si* II 3854, *Hη*, *He* I 3820, *Hθ*, *Hι*, *Ni* II 3769

SEC. 4: *Hκ*, *Hλ*, *Hμ*, *Hν*, *He* I 3705, *Hξ*, *Ho*, *Hπ*, *Hρ*, *Hσ*, *Hτ*, *Hυ*, *Hφ*, *Hχ*, *Hψ*, *Hω*, *H*27, *H*28, *H*29, *H*30, *H*31, Hydrogen continuum

curves of all elements. It was least marked for hydrogen and *Fe* II. In no case did the violet component show a corresponding change.

During this entire period the red component had been decreasing in strength until it completely disappeared at about JD 2428630.

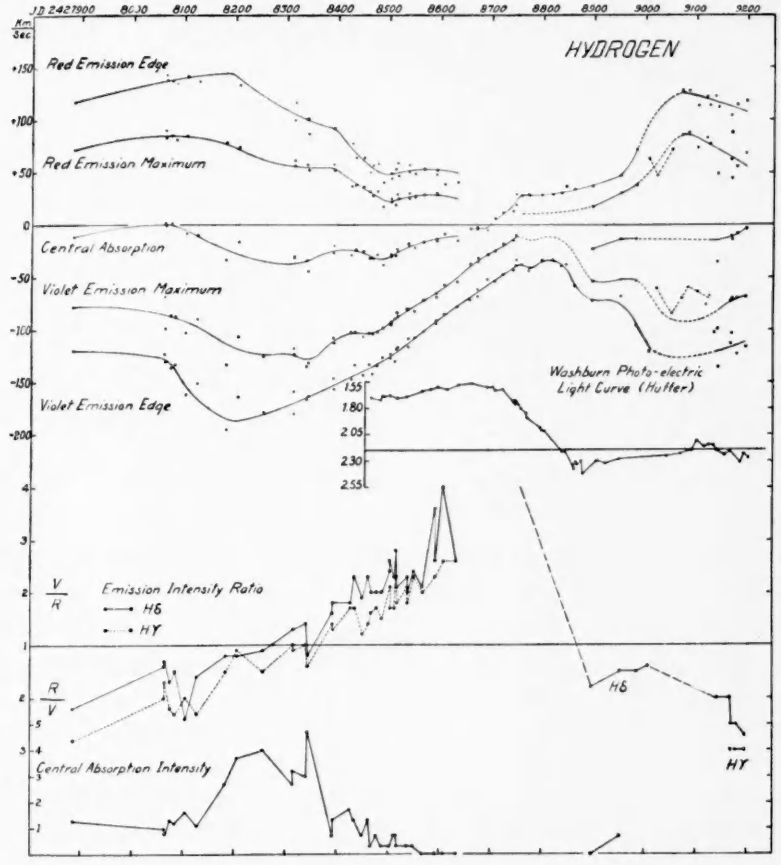

FIG. 1

For four months the violet component alone was visible and continually moved toward the then invisible red component. The latter reappeared as a blend with the violet line as is indicated by the abrupt increase of width during the single-line stage. The two components had finally separated far enough to be resolved at JD 2428900.

As the red component weakened, the violet strengthened correspondingly. V/R-curves are shown for $H\delta$ and $H\gamma$, the latter having a marked lag of the order of 60 days relative to the $H\delta$-curve. The other lines of the Balmer series show similar time lags over the line of next shorter wave length, but the lags decrease considerably for the shorter wave lengths and are not noticeable beyond $H\eta$. The largest lag, 80 days, is between $H\beta$ and $H\gamma$ ($H\alpha$ is not visible on these plates).

A marked variation in the V/R ratio took place between JD 2428340 and 2428342. It appeared to be correlated with a small change of velocity and with an increase in the strength of the central absorption line.

It should be noticed that the velocity-curve of the strong emission component runs along very smoothly, while the weaker component is displaced less than would be expected on a symmetrical model. No other element shows this effect, which suggests that the emission arising from atoms of higher velocity is completely absorbed before it can leave the atmosphere, while that from atoms of lower velocity is only partly absorbed, resulting in an apparent displacement which is actually too small.

The central absorption line showed an algebraic decrease of velocity in the period when the line was strong. As the emission components approached one another, the absorption decreased in strength and shifted toward the red with oscillations which are also shown by the other elements.

The light-curve[4] correlates closely with the V/R- and velocity-curves. During the increase of light the emission components were narrowing and the V/R ratio was becoming greater. The abrupt decline in brightness lasted throughout the single-line phase and ended in a nearly flat minimum as the emission again became double, this time with $R > V$.

Five additional light-curves are available. They are the *AAVSO* curve,[5] Cherrington's composite curve,[6] and a visual-curve by each

[4] Dr. C. M. Huffer has very kindly allowed me to use the light-curve of γ Cassiopeiae, prior to publication. It was derived at the Washburn Observatory with a photoelectric photometer.

[5] *Pop. Astr.*, **45**, 569, 1937. [6] *Ibid.*, **46**, 183, 1938.

of the following: Rigollet,[7] Loreta,[8] and Olivier.[9] These curves are all similar to the photoelectric light-curve, although the *AAVSO* curve and Cherrington's curve show oscillations which are not present in the others.

In Figure 1 the probable course of the two components during the single-line stage has been dotted in. Unless each component became very broad while blended together, they did not cross, as Lockyer[10] suggested for the similar phase in 1934. It seems likely that they approached each other with the violet component the stronger; they then blended, reversed their intensities, and separated.

As the two lines approached one another, the higher Balmer lines and the emission continuum appeared strongly. All lines increased in total strength. In an earlier paper[11] I announced measures as far as $H32$, while all higher members of the series and the continuum were strongly blended. The total strength of emission decreased considerably at the end of the single-line stage.

During the narrowing phase both components grew sharper. This phenomenon was more pronounced in the case of other elements than for hydrogen.

On any given date the Balmer lines were not all of the same velocity width but differed as much as 15 km/sec from line to line. Plates taken on the same or adjacent days yielded similar line velocities; but the number of spectrograms was not sufficient to give any sequence of the changes of velocities, line to line, or to correlate them with the V/R-curves. In general the changes seemed to progress to longer wave lengths, as did the changes of V/R; but this is not definitely established. The velocities given in Table 1 are the means of measures on all hydrogen lines clearly visible and not overexposed. The lines of longer wave length are wider, mainly because of the effect of the slit; but this introduces no appreciable error into the velocities.

Shortly after the end of the single-line stage a new complication arose. For the first hundred days after resolution, JD 2428900–2429000, the hydrogen lines appeared normal. They gradually

[7] *L'Astronomie*, March, 1938, p. 129.

[8] *Ibid.*, March, 1938, p. 130.

[9] Flower Observatory, unpublished.

[10] *M.N.*, **95**, 520, 1935.

[11] Baldwin, *op. cit.*

Table 1

Hydrogen

J.D. 242+	RE	RM	CA	VM	VE	AI	V/R Hγ	V/R Hδ	(RE)	(VE)	No.
7885	+117	+71	-11	- 78	-120	1.3	2.8R	2.2R	-	-	3
8063	143	90	+ 2	- 68	-123	1.0	2.0R	1.4R	-	-	2
8064	138	83	- 1	- 99	-130	0.8	1.7R	1.3R	-	-	1
8075	137	85	+ 2	- 86	-136	1.3	2.2R	1.7R	-	-	3
8084	135	81	- 6	- 87	-133	1.2	2.3R	1.5R	-	-	2
8105	141	85	- 8	-103	-162	1.6	2.0R	2.4R	-	-	4
8128	137	76	-10	- 90	-151	1.1	2.3R	1.6R	-	-	2
8182	151	79	-33	-133	-195	2.7	1.5R	1.2R	-	-	3
8206	133	74	-16	-107	-164	3.7	1.1R	1.2R	-	-	2
8256	115	55	-43	-125	-178	4.0	1.5R	1.1R	-	-	6
8315	116	61	-30	-124	-180	2.7	1.0	1.3	-	-	2
8315	100	56	-31	-118	-159	3.2	1.1R	1.3	-	-	15
8340	101	57	-34	-135	-166	3.0	1.0	1.4	-	-	4
8342	87	52	-44	-131	-163	4.7	1.4R	1.2R	-	-	16
8391	92	58	-26	-108	-146	0.7	1.4	1.6	-	-	6
8392	98	52	-20	-113	-156	1.3	1.3	1.8	-	-	3
8426	77	37	-28	-102	-147	1.7	1.7	1.8	-	-	5
8434	64	38	-24	-102	-134	1.3	1.7	2.3	-	-	17
8450	64	36	-25	-106	-143	0.7	1.2	1.9	-	-	17
8461	50	32	-31	-103	-133	1.3	1.4	2.3	-	-	17
8468	56	28	-32	-104	-142	0.3	1.6	2.0	-	-	17
8477	58	32	-28	-102	-134	0.7	1.7	2.0	-	-	14
8489	40	17	-38	- 98	-126	0.3	1.5	2.0	-	-	17
8503	49	22	-30	- 95	-126	0.3	1.7	2.4	-	-	17
8503	44	25	-28	- 93	-123	0.3	2.1	2.6	-	-	21
8511	53	19	-29	- 90	-130	0.7	1.7	2.3	-	-	6
8515	58	29	-23	- 84	-118	0.7	2.3	2.8	-	-	9
8517	46	25	-25	- 87	-117	0.3	1.8	2.1	-	-	21
8539	50	30	-18	- 80	-109	0.3	2.1	2.3	-	-	21
8539	56	25	-19	- 80	-116	0.3	1.8	2.0	-	-	12
8550	49	26	-21	- 82	-108	0.3	2.3	2.4	-	-	12
8567	53	29	-16	- 71	-101	0	2.0	2.1	-	-	22
8592	48	29	-15	- 69	- 94	0	2.3	3.6	-	-	22
8592	52	30	-14	- 65	- 91	0	-	2.6	-	-	17
8608	64	39	- 9	- 57	- 85	0	2.6	4.0	-	-	18
8633	+40	+15	-15	- 54	- 78	0	2.6	2.6	-	-	8
8659	- 3	-	-	- 37	- 71	-	-	-	-	-	22
8672	- 2	-	-	- 35	- 68	-	-	-	-	-	19
8672	- 4	-	-	- 32	- 61	-	-	-	-	-	22
8692	- 5	-	-	- 28	- 52	-	-	-	-	-	22
8706	+ 6	-	-	- 25	- 54	-	-	-	-	-	19
8721	11	-	-	- 18	- 47	-	-	-	-	-	22
8741	13	-	-	- 15	- 43	-	-	-	-	-	18
8746	19	-	-	- 10	- 39	-	-	-	-	-	25
8748	29	-	-	-	- 34	-	-	-	-	-	28
8759	28	-	-	-	- 38	-	-	-	-	-	28
8771	29	-	-	-	- 44	-	-	-	-	-	26
8773	28	-	-	-	- 41	-	-	-	-	-	27
8799	28	-	-	-	- 34	-	-	-	-	-	27
8819	29	-	-	-	- 34	-	-	-	-	-	22
8835	30	-	-	-	- 39	-	-	-	-	-	22
8844	36	-	-	-	- 38	-	-	-	-	-	13
8861	34	-	-	-	- 58	-	-	-	-	-	15
8896	36	+17	-23	- 54	- 72	0	-	1.8R	-	-	12
8951	47	30	-14	- 52	- 68	0.7	-	1.5R	-	-	9
8982	+71	+37	-14	- 53	- 96	-	-	1.5R	-	-	3
9007	-	-	-	-	-122	-	-	-	+62	-	2
9021	-	-	-	-	-	-	-	-	47	-60	6
9052	-	-	-	-	-	-	-	-	+72	-85	6
9071	+128	+86	-	-	-	-	-	-	-	-70	5
9084	127	88	-	-	-	-	-	-	-	-60	6
9102	114	73	-	-	-	-	-	-	-	-64	5
9119	121	83	-	-	-	-	-	-	-	-76	4
9125	113	77	(+15)	-	-	-	-	-	-	-68	9
9135	122	-	-	-	-102	-	-	-	-	-	6
9142	112	49	-35	-100	-135	-	-	2.0R	-	-	6
9166	104	62	-10	- 72	-113	-	-	2.0R	-	-	8
9169	88	44	-14	- 70	-104	-	3.0R	2.5R	-	-	2
9178	115	55	- 8	- 70	-123	-	3.0R	2.5R	-	-	3
9196	+118	+67	- 3	- 68	-116	-	3.0R	2.7R	-	-	12

NOTES TO TABLES 1–5

In Tables 1–5 the headings of the columns have these meanings:

JD Julian day

RE The velocity of the red edge of the red component of an emission line in kilometers per second

RM The velocity of the maximum of the red component

CA The velocity of the central absorption line

VM The velocity of the maximum of the violet component

VE The velocity of the violet edge of the violet component

(RE) The velocity of the red edge of the blend of the second pair of emission lines

(VE) The velocity of the violet edge of the blend of the second pair of emission lines

EI Estimated intensity ratio of emission line to adjacent continuous spectrum

$\frac{4472}{4481}$ The ratio of emission intensity of *He* I 4472 to *Mg* II 4481

No. The number of lines used in determining the foregoing values

The letter *R* after a *V*/*R* ratio indicates that the red component is stronger in that ratio.

The absorption intensities are merely the arithmetical averages of the estimates. In Table 1 the absorption intensity is the average of estimates of $H\gamma$, $H\delta$, and $H\epsilon$. In Table 2 the absorption intensity column gives the average of *He* I 3965, 4026, and 4472. Velocities and intensities of the central absorption line 3889 are tabulated separately.

In Table 3, for *Fe* II, the symbols (1), (2), and (3) refer to the $b^4P - z^4D^o$, $b^4F - z^4F^o$, and $b^4F - z^4D^o$ multiplets, respectively.

In Table 5, *Mg* II, the velocities are not reliable, because of grain effects, on JD 2428342, 2428426, 2428434, and 2428517. Probably an unknown emission line blends with the red component of *Mg* II 4481 and on occasions is strong enough to distort it.

widened with $R > V$ and with each part sharply delineated. Approximately at the latter date the lines became fuzzy and almost unmeasurable. Examination of the plates with a spectrocomparator disclosed that a second pair of emission lines, too narrow for perfect resolution, had appeared in the position previously occupied by the central absorption line. The new emission lines blended with the old pair, causing the whole configuration to appear indistinct.

The original emission components faded somewhat while the new lines were present, but recovered at least part of their strength as the second pair rapidly weakened near JD 2429125. It is probable that the new lines did not completely disappear until later, as there were indications of a weak emission core even on the last plate of the series, JD 2429196.

Dotted lines are used in Figure 1 to indicate probable, but unmeasured, changes of velocity. The curves of the velocity displacements of the outside edges of the second pair of emission lines are also shown as dotted lines during their brief appearance.

On the last four plates measured, the original pair of lines were again rather prominent but were not yet as distinct as in earlier phases.

A noticeable feature is the decrease of velocity width of the lines commencing about JD 2429070. This occurred near a secondary maximum of light.

THE HELIUM LINES

The same trends that are evident in the case of hydrogen are found in the helium spectrum (Fig. 2). Here, however, the two components of the emission remained equal in intensity throughout the entire period. The red component was much more displaced than the red component of hydrogen, but it also exhibited the secondary oscillation in velocity about JD 2428500.

During the period studied by Cleminshaw the helium lines were broad, shallow absorptions, very poorly defined and without emission edges. Emission was measured on the first plate of the present series and was seen, but not measurable, on plates taken during the next year. The lines, then, were generally broad without sharp edges. As the emission components approached each other they also sharpened, until they both appeared nearly monochromatic just before the single-line stage.

In the period JD 2427885–2428064, the helium central absorption lines were weak and were displaced approximately 30 km/sec toward the violet relative to the hydrogen. At the latter date this absorption began to sharpen and strengthen, and at the same time it shifted redward until it agreed in displacement with the hydrogen absorption. The increase of intensity coincided with a similar change in the hydrogen lines but occurred at lines of no other element studied. However, complete identifications were made only for emission lines found in the single-line stage. McLaughlin[12] found a few absorption lines of *O* II during the time when the *H* and *He* I

[12] *Ap. J.*, **84**, 235, 1936.

central absorptions were strong. Probably *O* II underwent the same general intensity changes.

As soon as the hydrogen and helium absorption lines agreed in velocity, they began to move toward the violet, except for a short

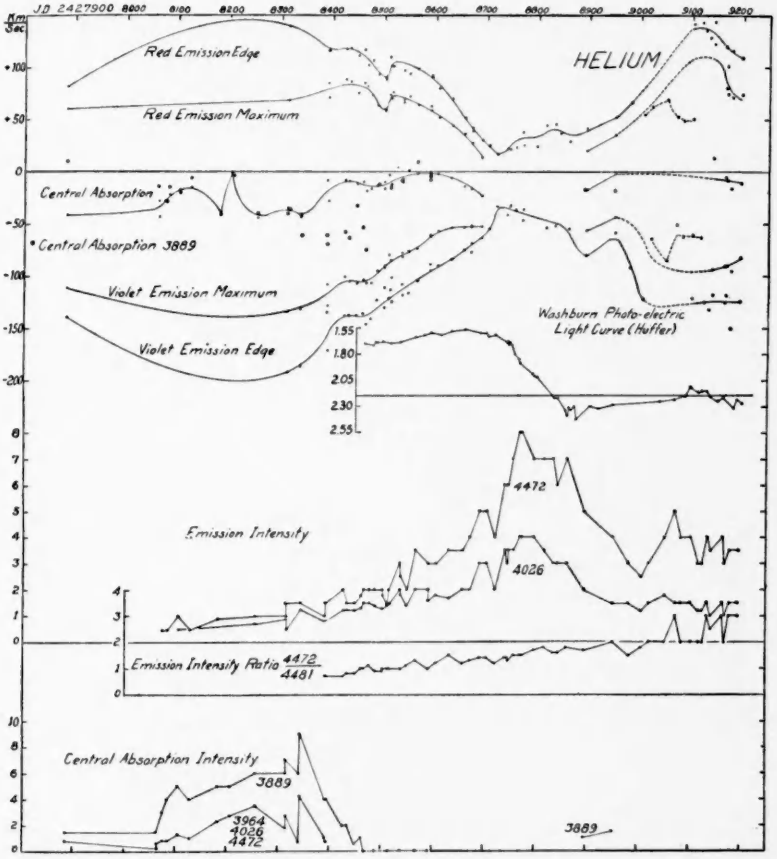

FIG. 2

fluctuation, until they reached the velocity previously shown by helium. This occurred about JD 2428250, just before the maximum absorption strength was attained.

In the previous stages the strongest *He* I absorption line, 3889, had agreed in velocity with the others; but at approximately JD 2428340 it suddenly diverged to higher negative velocities, while the

Table 2

Helium

J.D. 242+	RE	RM	CA	VM	VE	CA 3889	AI	AI 3889	EI 4026	EI 4472	4472/4481	(RE)	(VE)	No.
7885	+ 82	+ 60	-41	-111	-139	+10	0.8	1.5	-	-	-	-	-	2
8063	-	-	-28	-	-	-14	0.2	1.5	-	-	-	-	-	3
8064	-	-	-43	-	-	-	0.6	-	-	-	-	-	-	2
8075	-	-	-28	-	-	-28	0.8	3	-	0.5	-	-	-	3
8084	-	-	-22	-	-	-15	0.8	4	-	0.5	-	-	-	3
8105	-	-	-17	-	-	-20	1.3	5	0.5	1:	-	-	-	3
8128	-	-	-15	-	-	- 6	1.0	4	-	0.5	-	-	-	3
8182	-	-	-39	-	-	-41	2.3	5	-	1-	-	-	-	4
8206	-	-	- 2	-	-	- 4	2.7	5	?	?	-	-	-	4
8256	-	-	-44	-	-	-40	3.5	6	0.7	1	-	-	-	5
8315	-	-	-37	-	-	-41	1.8	6	1-	1	-	-	-	4
8315	+140	+ 68	-35	-134	-192	-37	2.7	7	0.5	1.5	-	-	-	5
8340	-	-	-44	-132	-196	-41	0.7	6	-	-	-	-	-	3
8342	-	-	-68	-	-	-62	4.2	9	1.2	1.5	-	-	-	5
8391	+116	+ 85	- 8	-108	-135	-62	1.0	4	0.8	1	0.7	-	-	3
8392	116	71	-28	-128	-171	-70	0.7	4	0.8	1.5	0.7	-	-	3
8426	118	88	- 8	-101	-138	-58	-	2	1.2	2	0.7	-	-	3
8434	119	86	- 9	-105	-138	-63	-	2	1.2	1.5	0.8	-	-	3
8450	111	75	-12	-107	-138	-33	-	0.5	1.2	1.5	0.8	-	-	4
8461	117	85	-10	-104	-136	-54	-	1	1.3	1.8	1	-	-	3
8468	102	82	-18	-107	-146	-75	-	0	1.5	2	1	-	-	4
8477	106	73	-16	-107	-141	-	-	-	1.5	2	1.1	-	-	3
8489	93	64	-13	- 95	-123	-13	-	0	1.4	2	0.9	-	-	3
8503	90	60	-10	- 91	-130	-	-	-	1.3	2	0.9	-	-	4
8503	88	58	-16	- 90	-111	-	-	-	1.3	1.8	1	-	-	4
8511	110	74	- 3	- 80	-121	-	-	-	1.5	1.5	1	-	-	2
8515	101	70	-13	- 85	-113	-15	-	0	1.5	2	1	-	-	4
8517	101	76	-12	-102	-125	-	-	-	1.5	2	1	-	-	4
8539	97	66	- 7	- 82	-108	- 9	-	0	2	3	1	-	-	5
8539	114	69	-10	- 78	-118	-	-	-	1.8	2.5	1	-	-	3
8550	94	72	+ 1	- 76	-116	-	-	-	1.4	2	1.1	-	-	2
8567	99	64	- 2	- 74	-105	+ 8	-	0	2	3.5	1.3	-	-	5
8592	92	62	- 2	- 62	- 89	- 6	-	0	2	3	1	-	-	5
8592	90	58	- 1	- 61	- 95	- 7	-	0	1.6	3	1	-	-	5
8608	80	52	- 2	- 57	- 90	-	-	-	1.8	3	1.2	-	-	3
8633	70	44	- 6	- 54	- 84	-	-	-	1.7	3.5	1.5	-	-	3
8659	52	36	-14	- 54	- 75	-	-	-	2	3.5	1.2	-	-	3
8672	41	27	-16	- 53	- 77	-	-	-	2	4	1.3	-	-	4
8672	38	26	-10	- 52	- 69	-	-	-	2	4	1.3	-	-	5
8692	30	+ 13	-23	- 53	- 63	-	-	-	3	5	1.4	-	-	5
8706	25	-	-	-	- 55	-	-	-	3	5	1.4	-	-	4
8721	16	-	-	-	- 34	-	-	-	2	4	1.2	-	-	8
8741	22	-	-	-	- 41	-	-	-	3.5	6	1.4	-	-	4
8746	21	-	-	-	- 34	-	-	-	3	6	1.4	-	-	9
8748	36	-	-	-	- 33	-	-	-	3.5	6	1.3	-	-	9
8759	23	-	-	-	- 36	-	-	-	3.5	7	1.5	-	-	11
8771	37	-	-	-	- 47	-	-	-	4	8	1.5	-	-	10
8773	25	-	-	-	- 36	-	-	-	4	8	1.5	-	-	12
8799	24	-	-	-	- 34	-	-	-	4	7	1.7	-	-	11
8819	44	-	-	-	- 54	-	-	-	3.5	7	1.8	-	-	6
8835	45	-	-	-	- 52	-	-	-	3	7	1.6	-	-	5
8844	36	-	-	-	- 41	-	-	-	3	6	1.6	-	-	4
8861	29	-	-	-	- 55	-	-	-	3	7	1.8	-	-	4
8896	41	+ 20	-17	- 57	- 80	-17	-	1	2	5	1.7	-	-	5
8951	53	+ 35	- 2	- 44	- 59	-18	-	1.5	1.5	4	2	-	-	5
8982	+ 65	-	-	-	- 92	-	-	-	1.5	3	1.5	-	-	2
9007	-	-	-	-	-122	-	-	-	1.2	2.5	1.8	+54	-	2
9021	-	-	-	-	-	-	-	-	1.5	3	2	62	-64	3
9052	-	-	-	-	-	-	-	-	1.8	4	2	70	-85	3
9071	-	-	-	-	-	-	-	-	1.5	5	3	52	-50	2
9084	-	-	-	-	-	-	-	-	1.5	4	2	48	-63	2
9102	+141	-	-	-	-122	-	-	-	1.5	4	2	+50	-61	2
9119	143	-	-	-	-	-	-	-	1.2	3	2	-	-63	2
9125	135	-	-	-	-125	-	-	-	1.2	3	2	-	-	2
9135	128	-	-	-	-132	-	-	-	1.5	4	3	-	-	2
9142	144	+122	+13	- 94	-118	-	-	-	1	3.5	2.5	-	-	2
9166	120	80	- 5	- 90	-125	-	-	-	1.5	4	3	-	-	2
9169	101	74	- 8	- 90	-119	-	-	-	1	3	2	-	-	2
9178	115	71	-16	- 95	-150	-	-	-	1.5	3.5	3	-	-	2
9196	+109	+ 74	-11	- 83	-124	-	-	-	1.5	3.5	3	-	-	3

remaining helium lines gave considerably smaller negative velocities than before. The hydrogen central absorption lines also moved to lower negative velocities, but not as abruptly as the helium lines.

Soon after this velocity separation, maximum absorption intensities occurred simultaneously at all helium and hydrogen lines, JD 2428342, followed by a precipitous decline in strength. At the end of the decrease all the lines except λ 3889 appeared merely as two widely separated emission lines, showing, apparently, only the continuous spectrum between them and no sharp absorption line. Underlying this was the great broad, shallow absorption, which was now less wide than formerly. At this point the absorption line λ 3889 appeared as a slight dip in the emission blend with $H\zeta$ and again agreed in velocity with measures of the space between the emission components of the other *He* I lines. *He* I 3889 was present in absorption until JD 2428592 and continually weakened until its final disappearance.

Probably the variations in the absorption intensity of the *He* I line 3965 should be shown in Figure 2 separately from those of λ 4026 and λ 4472, as the former is a singlet line and the latter two are triplets. Actually, their intensity changes were nearly identical.

As at the hydrogen lines, a second pair (blended) of emission lines developed after the single-line phase and caused the helium lines to appear fuzzy and poorly defined.

Dr. McLaughlin, of the University of Michigan Observatory, has very kindly made estimates of the emission intensities of the *He* I lines 4026 and 4472 relative to the neighboring continuous spectrum. They are, in effect, estimated ratios of energy per unit frequency difference. They are not total energies. He also estimated the ratio of intensity of *He* I 4472 and *Mg* II 4481. This ratio is approximately free from the effect of narrowing of the lines, as λ 4481 narrowed simultaneously with λ 4472. His estimates are given in Table 2 and are shown graphically in Figure 2. *He* I 4472 continually increased in strength relative to *Mg* II 4481.

Both λ 4026 and λ 4472 reach a maximum central intensity during the single-line stage. This is due mainly to the narrowness of the lines but partly to a real increase in total intensity, as the maximum strength occurred *after* the narrowest part of the single-line phase.

A second maximum of intensity occurred near JD 2429070 and is to be attributed to the combined effects of both pairs of emission lines, although mainly to the new set.

The velocity-curves for both pairs of lines are shown in Figure 2 and, in the main, are similar to those of hydrogen. The decrease in the velocity of the original red component is more pronounced, and the edge measures of the second set of lines are far more definitive than for hydrogen. For several plates in this interval the new lines were easily measurable, and the old pair appeared only as a shading at each edge. As the new pair faded out after JD 2429100, the old lines regained at least part of their former intensities.

THE *Fe* II LINES

Many lines of *Fe* II were present throughout the earlier phases[13] of γ Cassiopeiae and the first year of this study, but the majority were diffuse patches of emission. Only a very few of the strongest were accurately measurable, and these gave results strikingly similar to the hydrogen and helium lines (Fig. 3). Coincidentally with the narrowing, the *Fe* II lines began to sharpen and grew stronger until nearly sixty, counting blends, were measured in the single-line stage. As the components again separated, the intensity of the lines declined immediately.

The rate of narrowing of the two components of each emission line was somewhat less than for the other elements, and the lines were not quite as narrow in the single-line phase.

The central dip, or absorption line, underwent no large changes in velocity or intensity, although the velocity-curve showed some of the same variations as the curves of the other elements. The fluctuation in the velocity of the red emission component, JD 2428500, previously mentioned, was small but present.

The V/R-curve for the average of all lines visible in the $b^4P - z^4D^o$ multiplet[14] was similar to those of hydrogen, although of lesser amplitude. It preceded the $H\delta$-curve by about 150 days. The aver-

[13] Curtiss, *Pub. Obs. U. of Michigan*, **2**, 1, 1916; *ibid.*, **3**, 1, 1923; *ibid.*, p. 16; *ibid.*, p. 256. See also Lockyer, *M.N.*, **93**, 362, 1933; Cleminshaw, *Ap. J.*, **83**, 495, 1936.

[14] The strongest lines are λλ 4173, 4233, 4303, 4352, 4385, and 4417.

age curve for the $b^4F - z^4F^o$ multiplet[15] was in phase with the hydrogen-curves but was peculiar in that the two components tended to be equal. The $b^4F - z^4D^o$ curve[16] was similar to that for the $b^4P - z^4D^o$ multiplet but showed a tendency to approach unity

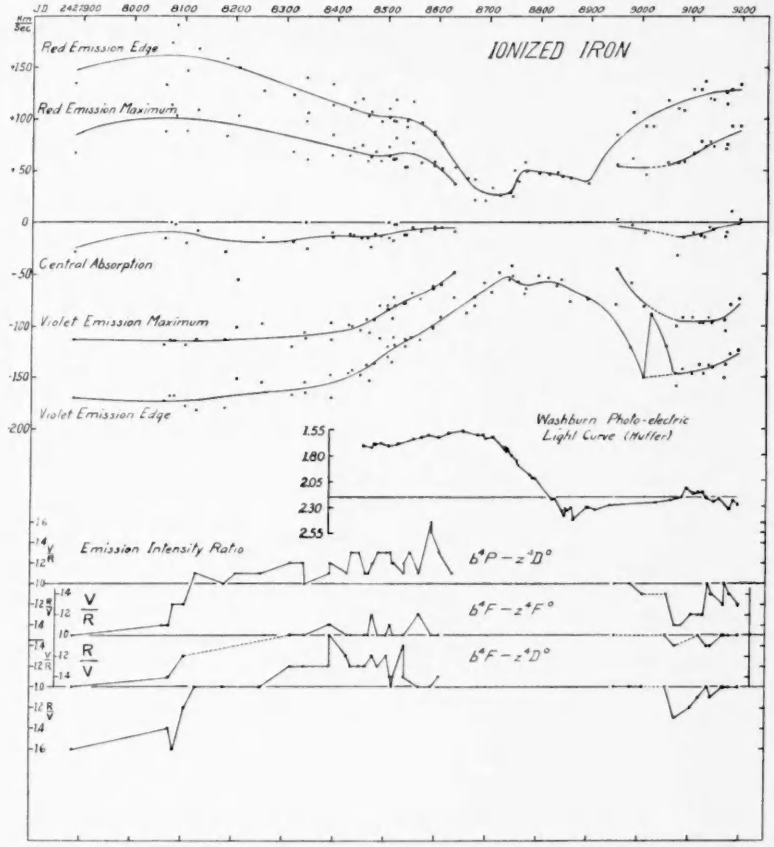

FIG. 3

just before the single-line stage. The lines of the first multiplet thus behaved like the hydrogen lines; those of the second resembled the *He* I lines in behavior; while those of the third were similar in their changes to the *Si* II lines. This may possibly be an indication of the

[15] The strongest lines are λλ 4489, 4491, 4515, 4520, 4556, and 4629.

[16] The strongest lines are λλ 4508, 4522, 4549, and 4584.

Table 3

FeII

J.D. 242+	RE	RM	CA	VM	VE	V/R (1)	V/R (2)	V/R (3)	No.
7885	+134	+ 67	-28	-113	-170	1.5R	1.5R	1.6R	3
8063	133	88	-15	-118	-173	1.4R	-	-	1
8064	-	-	-	-	-	-	-	-	-
8075	174	113	0	-114	-168	1.4R	1.4R	1.4R	3
8084	191	103	- 2	-114	-168	1.2R	-	1.6R	2
8105	147	89	-20	-119	-178	1.2R	1.2R	1.2R	3
8128	168	109	- 8	-113	-182	1.1	-	1.0	2
8182	159	84	-28	-113	-180	1.0	-	1.0	3
8206	150	103	-55	-101	-151	1.1	-	-	1
8256	127	78	-15	- 98	-155	1.1	-	1.0	1
8315	-	-	-	-	-	-	-	-	-
8315	123	69	-18	-120	-167	1.2	1.0	1.2	5
8340	140	98	0	-106	-155	1.2	-	-	1
8342	106	61	-25	-112	-165	1.0	1.0	1.2	5
8391	114	65	-10	- 97	-148	1.1	1.1	1.2	4
8392	134	85	-14	-114	-170	1.2	1.1	1.5	4
8426	110	65	-11	- 99	-146	1.1	1.0	1.3	4
8434	116	72	-12	-100	-144	1.3	1.0	1.2	8
8450	120	75	-15	-104	-148	1.3	-	1.2	6
8461	103	60	-15	- 93	-139	1.1	1.0	1.2	6
8468	107	64	-24	-106	-154	1.1	1.0	-	4
8477	103	69	-11	- 94	-136	1.2	1.2	1.3	4
8489	98	60	-13	- 80	-112	1.3	1.0	1.2	3
8503	101	65	-15	- 80	-130	1.3	1.0	1.3	4
8503	110	73	0	- 83	-120	1.3	1.0	1.3	4
8511	99	61	-17	- 92	-135	1.3	1.1	1.1	6
8515	98	61	- 2	- 72	-111	1.2	-	1.0	5
8517	119	82	- 2	- 80	-119	1.2	1.0	1.1	6
8539	98	54	-12	- 78	-113	1.1	1.0	1.4	5
8539	92	54	-12	- 78	-120	1.2	1.0	1.1	4
8550	117	77	- 5	- 68	-111	1.3	-	-	4
8567	96	58	- 9	- 73	-114	1.1	1.2	1.0	11
8592	88	59	- 5	- 64	-102	1.6	1.0	1.0	10
8592	85	55	- 6	- 62	-100	1.5	1.0	1.0	10
8608	77	52	- 5	- 60	- 91	1.3	1.0	1.1	14
8633	53	+ 37	- 9	- 48	- 72	1.1	-	-	1
8659	42	-	-	-	- 87	-	-	-	17
8672	41	-	-	-	- 80	-	-	-	10
8672	22	-	-	-	- 72	-	-	-	16
8692	21	-	-	-	- 59	-	-	-	17
8706	33	-	-	-	- 67	-	-	-	12
8721	26	-	-	-	- 49	-	-	-	25
8741	29	-	-	-	- 55	-	-	-	13
8746	25	-	-	-	- 42	-	-	-	23
8748	50	-	-	-	- 52	-	-	-	26
8759	40	-	-	-	- 57	-	-	-	27
8771	59	-	-	-	- 69	-	-	-	26
8773	50	-	-	-	- 64	-	-	-	27
8799	48	-	-	-	- 51	-	-	-	22
8819	47	-	-	-	- 53	-	-	-	11
8835	49	-	-	-	- 61	-	-	-	9
8844	45	-	-	-	- 55	-	-	-	6
8861	44	-	-	-	- 76	-	-	-	7
8896	38	-	-	-	- 74	-	-	-	2
8951	85	+ 56	+ 3	- 45	- 79	1.0	1.0	1.0	2
8982	106	62	- 2	- 58	-121	1.0	-	1.0	1
9007	94	+ 46	-10	- 81	-150	1.1R	-	1.0	1
9021	93	-	-	-	- 88	-	-	-	1
9052	118	+ 59	-	-	-120	1.1R	1.0	1.0	1
9071	110	58	-31	-100	-159	1.4R	1.1R	1.3R	4
9084	108	59	-15	- 92	-143	1.4R	-	-	2
9102	128	66	-10	- 92	-147	1.3R	-	1.2R	2
9119	128	78	-13	- 96	-138	1.3R	1.0	1.1R	1
9125	136	74	-14	- 97	-146	1.3R	-	-	1
9135	120	78	- 5	- 91	-139	1.0	1.1R	1.0	2
9142	118	73	- 6	- 97	-140	1.1R	1.1R	1.1R	5
9166	126	71	-14	- 94	-151	1.2R	1.0	1.0	1
9169	114	76	-10	-105	-139	1.0	1.0	1.0	1
9178	128	93	+11	- 79	-127	1.1R	1.0	1.0	2
9196	+133	+ 94	+ 2	- 74	-124	1.2R	1.0	1.0	2

heights in the atmosphere at which the lines were produced. No differences between the velocities of the three multiplets could be established, nor were there any correlations with the upper excitation potentials of the lines in question.

In the stages after the single-line phase when all other lines in the photographic spectrum appeared fuzzy, the *Fe* II lines retained nearly their original double appearance. The components gradually separated and, except for a short time, near JD 2429040, were easily resolved. It is probable that the secondary set of emission lines actually did develop but never became as prominent as in lines of other elements.

THE *Si* II LINES

The three lines, λλ 3854, 3856, and 3863, constituted the strongest features of the *Si* II spectrum, although λ 4128 and λ 4131 were present. The former lines were seen as diffuse, unmeasurable emissions during most of the first 200 days covered by this investigation. After that interval they soon became the sharpest emission lines in the spectrum and were approximately monochromatic in the last stages of the narrowing.

Because of the higher dispersion in the ultraviolet, the *Si* II lines could be resolved for a longer period than those of any other element. The hydrogen components were actually closer and thus became blended earlier than either the *Si* II or *He* I lines.

The same trends shown in Figures 1, 2, and 3 are also evident in Figure 4, and the lines in the single-line stage became the narrowest of all elements. The so-called "central absorption line" appeared to be merely the space between the emission components and was of the same strength as the adjacent continuous spectrum.

The weakness of the absorption lines of *Si* II, 3854, 3856, and 3863, in stages when the *H* and *He* I lines were strong, shows that they do not originate from the ground level of the ion.[16a] The lines behave very much as does *Mg* II 4481, which is strong in emission but weak in absorption. Miss Moore[16b] states that they originate from an $sp^2\ ^2D$ term, and there seems to be no reason why this level should

[16a] Grotrian, *Handbuch der Astrophysik*, **3**, Part II, 575, 1930.

[16b] *A Multiplet Table of Astrophysical Interest*, Princeton Observatory, 1933.

not combine with the odd ground level of the ion. Hence the observational evidence strongly supports the more modern spectroscopic theory.

The two curves for the maxima and the "absorption"-curve were shifted approximately 8 km/sec toward the violet relative to the

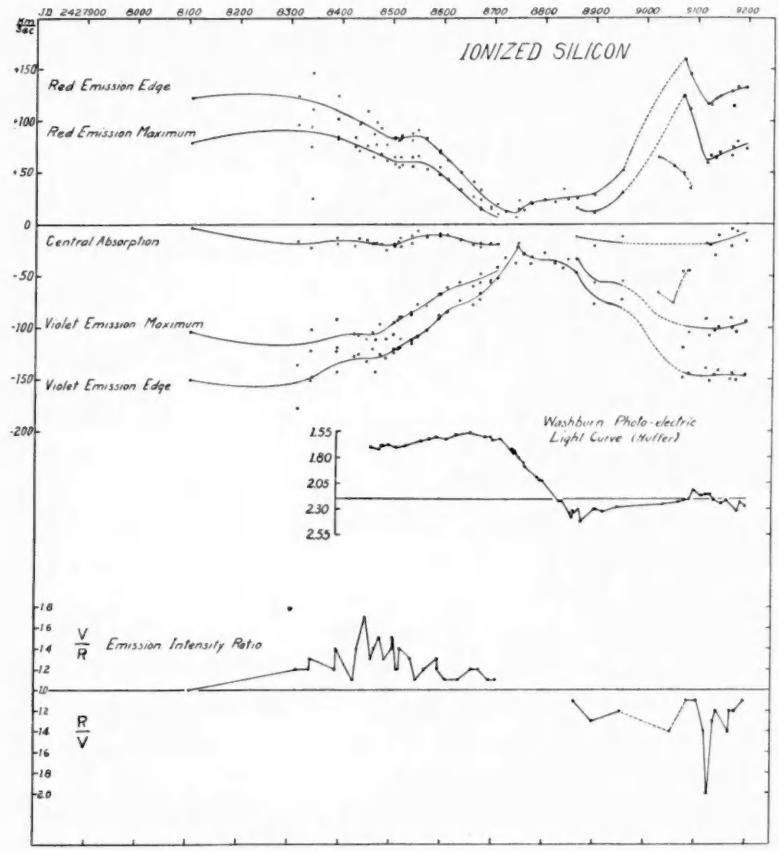

FIG. 4

He I curves. The velocity-curves of *He* I and *Si* II were more alike than those of any other pair of elements.

The V/R-curve behaved similarly to that of the $b^4F - z^4D^o$ multiplet of *Fe* II and reached a maximum during the narrowing, rather than during the single-line stage, while the decrease occupied

Table 4

SiII

J.D. 242+	RE	RM	CA	VM	VE	V/R	(RE)	(VE)	No.
7885	-	-	-	-	-	-	-	-	-
8063	-	-	-	-	-	-	-	-	-
8064	-	-	-	-	-	-	-	-	-
8075	-	-	-	-	-	-	-	-	-
8084	-	-	-	-	-	-	-	-	-
8105	+122	+ 78	- 4	-104	-151	1.0	-	-	1
8128	-	-	-	-	-	-	-	-	-
8182	-	-	-	-	-	-	-	-	-
8206	-	-	-	-	-	-	-	-	-
8256	-	-	-	-	-	-	-	-	-
8315	-	-	-	-	-	-	-	-	-
8315	+124	+ 96	-16	-137	-178	1.2	-	-	2
8340	94	75	-23	-123	-152	1.2	-	-	2
8342	146	111	+25	-102	-149	1.3	-	-	2
8391	102	82	-13	- 92	-123	1.2	-	-	2
8392	124	85	-19	-120	-144	1.4	-	-	2
8426	84	75	-21	-106	-128	1.1	-	-	3
8434	97	71	-14	-108	-126	1.4	-	-	3
8450	109	76	-15	-112	-133	1.7	-	-	3
8461	87	65	-18	-105	-121	1.3	-	-	3
8468	99	77	-18	-112	-144	1.4	-	-	2
8477	93	68	-19	- 97	-126	1.5	-	-	3
8489	77	61	-25	-111	-130	1.3	-	-	2
8503	82	58	-20	- 95	-121	1.4	-	-	2
8503	84	65	-21	-107	-125	1.5	-	-	3
8511	81	55	-17	- 93	-121	1.2	-	-	2
8515	82	65	-13	- 90	-120	1.2	-	-	3
8517	86	57	-21	- 90	-112	1.4	-	-	3
8539	88	65	-11	- 88	-112	1.3	-	-	3
8539	81	56	-18	- 86	-116	1.3	-	-	2
8550	91	66	- 6	- 78	-109	1.1	-	-	2
8567	83	53	-12	- 79	-103	1.2	-	-	3
8592	71	55	-11	- 68	- 88	1.3	-	-	3
8592	69	48	- 9	- 68	- 91	1.2	-	-	2
8608	62	43	-10	- 61	- 85	1.1	-	-	2
8633	50	34	-15	- 56	- 74	1.1	-	-	2
8659	41	27	-20	- 60	- 78	1.2	-	-	3
8672	33	14	-18	- 49	- 67	1.2	-	-	2
8672	24	15	-22	- 56	- 73	1.2	-	-	3
8692	17	15	-18	- 54	- 56	1.1	-	-	3
8706	20	+ 10	-19	- 41	- 52	1.1	-	-	2
8721	12	-	-	-	- 32	-	-	-	5
8741	7	-	-	-	- 38	-	-	-	3
8746	15	-	-	-	- 21	-	-	-	5
8748	23	-	-	-	- 19	-	-	-	3
8759	14	-	-	-	- 29	-	-	-	5
8771	21	-	-	-	- 39	-	-	-	5
8773	20	-	-	-	- 32	-	-	-	5
8799	24	-	-	-	- 28	-	-	-	5
8819	22	-	-	-	- 38	-	-	-	3
8835	34	-	-	-	- 42	-	-	-	2
8844	24	-	-	-	- 34	-	-	-	2
8861	25	+ 16	-12	- 34	- 47	1.1R	-	-	2
8896	28	11	-21	- 56	- 77	1.3R	-	-	2
8951	+ 52	+ 31	-12	- 55	- 73	1.2R	-	-	2
8982	-	-	-	-	-	-	-	-	-
9007	-	-	-	-	-	-	-	-	-
9021	-	-	-	-	-	-	+65	-66	2
9052	-	-	-	-	-	1-4R	56	-76	2
9071	+160	+124	-	-120	-149	-	50	-46	2
9084	145	111	-	-105	-145	1.1R	+35	-45	2
9102	-	-	-	-	-	1.1R	-	-	1
9119	116	59	-19	- 92	-140	1.4R	-	-	2
9125	115	66	-20	-108	-152	2.0R	-	-	2
9135	121	64	-30	-103	-146	1.3R	-	-	2
9142	123	70	-11	-100	-142	1.2R	-	-	2
9166	129	66	-21	- 90	-150	1.4R	-	-	2
9169	114	75	- 4	-100	-145	1.2R	-	-	1
9178	132	80	- 6	-104	-151	1.2R	-	-	1
9196	+132	+ 73	-16	- 94	-146	1.1R	-	-	2

as long a time as the rise. This is in sharp contrast to the abrupt declines shown by the hydrogen curves.

The behavior of the *Si* II lines subsequent to the single-line stage was again remarkably similar to that of the hydrogen and helium lines. The former became wider but also showed a sharper velocity

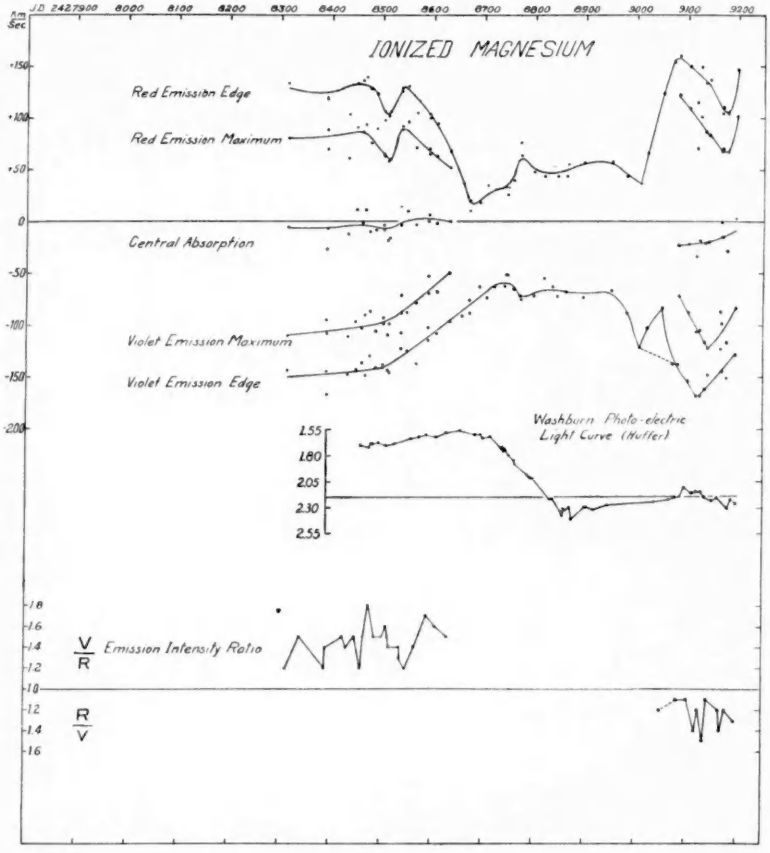

FIG. 5

decrease at the red component near JD 2429100 than did the latter two elements. The new pair of *Si* II lines was easily visible, and on plates of JD 2429071 and 2429084 was completely separated from the original pair. Each component of the original lines was approximately twice as broad as the corresponding line before the single-line phase.

Table 5

MgII

J.D. 242+	RE	RM	CA	VM	VE	V/R
7885	-	-	-	-	-	-
8063	-	-	-	-	-	-
8064	-	-	-	-	-	-
8075	-	-	-	-	-	-
8084	-	-	-	--	-	-
8105	-	-	-	-	-	-
8128	-	-	-	-	-	-
8182	-	-	-	-	-	-
8206	-	-	-	-	-	-
8256	-	-	-	-	-	-
8315	-	-	-	-	-	-
8315	+133	+ 81	- 5	-110	-144	1.2
8340	-	-	-	-	-	-
8342	198	155	+41	-106	-150	1.5
8391	120	89	- 6	- 95	-145	1.2
8392	119	70	-26	-108	-167	1.4
8426	189	143	+45	- 72	-134	1.5
8434	104	61	-12	-111	-148	1.4
8450	134	91	+11	- 97	-143	1.5
8461	137	87	- 2	-103	-137	1.2
8468	140	94	+11	- 90	-149	1.5
8477	128	76	-10	- 87	-130	1.8
8489	124	90	- 8	-106	-141	1.5
8503	106	65	- 8	- 93	-141	1.5
8503	98	64	- 4	- 99	-139	1.5
8511	102	58	-18	-110	-144	1.6
8515	107	60	-16	- 99	-146	1.5
8517	146	124	+ 8	- 66	-143	1.4
8539	129	92	- 3	- 89	-123	1.4
8539	126	89	+15	- 71	-108	1.3
8550	131	96	+10	- 88	-125	1.2
8567	105	71	- 3	- 79	-138	1.4
8592	104	70	+ 6	- 53	-102	1.7
8592	100	65	0	- 70	-115	1.7
8608	95	64	- 1	- 68	-108	1.6
8633	68	+ 52	0	- 50	- 96	1.5
8659	38	-	-	-	- 91	-
8672	20	-	-	-	- 89	-
8672	10	-	-	-	- 76	-
8692	18	-	-	-	- 63	-
8706	35	-	-	-	- 73	-
8721	30	-	-	-	- 63	-
8741	34	-	-	-	- 62	-
8746	26	-	-	-	- 51	-
8748	33	-	-	-	- 51	-
8759	40	-	-	-	- 65	-
8771	76	-	-	-	- 72	-
8773	64	-	-	-	- 75	-
8799	48	-	-	-	- 72	-
8819	44	-	-	-	- 55	-
8835	54	-	-	-	- 63	-
8844	43	-	-	-	- 72	-
8861	44	-	-	-	- 68	-
8896	57	-	-	-	- 73	-
8951	57	-	-	-	- 66	-
8982	43	-	-	-	- 89	-
9007	36	-	-	-	-122	-
9021	66	-	-	-	-104	-
9052	123	-	-	-	- 84	1.2R
9071	155	-	-	-	-138	-
9084	160	+122	-23	- 72	-138	1.1R
9102	150	109	-22	- 88	-154	1.1R
9119	115	70	-34	-106	-169	1.4R
9125	149	101	-19	-105	-168	1.2R
9135	134	86	-21	-116	-162	1.5R
9142	136	84	-20	-122	-149	1.1R
9166	104	67	- 1	- 86	-123	1.2R
9169	110	70	-15	- 99	-145	1.4R
9178	104	67	-28	-117	-151	1.2R
9196	+147	+101	+ 3	- 83	-129	1.3R

THE LINE OF *Mg* II λ 4481

This line, though present throughout all stages of the spectral variations, could be measured only during the narrowing and single-line phases and the subsequent widening. Its changes of emission intensity were extremely great, varying from a faint blur before JD 2428300 to one of the strongest lines in the spectrum. In this it behaved like the *He* I lines. It continually increased in strength until the end of the single-line stage, when it underwent a decided diminution of intensity.

The second pair of emission lines at *Mg* II 4481, while undoubtedly present, was never prominent. The most striking features of the post–single-line stage were the rapid fluctuations of the red component (Fig. 5), while the narrow part of the single-line phase lasted about 70 days longer than for the other elements.

The scatter of the points defining the velocity-curves is greater than for other elements, because of the lower dispersion at λ 4481 and because the velocities depend upon only one line. Nevertheless, the points are sufficiently accurate to define the velocity-curves, which differ somewhat from those of the other four elements measured. The narrowing phase occupied a shorter interval of time and was more abrupt than the others. The dip in the velocity-curve of the red component was by far the most pronounced, and the central absorption line was displaced toward the red more than in the other cases.

The V/R-curve did not display any pronounced trend during the short time it was visible; it resembled that of the $b^4P - z^4D^o$ multiplet of *Fe* II.

DISCUSSION

Whatever the forces which have produced the observed changes in γ Cassiopeiae, they have acted on elements of widely different atomic weights with rather similar effects.[17] From JD 2428400 to JD2428700 in the narrowing phases the violet maxima of the five elements measured showed the same displacements, within the errors of measurement. For four elements the violet component was stronger than the red in this time interval ($R = V$ for *He* I). In other

[17] *J.R.A.S. Canada*, **32**, 353, 1938.

phases the violet components showed real differences in displacement, although the same general forms were apparent (see Figs. 1–5).

Real differences between the velocity-curves for the red components were also observed, but again these were merely modifications of the common curve. A sudden fluctuation in velocity occurred around JD 2428500 at all red emissions but not at the violet. This oscillation was most marked for *Mg* II, while *He* I, *Si* II, *H*, and *Fe* II showed smaller changes, decreasing in amplitude in the order named; that for *Fe* II was barely perceptible.

The red hydrogen component, before the single-line stage, was displaced much less than the red emission lines of the other elements. The latter were nearly symmetrically displaced, although real differences, sometimes 50 km/sec, were observed between the curves for various elements.

The rates of approach of the two components were as follows: *Fe* II slowest, then *H*, followed by *Si* II and *He* I, which were equally rapid. *Mg* II took less than one-third as long to narrow as *Fe* II, i.e., 210 days as against 640 days.

Except for time lags, which were short compared with the length of the cycle, the four elements *H*, *Si* II, *Fe* II, and *Mg* II possessed simultaneously either a strong red and weak violet component or the reverse.

The central absorption line at the hydrogen, the helium, and possibly the *Fe* II lines must be considered as a combination of three effects. First, there is an apparent line produced by the lack of undisplaced emission; second, there is a deepening of this space by the broad underlying absorption; and third, a true absorption line is produced in a slowly moving layer of gas, probably exterior to, and perhaps overlapping, the region of effective emission.

Struve and Wurm[18] have shown that in several B stars there exists an outer atmospheric shell of gas capable of producing strong absorption lines. This shell lies approximately at five times the radius of the photosphere and is nearly at rest with respect to the photosphere. The region of effective emission must lie between the photosphere and this layer. Consequently, emission from atoms moving nearly at zero velocity with respect to the observer, except

[18] *Ap. J.*, **88**, 84, 1938.

for the actual radial velocity of the star, will have to penetrate a great thickness of similarly moving atoms; and very little of such emission will leave the star's atmosphere, because of self-absorption. This, of course, does not apply to lines arising from the ground level. It is exemplified by the gap between the violet and the red components of the *He* I and *Si* II lines. In addition, the same mysterious unknown cause may be active here, as in novae, to produce a dip in the emission near the undisplaced position of the line. If rotation of the central star is a factor aiding the ejection of matter, the low velocity emission would be cut down by a lack of ejections occurring in polar and near-polar regions. The poles must, in the case of a Bne star, lie nearly at right angles to the line of sight if rotation is an important aid to ejection. It is unfortunate that no forbidden lines are found in the spectrum, because they would aid in determining which mechanism is operating.

The great increase in absorption of the sharp hydrogen and helium lines at the beginning of the narrowing phase[19] followed the same course for both elements. This indicates that these lines were all produced in the same general region, while the separation of the velocity-curves of λ 3889 and the remaining *He* I lines suggests that different layers of the shell then produced the various lines.

It is reasonable that lines of different elements and individual lines of the same element originate at different effective atmospheric levels. This is well known in the chromosphere and has recently been demonstrated by Goedicke[20] in the atmosphere of the early-type star in the VV Cephei system.

The photoelectric light-curve of γ Cassiopeiae by Huffer is shown in each figure. It has a rather smooth rise, reaching magnitude 1.57 at the maximum in May, 1937, approximately at the beginning of the single-line phase. During this phase the brightness of the star decreased rapidly, reaching a minimum of 2.44 at the end of the single-line stage. It remained near that magnitude until at least the end of the time covered by this investigation, although there was a slight secondary maximum near JD 2429100.

[19] Lockyer, *M.N.*, **96**, 2, 1935; **96**, 679, 1936; McLaughlin, *Ap. J.*, **84**, 235, 1936; **85**, 181, 1937.

[20] *Pub. A.A.S.* **9**, No. 3, 122, 1938.

It has not been determined from the Michigan plates just what percentage of the rise in brightness was caused by the increase in the intensities of the emission lines. It was probably small, however. An analogous case concerns the strong lines in Mira stars which contribute less than 0.1 mag. to the variation.

Measures by Chalonge and Safir[21] during November, 1936, yielded temperatures in the neighborhood of 10,000° K. In September, 1935, they derived, by the same method, 12,500° K and 14,000° K from wave lengths greater than 3700 A and less than 3700 A, respectively. Vanderkerkhove[22] found a gradient (Greenwich scale) corresponding to 10,250° K in November and December, 1936. This constituted a drop of 6000° K from his own earlier measures made from 1926–1927 observations.

Greaves and Martin[23] at Greenwich have reported four different temperatures for γ Cassiopeiae. In 1926–1927 they derived 16,100° K from eleven plates. Four plates near 1936.9 yielded 10,500° K; and five plates, averaged at 1937.7, gave 9200° K. A single plate of 1938.2 yielded 12,000° K, but this value was somewhat uncertain because of the large zenith distance of the star. The 1926–1927 and 1936 temperatures were derived from the same plates as those of Vanderkerkhove.

The 1936 observations were made during the rising part of the light-curve; the 1937 observations came during the rapid decrease in brightness. The single 1938 temperature measure was made shortly after minimum light.

Williams[24] gives four color temperatures from individual plates. On September 6, 1937, the temperature was 8800° K. It was 8000° K on October 30, 1937; and two plates of July 14, 1938, give 13,000° K and 11,500° K. The first and third measures have α Lyrae[25] ($\phi_0 = 1.14$) as comparison star; α Andromedae is the comparison star for the remaining pair.

Williams and the Greenwich observers agree on relative gradients, but they find different zero points. If 0.14 is added to the Greenwich

[21] *C.R.*, **203**, 1329, 1936.

[22] *Observatory*, **60**, 329, 1937.

[23] *M.N.*, **98**, 435, 1938; *Observatory*, **61**, 118, 1938.

[24] U. of Michigan, unpublished.

[25] *Pub. Obs. U. of Michigan*, **7**, 93, 1938.

gradients, then they correspond to Williams' gradients. When this change of zero point is made, the Greenwich temperatures reduce to 13,500° K, 9400° K, 8400° K, and 10,700° K. They thus drop into line with the values found by Williams. Measures by all observers now fall along a smooth curve.

Woolley[26] has suggested that the low temperatures found for emission stars are apparent effects caused by fluorescent Paschen continuous emission overlying the normal continuous spectrum. For the drop in temperature of γ Cassiopeiae this view does not seem acceptable. Chalonge and Safir measured the decrease in temperature from the spectrum nearly 5000 A from the Paschen limit. In addition, Greaves and Martin[27] have shown γ Cassiopeiae to radiate as a black body while in the cool stage (from energies at 4284 A, 5308 A, and 6320 A). If the Paschen continuum were strong enough to produce the apparent low color temperatures, the spectral energy distribution would not be that of a black body. The Paschen continuum intensity decreases exponentially toward the violet.

To test this hypothesis let the energy radiated at 4284 A by a black body at 16,000° K be equal to that radiated at the same wave length by a brighter black body at 9000° K, and let sufficient Paschen continuous emission be added to the energy corresponding to 16,000° K to make the total radiation at 6320 A equal for each star. Then the combined radiation at 4284 A is 5.6 per cent greater than that emitted by the cool star. Similarly, the combined radiation of the hotter star at 5308 A is 9.8 per cent less than the energy emitted by the 9000° star at the same wave length.

Greaves and Martin[1] state that the residuals at 5308 A from black-body radiation from three plates are +2.7, +3.6, and −7.1 per cent. Two of these are of opposite sign, and all are much smaller than the residual computed in the foregoing paragraph. The black-body temperature for each plate was determined from the measured energies at 4284 A and 6320 A.

Woolley's hypothesis requires that the energy emitted purely as Paschen continuum between 8206 A and 7000 A be greater than the

[26] *M.N.*, **95**, 115, 1934.

[27] *Ibid.*, **98**, 434, 1938.

energy emitted at the corresponding wave lengths by the photosphere. The photosphere, of course, would remain approximately at 16,000° K, on the foregoing suggestion.

Another difficulty for this hypothesis arises, however. γ Cassiopeiae had a decidedly lower color temperature near minimum light (0.3 mag. fainter than normal) than formerly. In the visible spectrum approximately 75 per cent of the light is from the normal black-body photospheric radiation, while 25 per cent is Paschen continuum, if we are to accept Woolley's proposal. This would seem to mean that the photosphere contracted until it emitted roughly 60 per cent of its usual light and yet remained at 16,000° K.

The foregoing temperature measures by all authorities, combined with the light-curve, show that γ Cassiopeiae became brighter and cooler at the same time. An interpretation is that the increased radiation led to the formation of a much larger photosphere, which thus appeared cooler than normal. When the "inner star" itself cooled below its original temperature, the false photosphere cleared away, leaving the original star in view, cooler than formerly but slightly hotter than the false photosphere.

The clearing-away of the upper photosphere occurred during the rapid decrease in brightness in the fall of 1937. The latter state is shown by the nearly stationary light-curve after the decrease.

If this mechanism is the correct one, it is probable that similar, but far less important, changes took place in 1929 and 1934.

An observational result, correlating with the behavior of prominences and novae, is noted, namely, that atoms of various elements are moving in the atmosphere with essentially the same mean velocities. Theory is not able to explain this phenomenon; yet it has been observed in at least three different types of atmospheres.

CONCLUSION

The recent changes in the spectrum of γ Cassiopeiae are of such nature that they are inexplicable by means of any model heretofore advanced to explain Be variations. Struve's model[28] of a rapidly

[28] *Ap. J.*, **73**, 93, 1931.

rotating star with its equatorial ring does not explain the V/R changes and thus cannot be entirely accepted, although rapid rotation of the main body of the star may be the trigger which allows radiation pressure to eject matter. The diffuse underlying absorption may indicate rapid photospheric rotation, although the velocity shown, 300 km/sec, is rather high. Neither is McLaughlin's hypothesis[29] tenable, in spite of the fact that it works so beautifully in such a case of Be variation as 25 Orionis[30] exhibits.

In the latter model the rotational and pulsational components of the velocities of the atmosphere of the star combine in such a manner as to produce an alternation in the relative strengths of the two components of an emission line. The red component will be stronger during an expansion, and the violet stronger during collapse. On this explanation the velocity-curve of the red edge of the red component should remain roughly parallel to the velocity-curve of the violet edge of the violet component, unless the atmosphere had expanded to such a size that the rotational component had become negligible. In McLaughlin's hypothesis the red component should be stronger as the two lines approached each other. Actually, the violet component was far more intense. This nearly parallel condition is fulfilled by 25 Orionis, but is not even remotely satisfied by γ Cassiopeiae.

Gerasimovič[31] has also advanced a hypothesis, based on alternate expanding and quiescent states of the atmosphere under the influence of radiation pressure. His model does not explain the presence of the observed sharp central absorption lines of helium and hydrogen. The atoms producing these lines are nearly at rest and must be remote from the photosphere.[32] Gerasimovič's model postulates a large velocity of expansion in the region where the undisplaced absorption lines are now known to be formed. It also does not satisfactorily account for the observed unsymmetrical changes of velocity shown by the emission lines.

As all hypotheses fail to explain the observed phenomena, a new

[29] *Proc., Nat. Acad. Sci.*, **19**, 44, 1933.

[30] Dodson, *Ap. J.*, **84**, 180, 1936.

[31] *Observatory*, **58**, 115, 1935; *M.N.*, **94**, 743, 1934.

[32] Struve and Wurm, *Ap. J.*, **88**, 84, 1938.

theory must be found. To that end the observational data on γ Cassiopeiae have been collected and correlated. It remains for the future to determine the details of the new model.

A sequence, which may be purely fortuitous, should be mentioned. In 1928 and 1929, γ Cassiopeiae began its spectroscopic variations with a very mild fluctuation. About five years later, 1934, the star underwent a much stronger series of changes. The last cycle was in 1937 and 1938, only three years later, and was by far the most violent. Observations made during the next few years may be very interesting.

It is with great pleasure that I acknowledge my indebtedness to Director H. D. Curtis of the University of Michigan Observatory, who loaned me a long series of spectrograms of γ Cassiopeiae, and to Dr. D. B. McLaughlin, also of the University of Michigan Observatory, who proposed the problem and contributed many helpful suggestions. My thanks are also due to Director van de Kamp of the Sproul Observatory, who permitted me to use an excellent measuring engine, and to Director Olivier of the Flower Observatory, who allowed me to study γ Cassiopeiae as part of the regular program of the observatory during the school year 1937–38.

I also wish to thank Dr. C. M. Huffer of the Washburn Observatory for giving me his photoelectric light-curve prior to publication; Dr. R. C. Williams of the University of Michigan Observatory for sending me his unpublished color-temperature measures of γ Cassiopeiae; and Dr. O. C. Mohler of the Cook Observatory, with whom I had many interesting discussions.

APPENDED NOTE

A *Contribution* from the Mount Wilson Observatory, "The Excitation of Emission Lines in Late-Type Variables," by Thackeray,[33] may possibly furnish the clue to the identification of five of the numerous unidentified lines in the photographic spectrum of γ Cassiopeiae.[34] According to Thackeray, if certain far ultraviolet lines, known to be present in emission, lie close to the positions

[33] *Mt. Wilson Contr.*, No. 580; *Ap. J.*, **86**, 499, 1937.

[34] Baldwin, *Ap. J.*, **87**, 573, 1938.

of lines of other elements, line absorption can occur, producing, by a cyclical process, weak emission lines in the visible spectrum of the absorbing atoms.

Measured λ (I.A.)	Intensity	Identification	Exciting Agent	Notes
4037.01	0	*Fe* I 7.69 (1n)	Mg II 2795.52	1
4181.82	0	*Fe* I 1.76 (15)	*Fe* II 2562.54	.....
4307.42	0.3	*Fe* I 7.91 (35)	*Mg* II 2795.52	2
4325.49	0	*Fe* I 5.77 (35)	*Mg* II 2802.70	1, 3
4372.55	0.3	*Ti* I 2.41 (3)	*Mg* II 2802.70	4

NOTES TO TABLE

1. Questionable.
2. Previously identified as *Al* II 4307.20 (3), *Ti* II 4307.91 (40). May be a blend.
3. Provisionally identified as *Sc* II 4325.00 (20). May be a blend.
4. Near position of line found in A stars.

DEARBORN OBSERVATORY
NORTHWESTERN UNIVERSITY
EVANSTON, ILLINOIS
November 15, 1938

RECENT PROGRESS IN THE INTERPRETATION OF MOLECULAR SPECTRA AND IN THE STUDY OF MOLECULAR SPECTRA IN CELESTIAL OBJECTS*

INTENSITIES OF ELECTRONIC TRANSITIONS IN MOLECULAR SPECTRA

ROBERT S. MULLIKEN

In discussions of intensity relations in the spectra of molecules, attention has been devoted mainly to the relative intensities of the bands in a system of bands or of the lines in a band. The question of absolute intensities, that is, of absolute emission or absorption probability coefficients, has been rather neglected. Especially the question of the theoretical calculation of such absolute coefficients for molecules, or the theoretical interpretation of observed values, in relation to the electronic states involved, seems to have been neglected.

In the case of band spectra composed of many bands and fine lines, it is, of course, difficult to make direct measurements of absolute intensities, and less direct methods also offer difficulties. Results are most easily obtained with continuous spectra, such as occur when absorption of light in the molecule leads to dissociation. Careful measurements now exist on the visible and near-ultraviolet absorption continua of several of the diatomic halogen and hydrogen halide molecules in the vapor state, and on methyl halides and a great number of more complex organic and inorganic molecules in the liquid or dissolved state.

In attempting to determine the nature of the electronic structures of molecules, particularly for the excited states produced by absorption of light, it would be a great help if we could bring to bear some theoretical considerations relating absorption intensities to molec-

* The following papers were presented at a symposium held at the Yerkes Observatory, June 22–25, 1938. Publication has been postponed, or arranged elsewhere, in the case of the papers by Dr. John T. Tate, "Ionization and Dissociation Processes in Molecules by Electron Impact," and Dr. O. Struve and Dr. K. Wurm, "The Spectrum of the Earth's Atmosphere."

ular structure. For instance, if we were able to say that a high absorption intensity could only mean that certain types of molecular states were involved, while a low intensity could correspond only to certain other possibilities, it would be very helpful. It was from this point of view that I was led to make some simple calculations and comparisons with experiment, on which this is a preliminary report.

When, in the following discussion, I refer to the intensity or the Einstein coefficient, or the *f*-value, for an *electronic transition* in a molecule, I shall mean the sum total of intensity or of oscillator strength summed over all the separate bands and lines, or over the whole width of the broad continuous absorption, into which the spectrum belonging to this particular electronic transition is spread out.

In making any calculation on transition probability or *f*-value (number of dispersion electrons), one uses, according to quantum mechanics, the relations

$$f_{mn}^{(q)} = \frac{mhc^2\nu_{mn}}{\pi e^2} B_{mn}^{(q)} ; \qquad B_{mn}^{(q)} = \frac{8\pi^3 e^2}{3ch^2} [\int \Psi_m^* (\Sigma q) \Psi_n d\tau]^2 . \qquad (1)$$

The letter q stands for x, y, or z, where z is taken along the *axis of symmetry* of the molecule, x and y *perpendicular* to it. In diatomic molecules, all electronic transitions have either an electronic moment vibrating along z (parallel-type transitions) or along x or y (perpendicular-type transitions). In the latter case the B_{mn} or f_{mn} calculated for one direction (say y) must be multiplied by 2 to give the total intensity associated with the given transition. Experimentally, B_{mn} is determined from measurements of the absorption coefficient as a function of wave number, as follows:

$$B_{mn} = \frac{1}{nh} \int \frac{k_\nu d\nu}{\nu} . \qquad (2)$$

The theoretical problem consists chiefly in finding suitable approximations to the wave functions Ψ_m and Ψ_n which go into the integral in equation (1). At the present time we do not have anything better than rather rough approximations for the electronic wave functions of molecules, except for some states of hydrogen and

one or two other very simple molecules. It is, therefore, best to try the customary types of rough approximation, namely, the approximation using atomic orbitals and that using molecular orbitals.

As a simple example, let us consider the hydrogen molecule.[1] Let us try to calculate the over-all intensity of the first two of the ultraviolet absorption systems of this molecule. One of these is the so-called Lyman bands, which are an example of parallel-type bands (P_z), the transition being from a Σ_g normal to a Σ_u excited state. The second of these, called the Werner bands, is of the perpendicular type, being from the same Σ_g normal state to a Π_u excited state.

By calculation, the following approximate formulae are arrived at for the integral $e\int \Psi_m^*(\Sigma q)\Psi_n d\tau$ in equation (1). This integral may be called the "effective electric moment of the transition" and may be symbolized by P.

$$\left.\begin{array}{lll} \text{Atomic orbitals:} & \text{Lyman bands, } P_z \approx eSr & \\ & \text{Werner bands, } P_x = P_y \approx e\sqrt{2}\,(y_{s\pi} + Sy_{s\pi'}) & \\ \text{Molecular orbitals:} & \text{Lyman bands, } P_z \approx \dfrac{er}{\sqrt{2}} & \\ & \text{Werner bands, } P_x = P_y \approx e\sqrt{2}\,(y_{s\pi} + y_{s\pi'})\,. & \end{array}\right\} \quad (3)$$

Here $S = \int 1s_A 1s_B dv$, where $1s_A$ and $1s_B$ refer to a $1s$ atomic orbital of atom A or B, respectively. Further,

$$y_{s\pi} = \int 1s_A y 2p\pi_{yA} dv\,, \qquad y_{s\pi'} = \int 1s_A y 2p\pi_{yB} dv\,,$$

where y is simply the y-co-ordinate of an electron, and $2p\pi_{yA}$ indicates a $2p_y$ orbital of the A atom.

In the calculation using atomic orbitals the wave function of the Σ_u upper state of the Lyman bands has been taken to be of the *ionic* character H^+H^-, in accordance with suggestions by various people. The Σ_g normal state of H_2, using atomic orbitals, is of the character $H\cdot H$, or $1s_A 1s_B$, that is, the binding is covalent.

For the transition from a normal covalent H_2 to an ionic H_2, the calculation is seen to give for the electric moment P_z a value approxi-

[1] Some in part similar calculations have already been made by B. Mrowka, *Zs. f. Phys.*, **76**, 300, 1932; **84**, 448, 1933, in connection with polarizability and dispersion of H_2.

mately equal to the charge of an electron times the distance r between the nuclei in the normal state of H_2. This, however, is multiplied by the factor S, the overlapping or orthogonality integral, between two $1s$ wave functions, one on atom A and the other on B^-. The value of S here is about 0.8, but for most molecules it would be smaller. Thus, the calculated strength of the transition is as great as would be expected classically if an electron vibrated with an amplitude comparable to the distance between the nuclei. It is very interesting that the parallel-type transition to an ionic state gives this high predicted intensity.

Further investigation shows that the P_z equations in (3) should hold also for other molecules for transitions from a covalent to an ionic state. Moreover, it is possible to identify examples of such transitions in many molecules. The Schumann-Runge bands of O_2, the cis-trans-photoisomerizing absorption region in C_2H_4 derivatives, the strong C_6H_6 absorption just below λ 2000, and certain short-wave-length bands of the halogen molecules may be cited. The colors of many dyes probably arise from this kind of transition.

It is further very interesting that the second method of approximation, the method of molecular orbitals, also predicts very high intensities for the same transitions (cf. Eqs. [3]). It turns out also that, in terms of molecular orbitals, the electron jump involved in such cases is always from a bonding to a corresponding antibonding orbital.

On the other hand, if we calculate the intensities of perpendicular-type bands by each of the two methods, we find that the transitions may be weak or strong according to circumstances. They tend to be strong if the transition in terms of atomic orbitals is wholly or partly of the type $s \rightarrow p\pi$, but to be weak if it is essentially $p\sigma \rightarrow p\pi$. In H_2 the perpendicular-type Werner bands involve a transition $1s \rightarrow 2p\pi$, and they are predicted to be about as strong as the parallel-type covalent→ionic Lyman bands. On the other hand, there are in I_2 and other halogens and halides certain $\Sigma \rightarrow \Pi$ bands where the transition is essentially $p\pi \rightarrow p\sigma$; and the transition is predicted, and observed, to be weak.

Besides the covalent→ionic class of intense parallel-type transi-

tions, there is another related class for whose prototype we may take the transition $N \rightarrow E$ in the H_2^+ molecule (N = normal state, E = first excited state). There is, of course, just one electron in H_2^+. In state N this occupies a bonding, in E the corresponding antibonding molecular orbital, so that from this point of view the transition is of the same kind as in our previous class, exemplified by the Lyman bands in H_2. Furthermore, we find

$$P_z \approx \frac{er}{2}, \tag{4}$$

which is the same result as that obtained for the previous class by molecular orbitals, except for a factor $\sqrt{2}$.

If we regard the states N and E of H_2^+ from the atomic orbital or atomic viewpoint, their approximate wave functions are seen to be, respectively, a symmetrical and the corresponding antisymmetrical linear combination of the wave functions of two normal hydrogen atoms. This spectrum has its nearest classical analogue in the spectrum of an electron vibrating between two positively charged centers (here hydrogen nuclei).[2]

Extension of the present calculations promises to be useful in connection not only with problems of molecular structure but also with molecular spectra in astrophysics. From the discussion at the meeting, it appears that molecular spectra appearing in celestial objects are usually tacitly assumed to have f-values comparable to those of atomic lines. Calculations such as those made here offer a means of improving on this assumption. As an example, I should like to cite some preliminary calculations which I made after the meeting. According to these calculations, the CN bands (both red and violet) and the N_2^+ bands probably are something like a thousand times more intense than the OH bands. A very recent paper by O. Oldenberg

[2] New York: John Wiley & Sons, 1938. After the meeting, Professor E. Teller called my attention to a discussion in the new *Organic Chemistry* edited by H. Gilman. On p. 1889 of Vol. **2**, Pauling considers certain types of dyes; his explanation of their color is in terms of a transition which is entirely analogous to that here discussed for H_2^+.

and F. H. Rieke,[3] containing absorption intensity measurements on the *OH* band lines, gives results in rough agreement with the low intensity obtained by this calculation.

RYERSON PHYSICAL LABORATORY
UNIVERSITY OF CHICAGO

FORBIDDEN TRANSITIONS IN DIATOMIC MOLECULES

G. HERZBERG

There are essentially three possible reasons for the appearance of forbidden transitions, that is, transitions which violate the ordinary selection rules.

a) If the selection rule under consideration is derived with a certain approximation only, weak transitions violating such rules may occur. Examples are: (1) Singlet-triplet transitions, such as the Cameron bands of *CO* ($^3\Pi - {}^1\Sigma$) at 2000 A, which are observed in absorption as well as in emission, and the Vegard-Kaplan bands of $N_2(^3\Sigma_u^+ - {}^1\Sigma_g^+)$, which are observed in emission only, in certain discharges, and also in the aurora and the luminescence of the night sky. Another case would be the (not yet observed) transition from the ground state $^1\Sigma_g^+$ of H_2 to the $^3\Sigma_u^+$ repulsive state arising from two normal H atoms. Such a transition is possibly of importance in the atmospheres of the major planets in which large amounts of H_2 are available. This forbidden transition would then lead to the formation of normal H atoms by light of comparatively long wave length ($\sim$1800 A).[1] (2) $\Sigma^+ - \Sigma^-$ transitions, such as the near ultraviolet-absorption bands of oxygen at 2500 A, with their continuum starting at 2400 A.[2] This transition, although very weak, is responsible for the absorption of all sunlight in the region $\lambda\lambda$ 2400–2000 A and,

[3] *J. Chem. Phys.*, **6**, 439, 1938.

[1] According to Wildt (discussion in this symposium), these H atoms are needed in order to explain the stability of NH_3 in the atmosphere of Jupiter. On the other hand (as pointed out in a private discussion during the symposium by Drs. Mulliken and Teller), this forbidden transition in H_2 might cut out all light—say below 2000 A—that is likely to dissociate NH_3 and CH_4 in the planetary atmospheres.

[2] G. Herzberg, *Naturwissenschaften*, **20**, 577, 1932.

indirectly, also for the absorption of sunlight in the region λλ 3000–2400 A, since the O_3 molecules which absorb in this region are formed from the O atoms formed by absorption of light in the former region.

b) Some selection rules hold rigorously for electric dipole radiation; but transitions violating them may occur, though extremely weak, owing to quadrupole or magnetic dipole radiation. Examples of magnetic dipole radiation are the well-known atmospheric absorption bands of oxygen in the red, representing a ${}^1\Sigma_g^+ \leftarrow {}^3\Sigma_g^-$ transition, and the new infrared atmospheric absorption band of O_2 at 1.27 μ, representing a ${}^1\Delta_g \leftarrow {}^3\Sigma_g^-$ transition.[3] An example for quadrupole radiation would be the (not yet observed) vibration rotation spectrum of homonuclear molecules (H_2, N_2, etc.). Although this quadrupole rotation vibration spectrum is expected to be about 10^9 times less intense than ordinary rotation-vibration spectra, it should be detectable in the case of H_2 in the spectra of the major planets if the amounts of H_2 given by Wildt and others are actually present.[4] The 2–0 H_2 band would occur at 12,000 A, the 3–0 band at 8500 A. To observe the latter, 13 km atm of H_2 would be necessary. Since there would be only three or four very widely spaced and extremely sharp lines, high dispersion is needed to detect them. The corresponding N_2 spectrum might be observed as terrestrial bands in the infrared solar spectrum. It does not seem entirely impossible that the quadrupole rotation vibration spectrum of H_2 or H_2^+ may be observed in emission in suitable cosmic sources (e.g., the corona) if H_2 or H_2^+ can be formed and the density is sufficiently low.

c) Some selection rules, although rigorously valid for the free molecule, may break down in an electric field applied externally or due to the fields of the surrounding molecules (enforced dipole radiation). Thus, it has been found that in oxygen at high pressure or in the liquid, bands occur which do not occur at low pressure with a correspondingly longer absorbing layer.

UNIVERSITY OF SASKATCHEWAN

[3] G. Herzberg, *Nature*, **133**, 759, 1934.

[4] G. Herzberg, *Ap. J.*, **87**, 428, 1938; H. M. James and A. S. Coolidge, *ibid.*, **87**, 438, 1938.

DISSOCIATION, PREDISSOCIATION, AND RECOMBINATION OF DIATOMIC MOLECULES

G. HERZBERG

As is well known, every electronic state of a molecule has a continuous range of energy-levels corresponding to dissociation or recombination of the molecule. In absorption a transition from the ground state to the continuous part of an excited electronic state, according to the Franck-Condon principle, can take place only if the equilibrium nuclear distance r_e of the upper state is appreciably larger than that of the ground state. Many examples of such continuous spectra are known. Conversely, in cases where the internuclear distances are known from emission-band spectra, one may predict with certainty whether or not a continuous absorption spectrum leading to photochemical dissociation exists. Such is the case for C_2, for which the upper state of the new $^3\Pi - {}^3\Pi$ bands[1] has such a large r_e that in absorption a continuous spectrum will appear. This is of importance for Wurm's explanation[2] of the difference in the spectra of the head and the tail of comets: the C_2 molecules present in the head are dissociated by light absorption in the continuous spectrum just mentioned, and therefore no C_2 bands appear in the spectrum of the tail.

Depending on the relative positions of the potential curves, the two atoms produced by light absorption in the continuous region may have varying amounts of kinetic energy. If one of them is excited to the upper state of an atomic line, this line appearing in fluorescence will have an anomalously large Doppler broadening.[3] This process may be of importance in explaining the large Doppler width of the coronal lines.

The converse of the photochemical dissociation of a diatomic molecule is the recombination of two atoms in a two-body collision with emission of radiation. In consequence of the short time of collision, even in case of a completely allowed electronic transition, only every 10^5 collision leads to a recombination. Yet, at pressures

[1] J. G. Fox and G. Herzberg, *Phys. Rev.*, **52**, 638, 1937.

[2] K. Wurm, *Zs. f. Ap.*, **8**, 281; **9**, 62, 1934.

[3] T. R. Hogness and J. Franck, *Zs. f. Phys.*, **44**, 26, 1927.

below 0.1 mm *Hg* and if collisions with the walls are not important, this recombination by two-body collision is more important than recombination by three-body collision. For some elementary molecules, such as H_2 and N_2, recombination of normal atoms can occur only by way of a forbidden transition and is therefore much less frequent.

In three-body recombinations the energy of dissociation is carried away as excitation energy by one or both of the resulting systems. An interesting example is supplied by carbon: in discharges in *CO* of high pressure the Swan bands of C_2 appear with only the $v' = 6$ progression (so-called high-pressure carbon bands). The selective excitation of the one vibrational level can only be understood by assuming that molecules in this state are formed directly by the recombination of two *C* atoms (formed by dissociation of *CO*) in a three-body collision, the heat of dissociation $D(C_2)$ being transformed into energy of excitation of C_2.[4] Thus, $D(C_2) = 3.6$ volts follows.

A dissociation of a molecule can also be brought about by radiationless transition from a discrete state to one of equal energy that belongs to a continuous range of energy values. This so-called "predissociation" may be detected by the broadening of the band lines in absorption or by the breaking-off of a band system in emission at a certain value of the vibrational and rotational quantum number. For example, in the case of the new C_2 bands referred to in the first paragraph, only the $v' = 0$ progression appears. This is very probably due to predissociation of the higher levels. The predissociation limit fits well with the $D(C_2)$ value given above. Also, this predissociation of C_2 is an additional way in which this molecule may be dissociated in comets by absorption of sunlight.

An important question which, in some cases, is difficult to answer is whether the predissociation limit coincides with a dissociation limit or whether, owing to a potential maximum, predissociation sets in at a higher energy than corresponds to the dissociation limit. A decision can be reached if it can be ascertained whether the so-called "limiting-curve" of dissociation (obtained from several breaking-off points in different vibrational levels, plotted as a function of

[4] In the discussion Dr. Beutler pointed out that this is very probably a case of an inverted induced predissociation.

$J\ (J+1))$ is curved with a horizontal tangent for $J\ (J+1) = 0$ or is a straight line with nonzero slope. The latter is the case for *BH* and *AlH* in the excited $^1\Pi$ state. This shows definitely that in these cases the predissociation limit gives only an upper limiting value for the corresponding dissociation limit of the molecule.

UNIVERSITY OF SASKATCHEWAN

THE INFRARED SPECTRUM OF WATER VAPOR

DAVID M. DENNISON

The spectrum of water vapor which is to be correlated with changes in the vibrational and rotational energy of the molecule extends over a wide range. It begins in the very long heat waves and continues, with only a few gaps, through the near infrared up to about the middle of the visible spectrum. It has been measured with great precision from 135 μ to λ 5700 A. There are a number of features about the water molecule which make it particularly interesting to study, and the completeness with which the spectrum is known experimentally allows an accurate test of the theoretical predictions.

From an analysis of the vibration-rotation bands Mecke[1] and his collaborators have shown that the molecule possesses the form of an isoceles triangle where the central angle is about $104°36'$, while the distance between the oxygen and each hydrogen atom is 0.956×10^{-8} cm. This means that the water molecule is an almost perfect example of an asymmetric rotator, for its principal moments of inertia, A, B, and C, have the ratio approximately of $1:1.88:2.88$. A second point of interest arises from the lightness of the hydrogen atoms, and this has several consequences. The moments of inertia are small; and the fine-structure lines are rather widely spread, thus permitting them to be accurately mapped. The lightness of the hydrogens means that the vibrational frequencies will be high and that the overtone bands will extend well into the visible region. Finally, the small moments of inertia bring with them the circumstance that the angular velocities and the centrifugal forces will be large. There results a very appreciable interaction between vibra-

[1] R. Mecke, W. Baumann, and K. Freudenberg, *Zs. f. Phys.*, **81**, 313, 445, 465, 1933.

tion and rotation, an understanding of which will lead eventually to a detailed knowledge of the structure of the molecule.

The far infrared spectrum of water vapor corresponds to changes in the rotational energy alone and has been investigated in great detail by Randall, Dennison, Ginsburg, and Weber.[2] One hundred and seventy-three fine-structure lines have been measured and have been correlated with the transitions to be expected between the energy-levels of an asymmetric rotator. It was necessary to take into account the centrifugal-force stretching of the molecule, which for certain of the high energy-levels became as large as 280 cm^{-1}. The intensities of the lines were calculated by an approximate method which made use of the symmetrical rotator wave functions. The final result which was achieved showed a very accurate agreement between the observed and predicted lines, with respect to both their positions and their intensities.

The fundamental vibration bands of water lie in the near infrared, and these also may be well understood, although a less precise agreement is attained since the measurements are less complete.

The overtones of the fundamental vibration frequencies form a series of bands which extend through the photographic infrared up to the middle of the visible spectrum. Incidentally, the blue-green color of pure liquid water is due to the absorption of these overtone bands. The fine-structure lines of the overtone bands appear in the atmospheric absorption of the solar spectrum, and they have been very accurately determined. A partial analysis of their structure has been made by Mecke, Baumann, and Freudenberg,[1] and a discussion of their work follows. It was shown that there exist combination relations between these fine-structure lines, which may be correlated with combination relations derived from the far infrared lines. The agreement in most cases was excellent and was within experimental error. In other cases it was shown that Mecke had not correctly identified all the lines, but in those cases a line might always be found which fell in exactly the predicted position. It appears that all the atmospheric lines due to water vapor may eventually be identified and their positions and intensities understood.

Finally, the question of the interpretation of the vibration-rotation energy-levels of water in terms of the molecular contents is of

[2] *Phys. Rev.*, **52**, 160, 1937.

interest. The phenomenon of resonance degeneracy between two of the fundamental frequencies should play an important role in the eventual solution of the problem. I might say that a continuation of this work at the University of Michigan has proved the correctness of this opinion, and we hope to publish the complete details in the near future.

UNIVERSITY OF MICHIGAN

INFLUENCE OF PRESSURE AND TEMPERATURE UPON THE ABSORPTION AND FLUORESCENCE OF SPECTRAL LINES

H. BEUTLER

The width and shape of spectral lines are given by the Lorentz formula; for higher pressures, collision-damping occurs, increasing the width of the lines without changing their shape. For still higher pressures, Kuhn and Margenau gave a statistical treatment of the interaction forces and explained the observed shift of the lines and the shape of their wings. This shift varies within a series of the same atom, becoming constant for high quantum numbers. The sign of this shift in the absorption series of alkali atoms depends on the nature of the admixed gas. Reinsberg has shown, in continuation of Fermi's work, that a red shift occurs if the foreign gas has a minimum in its effective cross-section for electrons moving with small velocities; if there is no such minimum, a violet shift takes place. The amount of the shift is proportional to the cross-section for infinitely slowly moving electrons. The maximum of the pressure-broadening occurs in the alkali atoms for the series numbers between 4 and 8, and its height and position depend on the temperature. The theory of Reinsberg explains these facts.

For fluorescence phenomena coming out of deep gas layers the curves of growth, the multiple absorption, and re-emission have to be considered. By quantitative treatment of these effects on both D lines of sodium, Adel, Ladenburg, and Slipher determined the sodium concentration in the tail of a comet. The unknown term scheme for the helium atom with two excited electrons should give rise to many unknown spectral lines, perhaps to lines of the solar corona.

UNIVERSITY OF CHICAGO

CONTINUOUS SPECTRA

GEORGE H. SHORTLEY

After a brief review of the definitions and formulae for such quantities as line strengths, oscillator strengths, and transition probabilities in the case of discrete-discrete transitions, the corresponding quantities were defined for the case of continuous emission and absorption. By placing the atom or molecule at the center of a large spherical box, the proper normalization of the radial wave functions to use in the continuous spectrum was obtained. This is such that the asymptotic form for large r of the function with energy E is

$$\frac{1}{\sqrt{\hbar\pi}} \sqrt[4]{\frac{2\mu}{E}} \sin \sqrt{\frac{2\mu E}{\hbar}} (r - \delta) .$$

With this normalization the radiation probabilities refer directly to unit energy range in the continuous spectrum. Photoionization, autoionization, and predissociation were discussed. Then a new method of calculating the relative probabilities of transitions into the various levels of an atomic configuration in the case of electron capture by an ion was reported. These calculations were made with D. H. Menzel to furnish a possible explanation of peculiar intensities in the nebular spectra, but they have not been successful in this direction. The methods of calculation will be discussed in a note in the *Astrophysical Journal* in the near future.

OHIO STATE UNIVERSITY

ELECTRON AFFINITY IN ASTROPHYSICS

RUPERT WILDT

The carriers of the emission and absorption spectra observed in celestial objects have been identified as both neutral and positively charged atoms and molecules. A number of free electrons, equivalent to the charge of the positive ions, must be present to provide for electric neutrality. Collisions between electrons and certain neutral atoms or molecules should frequently lead to attachment, a negatively charged atomic or molecular ion being formed. The existence of such negative ions has been demonstrated by a great variety of experiments, among which the analysis of ionic beams in a mass

spectrograph affords the most direct evidence; and their stability is also accounted for by atomic theory.[1]

Although it has long been recognized that negative ions play an important role in the Kennelly-Heaviside layer of the terrestrial atmosphere, their presence in stellar atmospheres does not seem to have been envisaged. Several species of neutral atoms and molecules, abundant in stellar atmospheres, are able to attach electrons in stationary states. This tendency to attach electrons is generally re-

TABLE 1

ELECTRON AFFINITIES

Atom and Ground State	I.P.	E.A.	References
1 *H* ^{2}S	13.53	0.70	E. A. Hylleraas, *Zs. f. Phys.*, **65**, 209, 1930
3 *Li* ^{2}S	5.37	0.54	Ta You-Wu, *Phil. Mag.*, **22**, 837, 1936
8 *O* ^{3}P	13.55	2.2	W. W. Lozier, *Phys. Rev.*, **46**, 268, 1932
9 *F* ^{2}P	17.34	4.13	J. E. Mayer and L. Helmholz, *Zs. f. Phys.*, **75**, 19, 1932
16 *S* ^{3}P	10.31	2.8	J. E. Mayer and M. Maltbie, *Zs. f. Phys.*, **75**, 748, 1932
17 *Cl* ^{2}P	12.96	3.75	Mayer and Helmholz, *ibid.*
35 *Br* ^{2}P	11.80	3.53	Mayer and Helmholz, *ibid.*
53 *I* ^{2}P	10.55	3.22	Mayer and Helmholz, *ibid.*

ferred to, in physical and chemical literature, as "electron affinity" of the neutral particles, and the same term is used to denote the energy of binding measured in electron volts. The bond may be severed either by a subsequent collision or by photoelectric ionization. In thermodynamic equilibrium the concentration of the nega-

[1] A monograph on *Negative Ions* has just been published by H. S. W. Massey (Cambridge University Press, 1938). A letter received in March, 1939, from Dr. Massey communicates preliminary results of a new calculation of the absorption coefficients of H^-. Using the Hylleraas form for the ground-state wave function instead of the former rough approximation, he finds absorption coefficients of the same order of magnitude, in the astrophysically relevant range of wave lengths, as those given by Jen (*Phys. Rev.*, **43**, 540, 1933), to which reference has been made in a brief note to appear soon in the *Publications of the American Astronomical Society*. Utilizing Jen's data, it has been shown that the addition of the H^- absorption to the metallic absorption produces for the solar atmosphere that desired independence of the absorption coefficient from wave length which failed to emerge from Unsöld's and Pannekoek's theory. In the opinion of the writer this result is not likely to be changed materially when Jen's data eventually will be replaced by Massey's improved data. This would mean the removal of a serious discrepancy between theory and observation and, in fact, the identification, by their continuous absorption spectrum, of the negative hydrogen ions so abundant in the solar atmosphere.

tive ions is ruled by the general principles of statistical mechanics and can be evaluated numerically from the Saha equation, in which the electron affinity has to be substituted for the ionization potential. The number of reliably determined electron affinities is still very small, as will be seen from Table 1. Many astrophysically important diatomic molecules are known to form negative ions, like H_2, C_2, O_2, NH, OH, CN, and others; but there is scarcely any information available about the respective electron affinities. On inspecting Table 1 it will be noticed that all the electron affinities are small compared to the ionization potentials of the corresponding atoms. This circumstance counteracts the formation of negative ions in a system consisting of a single sort of atoms only, because at any temperature high enough to release electrons by ionization of the neutral atoms the negative ions would split up even more. However, in a mixture of two atoms differing greatly in ionization potential—say sodium and hydrogen—the electrons released from the sodium atoms at comparatively low temperatures may readily attach themselves to the hydrogen atoms. This is just the case realized in stellar atmospheres of medium or late spectral type. In addition, the great abundance of hydrogen will favor the formation of H^- ions. Therefore, the H/H^- equilibrium suggests itself as the most promising subject of an inquiry into the astrophysical significance of electron affinity.

If the pressure is measured in dynes per square centimeter, the Saha equation of the H/H^- equilibrium assumes the form

$$\log_{10} K = \log_{10}\left(\frac{P_H \cdot P_e}{P_{H^-}}\right) = -\frac{0.70 \cdot 5040}{T} + 2.5 \log_{10} T + 0.12 ,$$

the statistical weight of H^- being 1. The ratios P_{H^-}/P_H were computed as functions of the electron pressure and temperature, and for sake of comparison there are also given the ratios of the numbers of neutral hydrogen atoms in the second and first quantum state,

$$\frac{N_2}{N_1} = 4 \cdot 10^{-\left(\frac{10.16 \cdot 5040}{T}\right)} .$$

Table 2 contains these quantities as functions of the temperature and the total pressure in the "Russell-mixture" of elements.[2] This

[2] H. N. Russell, *Ap. J.*, **75**, 337, 1932.

mixture is rather rich in hydrogen. Unsöld's analysis of the vertical distribution of temperature and electron pressure throughout the solar atmosphere[3] is based on a smaller abundance ratio of hydrogen to metals and therefore is less favorable to the formation of H^-. Table 3 contains the same quantities as Table 2, for several optical

TABLE 2

IONIZATION EQUILIBRIUM OF NEGATIVE HYDROGEN IONS*

$T°$ K...	8400	6300	5040	4200	3600	3150	2800	2500	1680
$5040/T$.	0.6	0.8	1.0	1.2	1.4	1.6	1.8	2.0	3.0
$\log_{10} K$..	+ 9.51	+ 9.06	+ 8.68	+ 8.34	+ 8.03	+ 7.75	+ 7.48	+ 7.22	+ 6.08
Total pressure:									
10^4...	6.99	6.96	6.96	6.92	6.89	6.97	7.09	7.29	.....
10^3...	7.62	7.87	7.72	7.76	7.64	7.65	7.71	7.82	.....
10^2...	8.21	8.79	8.56	8.57	8.51	8.40	8.41	8.48	.....
10....	8.92	9.55	9.50	9.33	9.39	9.27	9.16	9.17	10.04
1....	9.83	10.17	10.48	10.20	10.19	10.18	10.02	9.92	10.54
10^{-1}..	10.81	10.78	11.41	11.15	10.97	11.04	10.94	10.78	11.06
10^{-2}..	.....	11.48	12.16	12.15	11.86	11.82	11.85	11.70	11.61
10^{-3}..	.....	12.37	12.77	13.14	12.84	12.66	12.71	12.64	12.32
10^{-4}..	.....	13.36	13.36	14.04	13.84	13.58	13.48	13.54	13.11
$\log_{10} \frac{N_1}{N_2}$	5.50	7.53	9.56	11.59	13.62	15.66	17.69	19.72	29.88

* The table gives $\log_{10} (P_H/P_{H^-})$, the total pressure being measured in dynes per square centimeter.

TABLE 3

NEGATIVE HYDROGEN IONS IN THE SOLAR ATMOSPHERE

Optical Depth	$5040/T$	P_{H^-}/P_H	N_2/N_1
0.12.....	1.0	$10^{-7.34}$	$10^{-9.56}$
0.53.....	0.9	$10^{-7.02}$	$10^{-8.55}$
1.25.....	0.8	$10^{-6.87}$	$10^{-7.53}$
2.62.....	0.7	$10^{-6.82}$	$10^{-6.52}$
5.40.....	0.6	$10^{-6.66}$	$10^{-5.50}$

depths under the solar surface, and reveals the surprising fact that, in the higher levels, the negative hydrogen ions are more abundant than the neutral hydrogen atoms excited to the ground state of the Balmer series. In view of the great strength of the Balmer series in the solar spectrum, it is obvious that the negative hydrogen ions

[3] A. Unsöld, *Zs. f. Ap.*, **8**, 262, 1934.

should produce conspicuous absorption lines in the medium and late spectral types if they possessed stable excited states capable of combining with the ground state.

At present, no definite answer can be given to the question whether or not there are stable excited states in negative ions. It has been established, as a general result, that their number could not be infinite, as in the case of an electron bound in a Coulomb field. The small binding energy of the attached electron in its ground state makes it most unlikely that any stable discrete excited states exist with appreciable binding energy, though there might be some states with very small binding energy, closely adjacent to the ionization continuum. With the coronal and certain interstellar lines defying all efforts of the spectroscopists at identification, it may not be untimely to remark upon the remote chance of negative ions being the carriers of these spectra. This has already been suggested, though rather perfunctorily, for the coronal lines by Goudsmit and Ta You-Wu.[4] This is the only reference, in astrophysical literature, to negative ions of which the writer is aware. Since the solar corona is now widely regarded, for its scattering properties, as a cloud of free electrons, it would seem to be the very place where negative ions are likely to be formed by collisions between the indigenous electrons and neutral atoms ejected from the sun during its eruptive activity. Unfortunately, there is little hope, if any, for the discovery, in the near future, of spectra of negative ions in the laboratory or for the theoretical prediction of their energy states.

The small electron affinity of hydrogen, 0.70 volt, would place any hypothetical discrete spectrum of the negative hydrogen ion far out into the infrared, beyond the ionization limit of H^-, near λ 17600. The rapid decay of atomic ionization continua toward greater frequencies might make one expect that the continuous absorption coefficient of H^- is negligibly small throughout the visual spectral region and the near ultraviolet. But the negative hydrogen ions show a strikingly different behavior, according to an investigation by Massey and Smith,[5] who computed the cross-sections for the capture of electrons by hydrogen atoms. Assuming thermodynamic equilibrium, these capture coefficients can easily be transformed, by Milne's formula,[6] into cross-sections for absorption or, by a different

[4] *Ap. J.*, **80**, 154, 1934. [5] *Proc. R. S.*, A, **155**, 472, 1936. [6] *Phil. Mag.*, **47**, 209, 1924.

name only, into the astrophysically relevant absorption coefficients pertaining to the bound-free transitions of the negative hydrogen ion. The absorption coefficient of H^- rises from zero, at the ionization limit, to a broad maximum at a distance of about 10 volts from the ionization limit. It then decreases gradually, extending with remarkable intensity into the region between 20 and 30 volts. Massey and Smith do not give any estimate of the accuracy of their cross-sections; but it may be hoped that their results are trustworthy for the astrophysically accessible spectral range, which is rather close to the ionization limit. Menzel and Pekeris[7] had already computed what they call the absorption resulting from the changes of kinetic energy of an electron traversing the field of a neutral hydrogen atom. From the point of view presented here, this absorption may be described as produced by the free-free transitions of the negative hydrogen ion. The absorption coefficient k_ν, resulting from the existence of negative hydrogen ions in a gas containing N_e electrons per unit volume, is, per neutral hydrogen atom,

for free-free transitions:

$$\frac{1}{3}\frac{e^2hN_e}{cm^3\nu^3}\left(\frac{mv_0^2}{2\pi kT}\right)^{3/2} v_0^4 A(T, v_0) = a \cdot P_e ,$$

and

for bound-free transitions:

$$\frac{1}{4}\frac{mc^2h(\nu - \nu^*)}{h^2\nu^2} Q^e N_e \left(\frac{h^2}{2\pi mkT}\right)^{3/2} e^{h\nu^*/kT} = b \cdot P_e .$$

The coefficients a have been taken from the paper of Menzel and Pekeris, and the coefficients b have been computed from the emission cross-sections Q^e published in the form of a graph by Massey and Smith, ν^* being the frequency corresponding to the electron affinity of hydrogen. As will be seen from Table 4, the bound-free transitions produce an absorption far greater than that of the free-free transitions, especially at lower temperatures. Now the latter, as found by Menzel, is still negligible at the solar temperature, amounting to about 5 per cent of the metallic absorption. However, they would become appreciable at lower temperatures, particularly in dwarf

[7] *M.N.*, **96**, 77, 1935.

stars. Therefore, with regard to the comparison given in Table 4, it would seem that the contribution by negative hydrogen ions to the opacity of stellar atmospheres cannot be neglected altogether, even at the solar temperature. It is generally agreed that the present theory of the atmospheric absorption coefficient is unsatisfactory,

TABLE 4

ABSORPTION COEFFICIENT OF NEGATIVE HYDROGEN IONS*

T° K	λ 8900	λ 6810	λ 5390	λ 4360	λ 3030
3000	6.82	4.12	2.70	1.88	1.04
	150	160	250	310	370
4000	5.81	3.41	2.20	1.50	0.81
	37	40	62	79	94
6000	4.83	2.71	1.69	1.12	0.55
	6.7	7.2	11.3	14.4	17.1
8000	4.33	2.36	1.44	0.93	0.47
	2.3	2.5	3.9	5.0	5.9

* Upper line: $a \cdot 10^{28}$ free-free transitions. Lower line: $b \cdot 10^{28}$ bound-free transitions.

and to take into account this new source of opacity may help to remove the discrepancies between theory and observation, at least partly. A detailed investigation is under way.

PRINCETON UNIVERSITY OBSERVATORY

MOLECULAR BANDS IN STELLAR SPECTRA

N. T. BOBROVNIKOFF

OBSERVATIONAL RESULTS

Bands due to diatomic molecules are the most important characteristic of the spectra of the majority of the stars. It is true that only 1.7 per cent of the total number of stars in the *Henry Draper Catalogue* belong to spectral class M, characterized by molecular bands due to the *TiO* molecule. This is, however, the result of observational selection, as most of the M stars are dwarfs with a very low absolute magnitude. In the sample supplied by the stars within 5 parsecs of the sun, more than 60 per cent are M-type dwarfs. On the other hand, the classes S (*ZrO*), N, and R (C_2 and *CN*) are

represented only by very few giants, the numbers being, respectively, 33, 160, and 58 stars. If there are any dwarfs in these classes, they must be exceedingly faint.

Observational conditions are vastly different for different classes of objects. In the case of the sun the highest dispersion may be employed (up to 0.25 A/mm), so that the details of the rotational structure of the bands can be easily studied. With the brightest stars, a dispersion of 4–5 A/mm can be employed. For the majority of the M giants, however, a dispersion of 25–30 A/mm is the highest obtainable. Only edges of bands can be measured under these conditions. The most fruitful source of molecular bands, the dwarf M stars, are so faint that only dispersions 75–100 A/mm or even 200 A/mm are usually employed.

This difference in the observational technique is reflected in the results of identification of molecules in stellar spectra. For instance, *MgH* can be observed even in the spectrum of the disk of the sun (class Go) and is shown on the high-dispersion spectrograms of Arcturus (K5), but ordinarily it is observable only in the stars of the later subdivisions of class M. On the small-dispersion spectrograms of red dwarfs,[1] however, it is impossible to distinguish between the bands of *TiO* and *ZrO*.[2]

A thorough study of stellar spectra in recent years has failed to establish any polyatomic molecules in the spectra of the stars. The most likely molecule of this kind to appear in stellar spectra, H_2O, has its fundamental bands in the infrared. In the usually observable region the transitions of H_2O result in faint lines, which are, moreover, masked by those in the atmosphere of the earth. The possibility of the existence of polyatomic molecules in stellar atmospheres should not, however, be overlooked.

The field for the study of molecules in stellar spectra is very rich, even if moderate dispersion (20–30 A/mm) is employed. In the spectrum of the sun, out of the 21,835 lines of the *Revised Rowland*, about 11,000 lines are still lacking identification. These fainter lines must be due largely to diatomic molecules. With the progress of the study of bands in the laboratory, new compounds are being found in the

[1] Öhman, *Stockholm Obs. Ann.*, **12**, No. 8, 1936.

[2] Wildt, *Ap. J.*, **84**, 301, 1936.

spectrum of the sun. Among recent identifications we may mention such molecules[3] as *SiH*, *SiN*, *PH*, and *CP*.

Since in stellar atmospheres we have to deal with thermal excitation, the probability of a molecule in an excited state is very small. The H_2 molecule, for instance, must be extremely abundant in cooler stars. However, the H_2 bands in the observable region have their lower electronic level 11–12 volts above the normal level of the molecule. In spite of many attempts to identify these bands in the spectrum of sunspots, their absence in the sun has been definitely proved. It is found that for 5000° the number of excited H_2 molecules is only 10^{-9} of the number of the *CN* molecule in its normal state, and the *CN* molecule is not particularly abundant in the sun.[4] The same considerations are applicable to ionized molecules, whose appearance in stellar spectra is even more improbable. In the stellar spectra we have to deal, therefore, with resonance bands of neutral diatomic molecules. There are no definitely proved exceptions to this rule. This is in marked contrast with the appearance of ionized molecules in the spectra of comet tails and in the ionosphere, which shows that the mode of excitation in these latter sources must be radically different from that of the stars.

Furthermore, stellar molecules manifest themselves only in absorption. *CN* and C_2 are indeed observable in the flash spectrum, in considerable intensity. In stars an appearance of molecular bands in emission would mean an unusually extensive atmosphere—that is, very low pressure—which would preclude the formation of molecules in large numbers. The only observation of a molecular emission spectrum is that of Joy,[5] who found in Mira Ceti three diffuse emission lines or bands. These were later ascribed to *AlO*.[6] It is doubtful, however, that this identification is correct.

Of especial interest is the occurrence of carbon isotopes in spectra of N- type,[7] resulting in the C_2 bands due to the molecules $C^{12} - C^{13}$ and $C^{13} - C^{13}$. It would seem that the abundance of C^{13} in N-type stars is far greater than in terrestrial sources, as the isotopic bands

[3] Nicolét, *Liége Coll. Mém. in 8°*, Nos. 205, 233, and 236, 1937.

[4] Swings, *ibid.*, No. 120, 1934; Nicolet, *ibid.*, No. 214, 1937.

[5] *Ap. J.*, **63**, 281, 1926.

[6] *M.N.*, **88**, 679, 1928.

[7] Menzel, *Pub. A.S.P.*, **42**, 34, 1930.

are very strong in the spectra of the stars. Lately, however, some doubt has been thrown on the estimates of intensities of isotopic bands leading to extreme figures of abundance of C^{13} in cosmic sources.[8]

Spectral classes M, S, N, and R are those especially distinguished by strong absorption bands of diatomic molecules. We have to deal here with the temperature range from about 3500° K (in class K5) to perhaps 1500° K (late class R).

Class M (including K5) has numerous bands attributable to *TiO*. In later subdivisions of this class the *TiO* bands are so strong that, in comparison with them, other bands and atomic lines are quite insignificant in intensity. About two hundred bands in the later M class can be attributed to *TiO*. There are at least three systems involved: α, $^3\Pi - {}^3\Pi$; γ, $^3\Sigma - {}^3\Pi$; and β, $^1\Pi - {}^1\Sigma$. The $^3\Pi$-level seems to be the normal level of the molecule. In that case, $^1\Pi$ is an excited level;[9] and if this is so, *TiO* is the only molecule showing bands in stellar spectra which come from an excited level. Many bands of *TiO* have not been analyzed yet, and it is possible that other systems may be present in stellar spectra.[10] In later M-type stars the *TiO* must be extremely abundant, as the vibrational transitions as high as α (10, 13) are quite prominent in the spectrum of α Herculis (M5). It would seem that with the increase in strength of the *TiO* bands the line spectrum of *Ti* should decrease in intensity. However, this is not the case. To as late a type as M2, the *Ti* I lines of rather high excitation potential (1.4 volts) increase in intensity along with the *TiO* bands,[11] and even in the spectrum of Mira (M7) the *Ti* I lines are quite strong. A study of the equilibrium between the *Ti* atomic lines and *TiO* bands is one of the most important aspects of the theory of the M-type spectra.

The stars of type S characterized by strong bands of *ZrO* are least numerous. It is at present impossible to assign any definite place for them in the stellar evolutionary sequence. They appear[12] to form a separate subbranch of the giant branch, beginning with *K2*

[8] Wurm, *Zs. f. Ap.*, **5**, 260, 1932.

[9] Lowater, *Proc. Phys. Soc.*, **41**, 557, 1929.

[10] Dobronravin, *Pulkovo Obs. Circ.*, No. 24, 1938.

[11] Roach, *Ap. J.*, **80**, 233, 1934.

[12] Davis, *Pub. A.S.P.*, **46**, 267, 1934.

and joining the main branch again at M5. Moreover, many S-type stars have also *TiO* bands; and on the other hand, the occurrence of *ZrO* band in ordinary M-type stars is not uncommon.[13] This molecule has also been identified in the spectrum of sunspots.[14]

The spectral types R and N are also separate branches of the giant sequence. In type R, cyanogen bands increase in strength along the sequence, attaining their maximum in R5. The Swan bands increase gradually in intensity from Ro to R8. In the N-type spectrum the cyanogen bands are very weak at No and are altogether missing in later subdivisions. The Swan bands increase in strength from No on. Neither the position of the classes R and N with respect to the normal classes K and M nor their relation to each other has been determined. Indeed, such a carbon star as R Coronae Borealis,[15] consisting of 70 per cent carbon, is classified not as R or N but as F7.

As an instance of the anomalous appearance of absorption bands in stellar spectra, we may mention Nova Herculis 1934, which for a few days showed[16] in its spectrum both *CN* and C_2, while the star, according to other criteria, was of class A. There are also a few long-variable stars having in their spectra high-excitation emission lines of *He* I and *He* II, together with strong bands of *TiO* (AX Persei, RW Hydrae, CI Cygni, and Z Andromedae).[17] Less striking examples are the stars SX Herculis[18] (*TiO* at G8), R Scuti[19] (*TiO* at G9), and U Monocerotis[20] (*TiO* at G4).

At the present time, twenty-seven diatomic molecules have been identified in stellar spectra. Most of them occur in the spectrum of the sun. To these we may add seven which are probably present in stars but whose resonance bands are situated unfavorably for observations. There are also seven molecules which were looked for but were not found. For many molecules, such as *FeO*, which may be present in stars, there are no sufficient laboratory data.

[13] Bobrovnikoff (β Pegasi), *Ap. J.*, **79**, 483, 1934; Davis (α Scorpii), *Pub. A.S.P.*, **49**, 110, 1937.

[14] Richardson, *Ap. J.*, **73**, 216, 1931. [15] Berman, *ibid.*, **81**, 369, 1935.

[16] *Pub. A.S.P.*, **47**, 209, 1935; *Stockholm Medd.*, No. 19, 1935.

[17] First three stars, *Ap. J.*, **77**, 44, 1933; Z Andromedae, *Pub. A.S.P.*, **44**, 328, 1932.

[18] *Ap. J.*, **75**, 127, 1932. [19] *Pub. A.S.P.*, **34**, 349, 1922. [20] *Ap. J.*, **77**, 120, 1933.

The existence of molecules in stellar atmospheres in sufficiently great numbers to produce observable absorption depends on the physical properties of the molecule and on the abundance of the atoms which make up the molecule.

Assuming Russell's analysis of the atmosphere of the sun to be applicable to other stars, we may divide the elements into groups according to the total number (T) of atoms in the atmosphere. The more abundant atoms, generally speaking, are more likely to produce molecules. The results are given in Table 1. In these diagrams

TABLE 1

BANDS IN STELLAR SPECTRA

log T	Element							Hydrides						Oxides					
10.5	*H*							*n*						*x*					
9.0	*O*							*x*						*n*					
8.0	*N*	*F*						*x*	*n*					*a*					
7.8–6.7	*Mg*	*C*	*Na*	*Si*	*Fe*	*K*	*Ca*	*x*	*x*	*x*	*x*		*a*	*x*	*x*	*n*		*n*		*a*	*x*
6.4–5.6	*Al*	*Ni*	*Mn*	*Cr*	*S*	*Co*		*x*							*x*		*x*	*x*	*n*		
5.2–4.9	*Ti*	*V*	*Cu*	*B*	*Zn*					*x*	*a*				*x*	*x*		*x*			
3.6–3.0	*Sc*	*Sr*	*Ba*	*Ge*					*a*	*a*					*x*	*x*		*n*			
2.6–2.4	*Y*	*Zr*	*Cd*	*Ce*											*x*	*x*					

the letter x means that the compound has been observed, n means that the resonance bands are not observable, and a signifies the established absence of the compounds.

To the hydrides and oxides we may add the compounds of *Si*, *SiN*, and *SiF;* compounds of phosphorus, *CP* and *PH;* and, of course, *CN* and C_2. The only other homopolar molecule so far observed in stellar spectra is Ca_2, but this is somewhat uncertain.

The most abundant molecule, H_2, cannot be observed in cosmic sources, as explained above. The next in abundance molecules, *OH* and *NH*, have been observed both in the sun and in the stars.

The *OH* bands fall very near the telluric ozone band and are, furthermore, in a region crowded with strong resonance lines of *Ni* I. The (0, 0) band of the system $B^2\Sigma - A^2\Pi$ has a head at λ 3063.71, almost at the limit of the observable spectrum. It was identified in

the spectrum of the sun by Fowler.[21] Recently Wildt[22] found, in the spectra of α Orionis and some M-type dwarfs, absorption at λ 3428.4, which he assigned to the (1, 0) band of *OH*. He suggests that the strong line at λ 3248.40 in the spectrum of Arcturus, observed previously by R. W. Shaw,[23] may be due to this band.

The *NH* bands of the resonance system $B^3\Pi - A^3\Sigma$ are at somewhat greater λ than the *OH* band and are therefore more easily observable. The (0, 0) band falls at λ 3360. It was found in the spectrum of the sun (both disk and spots).[24] It was also found by Shaw in Arcturus and suspected by Wildt in several R and K stars. However, this band coincides with the *CN* (2, 0) not observable in the laboratory but undoubtedly strong in the R and N stars.

The *FH* molecule must be quite abundant, but thus far there are no laboratory data concerning it.

ABUNDANCE OF MOLECULES IN THE STARS

We now have the task of explaining why certain molecules have strong bands in the stellar spectra while others have faint bands or none at all. The most complete exposition of the theory of compounds has been made by Russell[25] on the assumption that stars, in general, are of the same composition as the sun. The abundance of various elements has been computed by him on the basis of the study of the intensities of atomic lines in the sun.[26] These figures are given in Table 1.

The number of molecules (AB) will be determined by the equilibrium constant defined as $K(AB) = p(A)p(B)/p(AB)$, where p is the partial pressure. Since the partition function of a molecule involves translational motion and electronic, vibrational, and rotational energy,[27] we shall have all these quantities in the formula for K:

$$\log_{10} K = -\frac{5040}{T} D + \tfrac{1}{2} \log T - \frac{0.286\omega}{T} + \tfrac{1}{2} \log M - 2 \log r + \log \omega + \log G + 0.24 .$$

[21] *Proc. R. Soc.*, A, **94**, 472, 1918. [22] *Ap. J.*, **84**, 303, 1936. [23] *Ibid.*, **83**, 225, 1936.

[24] Fowler and Gregory, *Phil. Trans. R. Soc.*, A, **218**, 351, 1919; Nicolet, *Liége Coll. Mém. in 8°*, No. 215, 1937.

[25] *Ap. J.*, **79**, 317, 1934.

[26] *Ibid.*, **70**, 11, 1929. [27] Rosseland, *Theoretical Astrophysics*, p. 245.

Here D is the dissociation energy in volts; T, the absolute temperature of the star; ω, the fundamental frequency of the molecule in cm^{-1}; r, the equilibrium distance of the nuclei; and where $M = M_A M_B / M_{AB}$ (the masses of the atoms and of the molecule) and $G = g_A g_B / g_{AB}$ (the statistical weights).

Partial pressures of the atoms A, B, etc., and compounds AB are determined from the set of simultaneous equations:

$$p'(A) = p(A) + \frac{2p(A)^2}{K(A_2)} + \frac{p(A)p(B)}{K(AB)} + \ldots,$$

$$p'(B) = p(B) + \frac{2p(B)^2}{K(B_2)} + \frac{p(A)p(B)}{K(AB)} + \ldots,$$

where $p'(A)$, $p'(B)$, etc., are known from the previous analysis of the atmospheres of the giants and dwarfs. Finally, the number of molecules of a kind is computed from their partial pressure.

In order to apply these results properly we must remember the following points: (1) They are based on the analysis of the atmosphere of the sun, and they stand or fall with the results of this analysis. (2) Some stars certainly do not have the same composition as the sun, and they differ from each other (carbon and nitrogen branches in Wolf-Rayet stars). (3) Physical constants for most molecules are not sufficiently well known. The dissociation energy is especially important, as a small change in it greatly changes the value of the dissociation constant. (4) No direct comparison with observation is possible, as observations do not give the number N of molecules but rather the quantity Nf, where f is the oscillatory strength unknown for molecules. Therefore, no intercomparison between various kinds of molecules is possible. Even the amount of absorption due to the most common molecules, such as TiO, is not accurately known.

There are at present no reliable measures of the intensities of bands in stellar spectra. In the case of the sun we have the results shown in Table 2.

We notice that hydrides are much fainter than one would expect. CH is actually fainter in spots, whereas it should be stronger. OH and NH should be strong in spots, but their absence there is perhaps

due to the difficulties of observation. *CN* is practically absent in spots where it should be very strong. It would seem that in both *CH* and *CN* the maximum of concentration is arrived at earlier than it is calculated by Russell ($K2$ and $K4$ for dwarfs).

While Russell's theory gives, on the whole, a good approximation to the observed conditions, it is obvious that the problem of molecules in stellar atmospheres is much more complicated than it would seem from Russell's treatment. In the further development of this

TABLE 2

AVERAGE INTENSITIES OF LINES IN THE (0, 0) BANDS

MOLECULE	BAND	NO. OF LINES	AVERAGE INTENSITY		LOG S	
			Disk	Spot	Disk	Spot
OH	λ 3063	135	+0.3	?	5.3	6.7
NH	3360	68	−0.9	?	4.0	5.3
CH	4300	89	+1.1	+0.8	3.1	4.1
CN	3883	59	+0.7	?	2.3	3.9
SiF	4369	28	−0.9	?	0.9	2.6
C_2	5165	176	−2.2	−1.4	0.9	2.4
MgH	5211	143	−2.6	−0.6	1.4	2.9
CaH	6903	105	.....	+0.4	−0.4	1.5
TiO	5167	127	.....	−2.1	−0.6	2.2

problem, possible interaction of compounds, influence of compounds on general opacity, stratification of compounds, etc., will have to be considered. Before this can be done, however, both laboratory and observational data will have to be enlarged and improved.

CURRENT PROBLEMS

There are many astrophysical problems the solution of which depends on our better understanding of the role of compounds in stellar atmospheres. Perhaps the most complex problems of this kind are the physical processes involved in Me stars. It seems obvious that the variation in total light, color index, appearance and intensity of emission lines, etc., are bound somehow with the changes in the concentration of *TiO* molecules and perhaps with other molecules which do not produce observable absorption.[28] The abnormal

[28] For the role which may be played by the H_2 molecule, see Wurm, *Zs. f. Ap.*, **10**, 133, 1935.

Balmer decrement in the Me variables is ascribed to the layer of *TiO* superposed on the emission layer of hydrogen, as no physical theory can account at the present time for such decrement.[29] Yet the correlation between the strength of *TiO* bands, the amount of variability in total light, and the departure from the normal distribution of intensity among the members of the Balmer series is not very strong. In some irregular variables of Me type and in dwarf Me stars the Balmer decrement is normal. On the other hand, Se and Re stars show a decrement analogous to that of the Me stars.

Determination of temperature by the distribution of intensity among the vibrational transitions of the bands, evaluation of the relative abundance of isotopes, continuous absorption associated with the bands, etc., cannot be properly undertaken until we have better spectrophotometric data. It may be that with further study the classification of M stars will have to be refined to take cognizance of the occurrence of *ZrO*, *ScO*, and *YO* in some M stars and not in others. Above all, the exact relationship of classes R, N, and S to class M will have to be clarified.

PERKINS OBSERVATORY

MOLECULAR BANDS AS INDICATORS OF STELLAR TEMPERATURES AND LUMINOSITIES

W. W. MORGAN

In a recent paper[1] a number of the brighter K and M dwarfs have been reclassified from the strong *TiO* bands in the visual region. It was found that when these bands are used for classification the dispersion in luminosity for any given spectral type is exceedingly small; it can, in fact, be accounted for entirely by the accidental errors in the trigonometric parallaxes, in the apparent magnitudes, and in the spectral types. The strongest bands first appear at visual absolute magnitude 9.0 and increase steadily in intensity with decreasing luminosity. The connection between luminosity and spectral type is so close that absolute magnitudes of M dwarfs of un-

[29] Ambarzumian and Vashakidze, *Russ. Astr. J.*, **15**, 14, 1938.

[1] *Ap. J.*, **87**, 589, 1938.

known parallax may be deduced with good accuracy from the spectral type alone, on the revised system.

Accurate determinations of the colors of the M dwarfs are few; if we assume, however, that our classification represents a steady decrease in effective temperature and surface brightness, we may draw the following tentative conclusions concerning the *TiO* dwarfs having visual absolute magnitudes between 9.0 and 16.5:

1. For any one value of the surface brightness or effective temperature, there is one and only one value of the luminosity.

2. Since the luminosities and surface brightnesses of dwarfs of the same spectral type are identical, it follows that all dwarfs of the same spectral type are of the same size.

These results were obtained from the relatively small number of M dwarfs for which accurate absolute magnitudes are known. There was, however, no other selection of the data, and not one exceptional case has been found. Conclusions 1 and 2, therefore, seem to be justified, and we can draw the following final conclusion:

From the spectral type alone, determined from the intensity of the strong *TiO* bands in the visual region, the following data concerning M dwarfs can be obtained from reduction-curves based on well-observed stars: the absolute magnitude, the effective temperature, and the stellar diameter.

About two-thirds of all stars in the neighborhood of the sun are *TiO* dwarfs within the visual absolute magnitude limits 9.0–14.0. The close relationship between luminosity and spectral type is, therefore, of some general interest; the only exceptional objects are the relatively rare ordinary M giants and the still rarer M supergiants and long-period variables.

YERKES OBSERVATORY

SPECTROSCOPIC STUDIES OF PLANETARY ATMOSPHERES

ARTHUR ADEL

Planetary atmospheres form an important field for the study of molecular spectra in celestial objects, particularly because the prevailing low temperatures of these gaseous envelopes favor the existence of polyatomic molecular states.

Telluric spectrum.—Since the electronic bands of these molecules lie, for the most part, in spectral regions not transmitted by the earth's atmosphere, the absorption and emission bands of the planetary spectrum accessible to us are principally of the rotation-vibration type. Bands of this type having their origin in low-temperature sources become progressively stronger as we proceed toward the longest wave-length members of the spectrum. The damage done by our atmosphere to an incoming planetary spectrum is, therefore, most severe where the latter is richest in absorption and emission bands. A proper appreciation of the complete spectrum of a planet must be preceded by an understanding of the absorption spectrum of our own atmosphere. Accordingly, a detailed study of the telluric spectrum from 6000 A to 150,000 A has been made at the Lowell Observatory.

Planetary emission spectra.—The infrared emission spectra of the planets were next briefly reviewed in the light of the corrections supplied to the radiometric observations by the previously discussed infrared telluric spectrum.

Planetary absorption spectra.—The photographic absorption spectra of the planets were analyzed in detail.

Conclusion.—Finally, the analysis of the planetary spectrum was applied to the deduction of such physical properties of planetary atmospheres as atmospheric composition and temperature.

LOWELL OBSERVATORY

ON THE INTERPRETATION OF THE SPECTRA OF COMETS AND THEIR FORMS

K. WURM

In this paper I shall report some recent results concerning the interpretation of the observations of comets. The problem of the spectra of comets and of their shapes, which is closely connected with the question of the physical state of the atmospheres of comets, has not yet been solved satisfactorily. Nevertheless, during the last few years certain progress has been made toward a final solution, principally by the application of modern physical theories and especially the theory of band spectra.

I shall start with a description of the most outstanding features of the observations. It is well known that the activity of comets, their luminosity, the variations in their shape, and their spectra, all depend very largely upon their heliocentric distances. Far away from the sun, near aphelion, the comets show little or no luminosity; and we can take it for granted that in this stage they are merely accumulations of meteoric bodies. As a comet approaches perihelion, it develops around its solid nucleus a rather extended luminous atmosphere, the brightness of which increases with decreasing solar distance. This variation in brightness is absolute. The tails of comets make their first appearance usually at a solar distance r of 2 astronomical units, or somewhat less. Outside this range the comets consist only of a coma, which, projected on the background of the sky, appears as a nearly circular nebulous image around the nucleus. The nucleus reveals itself usually by a somewhat greater brightness.

For a number of comets which could be observed over a long interval of time, and hence over a large range of heliocentric distance, r, it has been established that the coma (also often called the "head") contracts strongly with decreasing r. It is hardly possible to give exact values of the diameter, D, of the head, since the outer borders are seldom well defined. Irregular fluctuations are quite frequent. But since the contraction is very strong, even the order of magnitude of the diameter D for different values of r is sufficient to show the effect of contraction very clearly.

Averaging the available data,[1] we get the values shown in the accompanying table. After perihelion passage the coma expands again.

r (in Astronomical Units)	D (in 10^3 Km)	r (in Astronomical Units)	D (in 10^3 Km)
1.5	300–600	0.5	20–100
1.0	100–300	0.3	5– 20

The gas atmospheres of comets contain, as far as the spectra reveal, the following molecules: CN, C_2, CH, CO^+, and N_2^+. If a

[1] See especially Bredischin and Jägermann, *Untersuchungen über Cometenformen*, St. Petersburg, 1903; N. T. Bobrovnikoff, *Pub. Lick Obs.*, **17**, 1931.

comet approaches the sun very closely, say to within 0.2 astronomical units, one observes also the emission of metallic elements. Sodium, with its very low boiling-point, exists in comet atmospheres already at distances of 0.5–1.0 astronomical units. Comets which come so near to the solar surface that other elements than sodium become conspicuous by their line emission are very rare. We can take it for granted that the generation of the atmospheres of comets is produced by the heating of the meteorites, which give off their occluded gases. At smaller distances r we have additional evaporation. Since the gravitational attraction of the nuclei is negligibly small, the freed gases will move away from the nucleus with a speed corresponding to their thermal velocities, and they are then exposed only to the influence of the solar radiation. We may, therefore, expect that all observational facts would be understood if we considered closely how the solar radiation acts on the freed gases. On the other hand, all comets should be very similar in their essential features. That the latter is really the case is especially indicated by the spectra, which show little difference from comet to comet. Regarding the forms of comets, their far-reaching similarity is often hidden by a large variation in the structure of the tails. There is no doubt that the shapes of different comets are very similar in their essential features. This becomes evident if one considers the distribution of the various emitting molecules over the different parts of the comets. We do not find the same emitting particles in all parts of a comet. The local distribution is as follows: CN and C_2 are found only in the coma or head, and the extension of the CN molecules is somewhat larger than the extension of the C_2 molecules. In the tail we find CO^+ and N_2^+ (see Fig. 1). This curious distribution was first confirmed by Baldet.[2] As can be seen from Figure 1, the CO^+ and N_2^+ molecules exist also in the head, but only in that part which lies behind the nucleus in the direction of the tail. If we define the tails of comets, according to the extension of the CO^+ and N_2^+ emission, we may say that the tail of a comet originates near the nucleus. There is no doubt that the CO^+ and N_2^+ ions are formed near the nucleus and are then driven off by light pressure. Both CO^+ and N_2^+ have a strong absorption system in the visible region,

[2] *Ann. de l'Obs. l'Astronomie Physique de Paris*, **7**, 1926.

the bands of which are observed in emission. The N_2^+ system is generally weaker than the CO^+ system. The latter is known as the "comet-tail band system." Whether the greater strength of the CO^+ bands is caused by a higher abundance of the CO^+ molecules or by a higher transition probability (compared with N_2^+) is not yet known. The first cause seems to be more probable.

Explanation of luminosity of comets as a fluorescent phenomenon was first given by Schwarzschild. This idea has found support in an

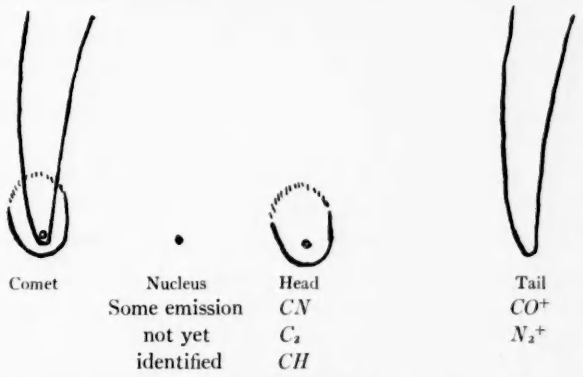

FIG. 1.—Schematic representation of the distribution of the emitting molecules in comets.

investigation of Zanstra,[3] who made some quantitative computations regarding the connection between the brightness of comets and the total masses of the particles which are excited to fluorescence by the continuous solar radiation. This investigation by Zanstra and one by the writer[4] indicated that the density in comet atmospheres must be very low, the free path of the particles being of the same order as the diameter of the head or even larger. From the intensities of the C_2 bands or from the visual brightness of comets, which depend chiefly on the intensity of the C_2 bands, we can estimate the total number of absorbing and emitting molecules and, thereby, the number of C_2 molecules per cubic centimeter. It turns out that the total number of the C_2 molecules is of the order of 10^{30} and that the number per cubic centimeter is 1. Naturally, this gives only a lower limit for the density, since other particles exist, some of which may

[3] *M.N.*, **89**, 178, 1928. [4] *Zs. f. Ap.*, **8**, 281, 1934.

have a higher abundance. Another definite indication which reveals the existence of a very low density is given by the structure of the bands, especially if we compare the CN and C_2 bands. If the density were not extremely low, the structure of the CN and C_2 bands could not show those differences which arise from different "rotational" and "vibrational" temperatures of the particles. The distribution of the molecules over the different rotational and vibrational states cannot be influenced by collisions but can be very well explained, as the writer has shown, if we assume that collisions play no role and that the distribution of the molecules over the various quantum levels is governed by the absorption and emission processes alone.[5] In this connection the individual properties of the molecules are of importance, such as the existence of a permanent dipole moment (CN, CH), the nature of the electronic transition, and the relative situation of the potential curves in the upper and lower states. As the writer has shown,[6] the variation of the structure of bands in their dependence upon the heliocentric distance, as observed by V. M. Slipher[7] and A. Adel,[8] can also be explained in this way by taking especially into account the individual character of the molecule, the nature of the electronic transition, and the lifetime of the rotational and vibrational states. In the case of the CN $^2\Sigma \rightarrow {}^2\Sigma$ bands, which have only P and R but no Q branches, the molecules are moved into higher rotational levels as soon as the time T between the successive absorption processes in the $^2\Sigma \rightarrow {}^2\Sigma$ system becomes shorter than the lifetime T_r of the rotational states. The reason for this is that in absorption we have a stronger R branch, while in emission the P branch is more intense. If we have a system with Q branches, the process is slowed up, since the Q branch is generally strongest.[9]

All these facts show clearly that we have to deal with extremely low densities in the atmospheres of comets and that collisions play no role.

Now we may see how far we can explain the other observations mentioned above if we take into account only the direct influence of the solar radiation. We have especially to account for the local

[5] K. Wurm, *Handbuch d. Ap.*, **7**, 305.

[6] *Zs. f. Ap.*, **15**, 115, 1937.

[7] *Bull. Lowell Obs.*, **2**, 74.

[8] *Pub. A.S.P.*, **49**, 254, 1937.

[9] See the remarks on a paper by Swings and Nicolet at the end of this report.

distribution of the molecules, the contraction effect, and, further, for the appearance of the C_2 molecules in the gas. The C_2 molecules cannot be supposed to be created by vaporization, since they exist already at very large solar distances—in fact, they appear much earlier than the sodium.

Besides the process of fluorescence, there are two other processes which we can expect with certainty to take place and to play an important role: ionization and dissociation by light absorption. The whole problem becomes greatly simplified by the fact that all processes which depend upon collisions can be excluded. Hence, the appearance of particles which we cannot expect to be freed from the solid nucleus directly, such as C_2, CO^+, N_2^+, and perhaps others, must be formed by one of the two processes mentioned, namely, by ionization or by dissociation by light absorption of another particle, which we may call the "parent-molecule." The presence of the C_2 molecule in the atmospheres of comets is to be explained by photo-dissociation of a parent-molecule which may be a poliatomic carbon nitrogen or carbon hydrogen compound, such as dicyanogen or acetylene. Until now we have had no spectroscopic evidence of these molecules; but we have to keep in mind that our observations are restricted to the wave-length region λλ 3000–7000, and it is very probable that the resonance system of this parent-molecule lies outside of this range. The simultaneous appearance of carbon and cyanogen permits us to suppose that the parent-molecule is represented by dicyanogen and also that the diatomic cyanogen is created by photo-dissociation. A direct indication in favor of this supposition can be seen in the following: The ionized carbon monoxide does not extend over the whole coma but only over that part which lies behind the nucleus. Without doubt the carbon monoxide ion is created by ionization either of carbon monoxide or dioxide. In the latter case the ionization must be accompanied by the simultaneous dissociation of one oxygen atom. Now, there is the question why this molecule does not have the same extension as the C_2 and CN molecules. The difference between the masses cannot account for the lower velocity of expansion if we think of a thermal motion only. But there is the possibility that the different velocities originate in the process of photo-dissociation. As is well known, we can expect

that in the process of photo-dissociation the newly created components separate with a certain relative velocity which can greatly exceed the average thermal velocity. It is quite natural to think of this effect in our case. The limited extension of the carbon monoxide ions in the head can be explained in this way by the different velocities of expansion for cyanogen (and C_2), on the one side, and the parent-molecule of CO^+, on the other.

As we come now to the contraction of the head with decreasing heliocentric distance, it is quite clear that this contraction can be explained by assuming that at the outer border of the head the cyanogen and also the C_2 molecules are either dissociated or ionized by the absorption of light. In consequence of this process, the rise of the head must diminish with decreasing heliocentric distance. With increasing radiation intensity the time which passes between the appearance of cyanogen (and C_2) molecules in space and their dissociation will be shortened. This means that the distance which they may reach traveling from the nucleus away into space will be shortened. This explanation accounts quite naturally also for the fact that the cyanogen and C_2 molecules do not appear in the tail. On the other hand, from the fact that CO^+ and N_2^+ form long tail images, we have to conclude that these particles are difficult to ionize or to dissociate by the absorption of solar radiation and that this circumstance alone makes possible the phenomenon of bright comet tails. When the idéa outlined here was first mentioned by the writer,[10] there was no definite evidence for any particle as to whether we were dealing with ionization or with dissociation. From an investigation by Dr. Herzberg[11] we know now that in one case, namely, that of C_2, there exists an electronic state about 6 volts from the ground state which leads to dissociation by the absorption of light shorter than λ 2000. Since the ionization energy of C_2 is about 12 volts, we can assume that the ionization process is negligible, as compared with the efficiency of dissociation.

Addendum.—Swings and Nicolet, in a paper published recently in this *Journal*,[12] suggest an alternative explanation for the variation of the intensity distribution within the band systems, in their dependence upon the solar distance *r*. The authors are of the opinion that the very different distribution of

[10] *Zs. f. Ap.*, **9**, 62, 1934. [11] See this issue, p. 290. [12] *Ap. J.*, **88**, 173, 1938.

the *CN* and *CH* molecules brings complications with regard to the explanation given by the writer and probably imply very different values of T_r (lifetime of the rotational states) for *CN* and *CH*. There is no reason why T_r should be equal for *CN* and *CH*, and we may expect that *CH* shows a shorter lifetime. The higher asymmetry of *CH* points to the higher electric moment of the *CH* rotator, and the higher rotational quantum of *CH* (ΔE_r of *CH* is seven times larger than ΔE_r for *CN*) points to a higher transition probability. These factors suggest a shorter lifetime of *CH* and may explain why we find the *CH* molecules in lower rotational levels than the *CN* molecules. There is still another point: Since the *CH* system in question has a strong Q branch, the moving-up into higher rotational states should go more slowly than in the *CN* system. Swings and Nicolet point out that the radiation in comet atmospheres in the far infrared in the region of the pure rotational spectra originates chiefly from the nucleus of the comet, which is warmed up by the absorbed solar radiation. They give $T=300r^{-1/2}$ for the temperature of the nucleus, applying Stefan's law (r is the heliocentric distance). The direct solar radiation has for $r=1$, for instance, a density near $\lambda=100\,\mu$ which corresponds to only $T_\lambda=5°$. The authors assume that the radiation of the nucleus influences chiefly the rotational distribution, since the pure rotational transitions of molecules in equilibrium at $T=300°$ are at least as frequent as the electronic transitions (absorption) near λ 4500 for an equilibrium temperature $\sim 2000°$, which corresponds to the density of radiation in this wave length and to $r=1$. But, besides the fact that the number of rotational transitions can hardly be computed, the radiation density in the far infrared region may correspond to $T=300°$ only near the nucleus. But the dimensions of the nuclei of comets are always small, compared with the size of the head. Therefore, the molecules are exposed not to a temperature radiation of 300° but to a diluted radiation, and the average dilution factor may be between 20 and 200 (assuming that the diameter of the nucleus is 1000 km and that the diameter of the head is 100,000 km). Hence, we have to assume that the molecules are exposed to a radiation corresponding roughly to 5°–15° ab. This means that the conclusions of Swings and Nicolet are hardly tenable.

YERKES OBSERVATORY

NOTES

NEW LINES IN THE ROCK-SALT PRISMATIC SOLAR SPECTRUM

Results of observations on the rock-salt prismatic solar spectrum, made during the 1938 rainy season at the Lowell Observatory, include telluric lines previously unknown and probably mainly due to absorption by water vapor.

The new lines range in position from the great water band at 6.3 μ to the limit of atmospheric transmission. They appear, for the most part, as small indentations in the new curves of Plates XVIII and XIX, where they are shown in relation to previously known weak water-vapor absorptions, now enhanced, as well as in relation to the better-known absorption bands of atmospheric water vapor, carbon dioxide, ozone, and nitrogen pentoxide.[1]

The observed continuous absorption spectrum of the earth's atmosphere overlying this spectral region, and upon which the above-mentioned discrete absorptions are superimposed, has been discussed in an earlier paper.[2]

ARTHUR ADEL

LOWELL OBSERVATORY
FLAGSTAFF, ARIZONA
January 1939

[1] The heretofore known but unidentified band q_1 (11.7 μ) exhibits a strong correlation with the water-vapor content of the atmosphere and would therefore appear to be due to water vapor. The band q_2 (12.6 μ) previously attributed entirely to carbon dioxide also exhibits this correlation and would therefore appear to be at least in part due to water vapor. Absorption lines due to water vapor (steam was actually used in the experiment) at the positions of q_1 and q_2 are given by L. R. Weber and H. M. Randall (*Phys. Rev.*, **40**, 835, 1932, Fig. 4). This paper also lists water lines between 13 μ and 14 μ of the order of the intensity of q_2 which consequently contribute to the structure of the infrared limit of transmission in previously unrecognized fashion.

[2] A. Adel, *Ap. J.*, **89**, 1, 1939.

PLATE XVIII

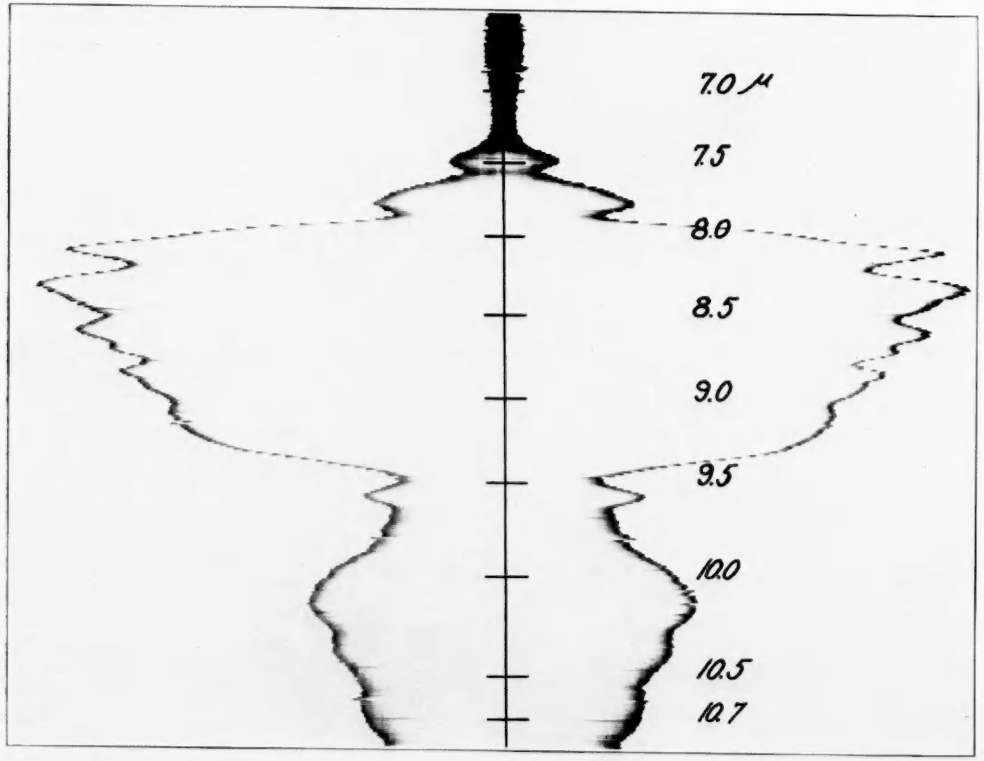

ROCK SALT PRISMATIC SOLAR SPECTRUM

PLATE XIX

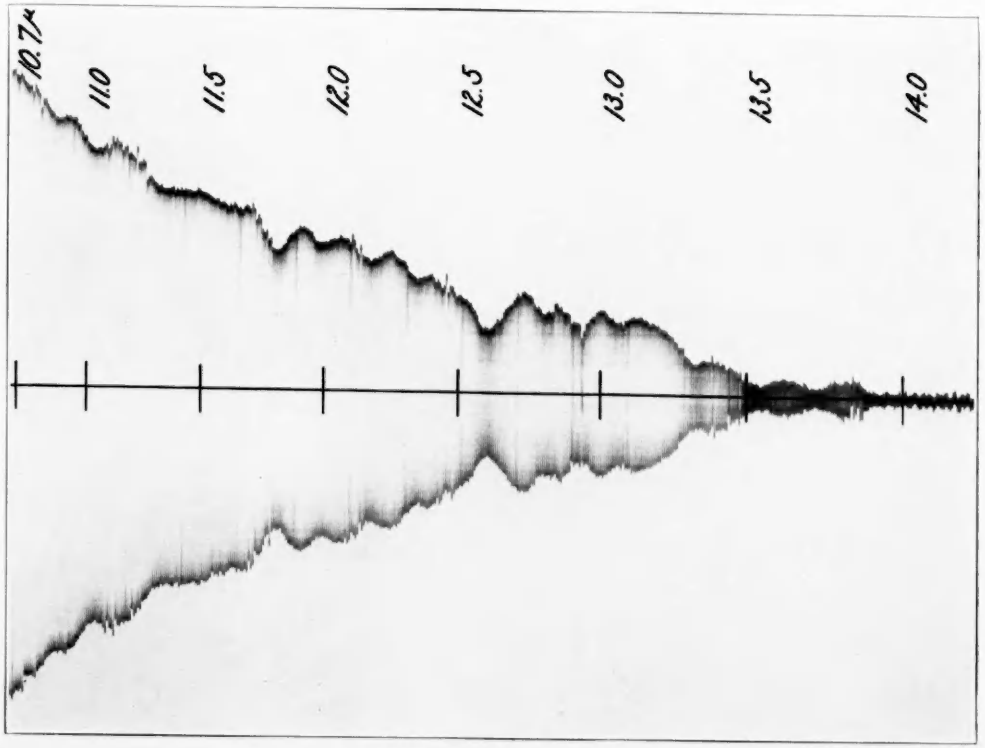

ROCK SALT PRISMATIC SOLAR SPECTRUM

PRESSURE SHIFTS OF LINES OF *N* I

ABSTRACT

The discrepancy previously reported in the mean displacement of the infrared *N* I lines in the spectrum of α Cygni is removed by the use of the wave lengths recently measured by Edlén. Laboratory studies of the large pressure shifts of these lines are suggested.

The large systematic differences (Table 1) between the wave lengths of infrared lines of *N* I recently measured by Bengt Edlén[1] and those previously published by the writer[2] are doubtless pressure effects. C. C. Kiess's wave lengths[3] are intermediate, and he has informed me that in his experiments the pressure also was intermediate. A comparison of various measures indicates that the shifts in lines of the multiplet $^2P - {}^2P$ are considerably greater than those of the quartets, and that the quartet shifts may differ slightly among themselves.

TABLE 1

WAVE LENGTHS OF LINES OF *N* I

Edlén	Merrill	Δλ	Multiplet
7423.63 A	24.04	+0.41	$^4P-{}^4S$
42.28	42.70	.42	.....
68.29	68.72	.43	.....
8184.80	85.26	.46	$^4P-{}^4P$
87.95	88.42	.47	.....
8200.31	00.72	.41	.....
10.64	11.12	.48	.....
16.28	16.72	.44	.....
23.07	23.48	.41	.....
42.34	42.80	.46	.....
8629.24	30.02	.78	$^2P-{}^2P$
8680.24	80.63	.39	$^4P-{}^4D$
83.38	83.70	.32	.....
86.13	86.41	.28	.....
8711.69	12.00	+0.31	.....

Since the displacements at atmospheric pressure are large compared to the accuracy of measurement easily attained in ordinary

[1] *Festskrift tillägnad Östen Bergstrand*, September, 1938.

[2] *Mt. W. Contr.*, Nos. 183 and 207; *Ap. J.*, **51**, 236, 1920; **54**, 76, 1921.

[3] *J. Opt. Soc. Amer.*, **11**, 1, 1925.

spectroscopic observations, these lines might prove especially useful for studies under controlled conditions of the effects of pressure (and other variables?) on wave length.

Numerous lines of *N* I, including all in Table 1, were measured in the spectrum of α Cygni,[4] with the curious result that, upon the basis of Kiess's wave lengths, the nitrogen lines were systematically displaced toward shorter wave lengths with respect to other lines by about 0.23 A. Edlén's values, however, yield a displacement which agrees with the mean displacement of all other lines well within errors of measurement, and thus remove a puzzling discrepancy.

The new data indicate that the pressure in the reversing layers of stars like α Cygni does not exceed a small fraction of an atmosphere, a conclusion of course now well established on other grounds.

PAUL W. MERRILL

CARNEGIE INSTITUTION OF WASHINGTON
MOUNT WILSON OBSERVATORY
December 1938

NOTE ON THE PAPER "A NEW ECLIPSING VARIABLE OF LARGE MASS"[1]

Through the use of a wrong elongation angle, corresponding to $D = 0^{p}.085$, the dimensions of the system were incorrectly computed. The correct values of the masses are 42.5 and 39.1; of the mean radii (corrected for the ellipticity $b/a = 0.972$), 13.40 = 0.134 A and 12.1 = 1.123 A; of the mean densities, 0.018 and 0.022; and of i, 85°.5. The ordinates for the figures should be 6.45, 6.58, 6.71, 6.84, 6.96, and 7.09. With these values the system does not deviate greatly from the mass-luminosity relation.

SERGEI GAPOSCHKIN

[4] *Mt. W. Contr.*, No. 486; *Ap. J.*, **79**, 183, 1934.

[1] *Ap. J.*, **89**, 125, 1939.